The Effect of Phosphodiesterase Inhibitors on Improving the Outcomes of Assisted Reproductive Technologies

Hesham Ibrahim Mohamed Eltemimy

The University of Sydney

Faculty of Medicine and Health

Sydney Medical School

Reproduction and Perinatal Centre

2026

A thesis submitted to fulfil the requirements of the degree of Master of Philosophy

Table of Contents

Morphokinetic Consequences of ICSI-mediated Phosphodiesterase Inhibitor Exposure in Preimplantation Mouse Embryos

Evaluation of Different Sperm Preparation Methods and their Impact on Fertility Treatment Outcomes; a Retrospective Cohort Study

Statement of Originality

I certify that the intellectual content of this thesis is the product of my own work, and that all assistance received in preparing this thesis and all sources have been acknowledged.

Hesham Eltemimy

Generative AI attribution statement

During the preparation of the thesis the author used some editorial assistance (e.g. paraphrasing, sentence structure, spelling, etc) which was supported by Microsoft Copilot.

Commands included:
“Check grammar and spelling UK English pls”
“Improve sentence and check grammar / spelling”

No AI system contributed to data analysis, interpretation, or scientific conclusions.

The author confirms that where text was modified by generative AI, the content was reviewed for possible errors, inaccuracies, and bias. The author takes full responsibility for the submitted thesis and ensures the work is their own and has used generative AI within the parameters of use in accordance with *“Guidelines on attribution of generative AI use for research students”* (The University of Sydney, 2024).

RTP Offset Statement

I, Hesham Eltemimy acknowledge that I have received The Australian Government Research Training Program (RTP) Fees Offset.

Authorship Attribution Statement

No part of this thesis has been published already or forthcoming.
This thesis does not contain material previously published

Acknowledgements

First and foremost, all praise and thanks are due to Allah (SWT), the Most Gracious and Most Merciful, for providing me with the strength, patience, and guidance to complete this work.

"My success is not but through Allah. Upon Him I have relied, and to Him I return."
(Surah Hud, 11:88)

The completion of this thesis would not have been possible without the unwavering support, guidance, and encouragement of many individuals to whom I owe my deepest gratitude.

I extend my most sincere thanks to my lead supervisor, **A.Prof. Cecilia Sjoblom**. I am profoundly moved by your dedication; despite the personal challenges and difficult times you have been facing, you remained a steadfast pillar of support and made this achievement possible. Your mentorship has been invaluable, and I am forever grateful for your resilience and commitment to my growth.

My sincere thanks also go to my co-supervisor, **Dr. George Liperis**. Your expert guidance, limitless patience, and unwavering belief in this project were its cornerstone. Thank you for sharing your profound knowledge and for your constant encouragement through both the challenging and rewarding phases of this work.

I must also express my great gratitude to my previous clinic, **Adam International Clinic**, and its founder, **Prof. Medhat Amer**. It was within this clinic that I began my practical career; I am deeply thankful for the opportunity to have gained such extensive experience and a solid professional foundation under your leadership.

I am also immensely grateful to the entire embryology team at **WFC**. Your understanding and flexibility in accommodating the demands of this research were crucial. Thank you for your collegiality and for providing me with the time and space necessary to bring this project to completion.

Finally, my deepest and most personal gratitude is reserved for my family. To my **Father**, thank you for a lifetime of love and for instilling in me the value of education. To my **late Mother**, though you are not here to witness this moment, your prayers and the values you raised me with remain my guiding light; I dedicate this success to your memory.

To my wife, **Mona**, thank you for your endless patience and for your constant encouragement that kept me going. To my beloved daughters, **Hana and Hala**, you were my anchor and my greatest motivation. This achievement is as much yours as it is mine.

- For Cecilia and George: "Your door was always open, and your guidance was my firm foundation."
- For the Adam Clinic team: "Thank you for the foundation and the years of invaluable experience."
- For the WFC team: "I greatly appreciate the collaborative spirit and support at WFC."
- For my Family: "Mona, Hana, and Hala—you are my heart, my anchor, and my motivation."

Hesham Eltemimy

Thesis Abstract

In assisted reproductive technology (ART), phosphodiesterase (PDE) inhibitors such as pentoxifylline (PTX) and theophylline (THEO) are widely used to enhance sperm motility. By increasing intracellular cAMP, these agents stimulate movement, yet concerns persist regarding potential embryotoxicity. Robust experimental evidence is therefore required to balance their clinical utility against possible risks. This study investigated the developmental impact of PTX and THEO using a mouse model of human pre-implantation development. Zygotes were microinjected with PTX or THEO using a technique that closely mimics intracytoplasmic sperm injection (ICSI), then cultured in vitro under standardised conditions. Embryo development was assessed alongside total cell number following propidium iodide staining. Multiple control groups, including non-injected embryos, medium-injected embryos, and PVP-injected embryos, were included to distinguish compound-specific effects from procedural artefacts.

Early developmental outcomes were broadly comparable across groups. There was no significant difference in cleavage rate between the groups, indicating that neither PTX nor THEO impaired early viability and that the microinjection procedure itself was well tolerated. All embryos that cleaved progressed to the blastocyst stage by 114 h, and all groups met or approached the ≥80% FDA benchmark commonly referenced in mouse embryo assay (MEA) validation guidelines.

Total cell-number analysis showed that PTX-injected embryos exhibited a significant reduction in total cell number compared with untreated controls. In contrast, THEO-injected embryos displayed cell numbers indistinguishable from controls, indicating that THEO does not adversely affect proliferation. These findings align with clinical and experimental literature showing that PTX exposure can reduce blastocyst cell number and increase apoptosis, whereas modified PTX analogues or THEO do not produce these effects.

Time-lapse imaging showed no significant morphokinetic differences between groups when normalised to pronuclear fading. Neither PTX nor THEO disrupted cleavage-cycle duration or

synchrony, and key morphokinetic indicators of embryo health, ECC2, ECC3, s2, and s3, were comparable across all groups. Because early cleavage timings are highly sensitive to environmental stressors, the preservation of these parameters suggests that neither compound perturbs the intracellular regulatory mechanisms governing early development.

Taken together, these findings demonstrate that PTX and THEO differ in their effects on pre-implantation development. Both compounds supported normal cleavage and blastocyst formation, and neither disrupted the fundamental kinetic architecture of early development. However, PTX exerted a clear suppressive effect on proliferative capacity, reducing total cell number despite otherwise normal morphokinetics. THEO, by contrast, appeared benign across all measured endpoints. Overall, this study provides a detailed and functionally relevant assessment of PDE inhibitor exposure during zygote microinjection and reinforces the need for careful evaluation of compounds used during gamete manipulation in ART.

Chapter 1

Literature Review

1.0 Introduction

Assisted reproductive technologies (ART) have evolved rapidly over recent decades, driven by continual refinement of laboratory techniques and the introduction of new strategies aimed at improving fertilisation, embryo development, and ultimately live-birth outcomes. Central to these advances are the procedures of *in vitro* fertilisation (IVF) and intracytoplasmic sperm injection (ICSI), which rely on the availability of functionally competent gametes to achieve successful fertilisation. Sperm motility, in particular, is a critical determinant of fertilising capacity, and impaired motility remains a major contributor to male-factor infertility. To overcome this limitation, ART laboratories frequently employ pharmacological agents such as the phosphodiesterase inhibitors pentoxifylline (PTX) and theophylline (THEO) to enhance motility *in vitro*. Despite their widespread clinical use, the mechanisms by which these agents act on gametes and early embryos, and their potential implications for embryo viability and downstream reproductive outcomes, remain insufficiently characterised. Understanding the biological effects and safety profile of these agents is therefore essential to inform evidence-based practice and optimise outcomes for patients undergoing fertility treatment.

1.1 Infertility

Infertility is a multifactorial reproductive health disorder characterised by the inability to achieve pregnancy after a year or more of regular, unprotected sexual intercourse (Zegers-Hochschild et al., 2017). It affects millions of individuals worldwide, with approximately one in six couples experiencing challenges in conceiving a child (Agarwal et al., 2015). Infertility aetiologies can vary, including physiological abnormalities in either partner, hormonal imbalances, genetic predispositions, lifestyle factors, and environmental influences (Chiang et al., 2017). In women, infertility may result from ovulatory disorders, fallopian tube abnormalities, uterine issues, or age-related decline in fertility ("Female age-related fertility decline. Committee Opinion No. 589," 2014). In men, factors such as low sperm count, poor sperm motility, abnormal sperm morphology, or structural abnormalities of the reproductive tract can contribute to infertility (Carson & Kallen, 2021).

The diagnosis of infertility often involves a comprehensive evaluation of both partners' medical history, physical examinations, and specialised fertility tests, including semen analysis, hormone assessments, and imaging studies (Merritt et al., 2020). Treatment options for infertility depend on the underlying cause and may include lifestyle modifications, medication, surgical interventions, or ART such as IVF or ICSI. Infertility not only impacts individuals' physical health but also has profound emotional, psychological, and social implications, underscoring the importance of holistic approaches to diagnosis, treatment, and support for those affected (Linehan et al., 2025). The World Health Organisation (WHO) have recently issued the first WHO Guideline for the prevention, diagnosis and treatment of infertility, which aims to improve the implementation of evidence-based interventions related to infertility (World Health Organization, 2025).

1.1.1 Assisted Reproductive Technology

ART has demonstrated high efficacy in helping infertile couples achieve pregnancy (Lazzari et al., 2023). Techniques such as IVF and ICSI provide alternative pathways to conception for individuals affected by a wide range of infertility factors. Since the birth of Louise Brown in 1978, IVF has become a cornerstone of ART, enabling fertilisation to occur outside the body followed by embryo transfer and successful pregnancy. Embryo cryopreservation has optimised the cumulative chances by allowing for excess embryos of good quality to be frozen and transferred in a subsequent cycle. Innovations such as time-lapse embryo monitoring have provided tools for embryo selection (Maezawa et al., 2014). The incorporation of advanced technologies, including preimplantation genetic testing for aneuploidy (PGT-A), has further improved ART outcomes by allowing embryos to be screened for chromosomal abnormalities prior to transfer, particularly benefiting patients of advanced maternal age (Sacchi et al., 2019). In addition, sperm, oocyte and embryo cryopreservation techniques offer vital opportunities for fertility preservation in individuals undergoing gonadotoxic medical treatments, such as chemotherapy or radiotherapy, which may compromise future reproductive potential (Sönmezer & Oktay, 2008).

The emergence of personalised medicine approaches, including ovarian reserve testing and tailored stimulation protocols, has enabled more precise and individualised fertility treatments. Techniques such as mitochondrial replacement therapy (MRT) have also been introduced which offer promising solutions for individuals with mitochondrial DNA disorders, mitigating the risk of transmitting genetic diseases to offspring (Mayeur et al., 2024).

In 2020, the most recent year for which comprehensive European data are available, 923,318 ART treatment cycles were reported across 41 countries, representing a decline from the 1,077,813 cycles recorded in 2019, largely reflecting COVID-19-related service interruptions (Smeenk et al., 2023; Smeenk et al., 2025). By comparison, the United States reported 330,773 cycles (Gleicher et al., 2026), while Australia and New Zealand reported 95,699 cycles for the same period (Newman et al., 2022). More recent data from the Australia and New Zealand Assisted Reproduction Database (ANZARD) 2023 report indicate that ART activity has since rebounded, with approximately 112,000 treatment cycles performed across Australia and New Zealand (Kotevski et al., 2025).

In many developed countries, ART activity has historically grown at an annual rate of 5–10%, although this expansion is now showing signs of plateauing. According to the most recent global data report from the International Committee for Monitoring Assisted Reproductive Technologies (ICMART) covering outcomes from 2019, China now performs more than one million ART cycles per year (1,120,000), making it the single largest contributor to global ART volume, followed by Japan with 454,621 treatment cycles (Dyer et al., 2025). The report further notes that more than 3.5 million ART cycles are reported for 2019, resulting in 783,073 babies born. As registry data are estimated to capture only around 75% of all ART activity, the true global figure is likely closer to 4 million cycles per year, with approximately 1 million ART-conceived infants born annually.

Australia and New Zealand consistently report some of the highest ART utilisation rates globally, with ART-conceived births representing approximately 1 in every 14 babies, reflecting both high accessibility and strong public acceptance of fertility treatment.

1.1.2 Male Factor Infertility

Infertility is often perceived as predominantly a female issue; however, male infertility contributes substantially to the overall burden of reproductive difficulty. Of the 88,764 cycles undertaken in Australia and New Zealand in 2023, 44.4% reported only female infertility factors, 10.4% reported male infertility factors as the only cause of infertility and 15.2% reported combined female-male factors (Kotevski et al., 2025). It is estimated to that male factors alone explain 20–30% of cases of infertility and there is a male contribution to the difficulty to conceive in half of all infertile couples (Dhikhirullahi & Zhang, 2025; Winters & Walsh, 2014). Male infertility arises from a wide range of underlying causes. Disorders of spermatogenesis, such as reduced sperm concentration, impaired motility, or abnormal morphology are among the most common and can markedly diminish the likelihood of natural conception (World Health Organisation, 2021). Hormonal disturbances, including conditions such as hypogonadism, may disrupt the endocrine regulation required for normal sperm production (Jacobs & Vaughn, 2012). Genetic abnormalities, including Klinefelter syndrome and Y-chromosome microdeletions, are also well-recognised contributors to male infertility (Houston et al., 2021).

Lifestyle and environmental factors further influence male reproductive potential. Smoking, excessive alcohol intake, recreational drug use, obesity, and exposure to environmental toxins have all been associated with impaired semen quality (Aitken, 2024). Structural or functional disorders of the reproductive tract, such as varicocele, infection, or congenital anatomical anomalies, may interfere with sperm production, maturation, or transport, thereby reducing fertility (de Kretser, 1997). Collectively, these factors can have profound emotional, psychological, and relational consequences for individuals and couples, underscoring the importance of effective diagnostic assessment and access to appropriate fertility treatment.

A cornerstone of male infertility evaluation is the semen analysis, which provides quantitative and qualitative information on ejaculate characteristics (Barratt, 2007). Reference limits for semen parameters are defined by the WHO, in the WHO Manual for Human Semen Analysis, currently in its 6th edition updated in 2021 (Boitrelle et al., 2021; World Health Organisation, 2021). The manual includes reference values for parameters such as semen volume, pH, total sperm number per ejaculate, total and progressive motility, vitality, and morphology

(summarised in Table 1.1). The recently published Australian clinical practice guidelines for male infertility (Katz et al., 2025) reinforce the importance of standardised semen analysis and emphasise the need for repeat testing, appropriate interpretation of borderline results, and integration of semen parameters with clinical history and examination findings.

Fortunately, advances in reproductive medicine offer a range of effective interventions for male infertility. ART, including IVF, ICSI, and surgical sperm retrieval, enable conception even in cases of severe sperm dysfunction. Hormonal therapies may correct endocrine abnormalities contributing to impaired spermatogenesis, while surgical procedures such as varicocele repair or correction of obstructive lesions can restore or improve fertility potential. Lifestyle modifications also play a meaningful role; adopting a healthy diet, engaging in regular physical activity, avoiding tobacco, alcohol, and recreational drugs, and reducing stress have all been shown to positively influence sperm quality (Skoracka et al., 2020). Psychological support, counselling, and peer support groups provide additional benefit by helping individuals and couples navigate the emotional impact of infertility and the complexities of treatment decision-making.

Table 1.1. Semen Analysis Reference Values According to WHO 6th Edition (2021)

Semen Characteristic	Lower Reference Limit
Volume	≥ 1.4 ml
pH (acidity)	7.2 – 7.8
Total sperm number	≥ 39 million sperm per ejaculate
Total motility	≥ 42% (progressive + non-progressive)
Progressive motility	≥ 30%
Vitality	≥ 54% live spermatozoa
Morphology	≥ 4% normal forms (strict criteria)

Reference limits for semen parameters based on the WHO *Laboratory Manual for the Examination and Processing of Human Semen*, 6th Edition (World Health Organisation, 2021). Thresholds represent the 5th centile of fertile men with partners conceiving within 12 months.

1.2 Spermatogenesis

Spermatogenesis is the process by which the testes produce mature spermatozoa capable of fertilising an oocyte. It is a continuous, highly coordinated developmental pathway that begins at puberty and continues throughout adult life. In humans, spermatogenesis takes approximately 64–70 days to complete (O'Donnell & Smith, 2000), whereas in mice the process is faster, taking around 35 days (O'Shaughnessy, 2014). Despite differences in timing and staging, the fundamental organisation of spermatogenesis is conserved across mammals.

1.2.1 Testicular Organisation and Early Development

By 16–20 weeks of gestation, the fetal testis has formed seminiferous cords composed of Sertoli cells, a basement membrane, and prespermatogonia, surrounded by interstitial tissue containing Leydig cells (Svingen & Koopman, 2013). These prespermatogonia remain quiescent until puberty, when activation of the hypothalamic–pituitary–testicular axis initiates spermatogenic activity. At puberty, the testes assume their two principal functions: the production of spermatozoa and the synthesis of androgens. Sperm develop within the seminiferous tubules in association with Sertoli cells, whereas testosterone is produced in the interstitial compartment by Leydig cells. These two regions become physiologically separated by the development of a specialised blood testes barrier around puberty.

As puberty progresses, the seminiferous cords remodel into seminiferous tubules, the functional units of sperm production. Each human testis contains approximately 500 tubules, providing a large surface area for germ-cell development (O'Donnell & Smith, 2000). Within each tubule, Sertoli cells form the structural and metabolic foundation of the seminiferous epithelium. They support developing germ cells, regulate the luminal microenvironment, and form the blood–testis barrier (BTB), a specialised junctional complex that divides the tubule into basal and adluminal compartments (Cheng & Mruk, 2012).

The BTB serves two key purposes. First, it prevents sperm antigens from entering the systemic and lymphatic circulations, where they could trigger an immune response and lead to the formation of anti-sperm antibodies, a possible contributor to a reduced ability to conceive naturally. Second, it creates a highly controlled biochemical microenvironment that allows the different stages of spermatogenesis to proceed in a protected and tightly regulated space.

Although often described as an immune barrier, true testicular immune privilege is maintained largely through immunomodulatory factors secreted by Sertoli cells rather than the BTB alone (Kaur et al., 2013).

Outside the tubules, Leydig cells synthesise testosterone in response to luteinising hormone (LH). Intratesticular testosterone concentrations are exceptionally high—up to 100-fold greater than circulating levels in humans reflecting its essential role in meiosis, spermiogenesis, and maintenance of Sertoli-cell function (Handelsman et al., 2018).

1.2.2 Hormonal Regulation of the Spermatogenesis

Spermatogenesis is regulated by the hypothalamic–pituitary–testicular axis. Gonadotropin-releasing hormone (GnRH) from the hypothalamus stimulates the anterior pituitary to release LH, which acts on Leydig cells to produce testosterone and follicle stimulation hormone (FSH), which acts on Sertoli cells to support germ-cell proliferation, differentiation, and metabolic activity. FSH and testosterone act synergistically to maintain the seminiferous epithelium. In primates, FSH promotes spermatogonial differentiation while testosterone is indispensable for meiosis and spermiogenesis (O'Donnell & Smith, 2000; Plant & Marshall, 2001). Disruption of either hormone leads to impaired sperm production.

1.2.3 Phases of Spermatogenesis

Spermatogenesis proceeds through three major phases, each characterised by distinct cellular events: mitotic proliferation, meiotic division and spermiogenesis (Figure 1.1).

In the mitotic proliferation phase, spermatogonial stem cells (SSCs) reside on the basement membrane of the seminiferous epithelium. In humans, type A spermatogonia include dark (Ad) reserve stem cells and pale (Ap) progenitors, the latter undergoing mitotic divisions to produce type B spermatogonia (O'Donnell & Smith, 2000; O'Donnell et al., 2015). These divisions generate clones of interconnected cells that will become primary spermatocytes. SSC maintenance depends on paracrine factors from Sertoli cells, peritubular myoid cells, and vascular elements, forming a specialised stem-cell niche (Liu et al., 2024).

Primary spermatocytes enter meiosis I, undergoing homologous recombination and segregation of chromosome pairs to form secondary spermatocytes. These rapidly complete

meiosis II to produce haploid round spermatids. Unlike somatic cells, spermatocytes and spermatids rely almost exclusively on lactate supplied by Sertoli cells as their metabolic substrate (Boussouar & Benahmed, 2004). Defects in meiosis can lead to maturation arrest, a common cause of non-obstructive azoospermia (Sun et al., 2007).

Spermiogenesis is the transformation of round spermatids into elongated, motile spermatozoa. This involves acrosome formation, nuclear condensation and chromatin remodelling, flagellum development and cytoplasmic reduction and formation of the residual body. Residual bodies are phagocytosed by Sertoli cells, highlighting their central role in germ-cell turnover. The final step, spermiation, releases mature spermatozoa into the tubule lumen, from where they are transported to the epididymis for further maturation (O'Donnell et al., 2011).

Although the overall process is conserved, several species differences are relevant. Humans have 6 stages of the seminiferous epithelial cycle, whereas mice have 12 (Russell et al., 1993). The epithelial cycle lasts ~16 days in humans versus ~8.6 days in mice. Sertoli-cell number strongly correlates with sperm output; humans have ~500 million Sertoli cells per testis, compared with ~4.5 million in mice. These differences influence experimental interpretation and highlight the importance of cautious extrapolation from rodent models to human sperm biology (Russell et al., 1993).

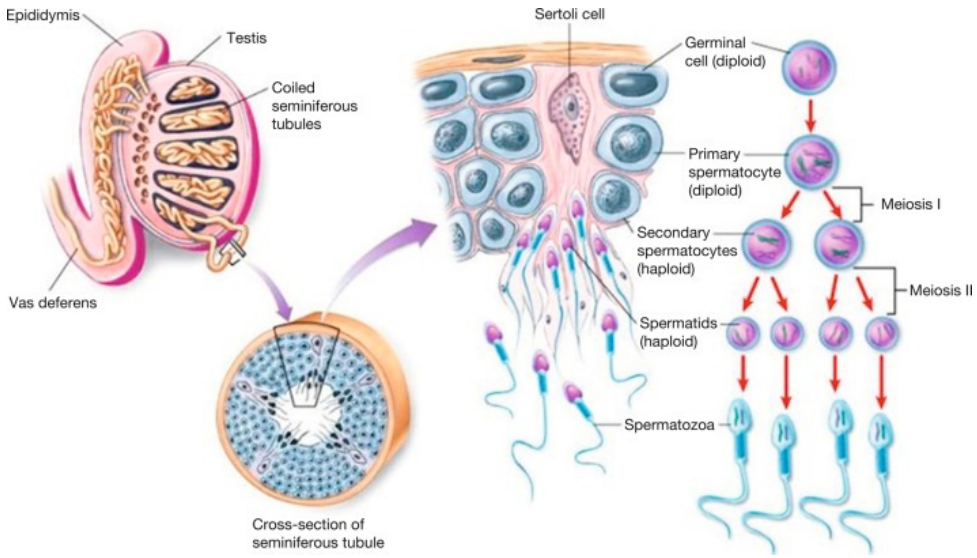

Figure 1.1. Diagram Showing Stages of Human Spermatogenesis (from (Lin & Troyer, 2014)).

1.2.4 The Spermatozoon

The mature spermatozoon is a highly specialised cell designed for motility and delivery of the paternal genome. Its structure is divided into the head, midpiece, and tail, each contributing to the functional requirements for successful fertilisation (Figure 1.2).

The sperm head contains the paternal nucleus and the acrosome, a Golgi-derived vesicle that stores hydrolytic enzymes required for penetration of the zona pellucida. Chromatin is tightly compacted by protamines, producing a streamlined, hydrodynamic profile that protects DNA during transit (Toshimori & Eddy, 2015).

The midpiece serves as the primary site of adenosine triphosphate (ATP) production in the spermatozoon, essential for flagellar motility. It features a helical arrangement of tightly packed mitochondria encircling the axoneme and outer dense fibres (Olson & Winfrey, 1990). These mitochondria generate ATP via oxidative phosphorylation of pyruvate and other Krebs cycle intermediates derived from glycolysis and fatty acid oxidation, which diffuses along the flagellum to power dynein-mediated microtubule sliding (Bhabha et al., 2016).

The number of mitochondria varies between species but in mammals it ranges from 22–75 per spermatozoon (St. John et al., 2000). This reflects the high energetic demand of sustained motility and the long distances sperm must travel within the female reproductive tract.

The sperm tail is a highly organised flagellum responsible for propulsion. It consists of the midpiece, principal piece and end piece, all built around the axoneme, a conserved 9+2 microtubule structure (Luck, 1984). Dynein arms attached to the outer doublets hydrolyse ATP to generate sliding forces between microtubules, which are converted into bending waves by nexin links and radial spokes (Linck et al., 2016). The principal piece forms the majority of the flagellum and is surrounded by a fibrous sheath that provides rigidity and houses glycolytic enzymes. This arrangement allows ATP to be generated locally along the flagellum, complementing mitochondrial ATP from the midpiece (Turner, 2005). The terminal end piece contains only the axoneme without the surrounding dense fibres or fibrous sheath, allowing flexible propagation of flagellar waves necessary for navigating the viscous environment of the female reproductive tract

After ejaculation, spermatozoa must undergo capacitation, a biochemical and physiological maturation process happening within the female reproductive tract, to acquire the ability to fertilise the oocyte. In humans, capacitation occurs primarily in the cervical mucus and fallopian tube, where sperm are exposed to a controlled environment that promotes membrane remodelling and functional activation (Austin, 1952). The process involves cholesterol efflux from the sperm plasma membrane, increased membrane fluidity, and changes in ion permeability, particularly elevated intracellular calcium and bicarbonate, which stimulate cyclic adenosine monophosphate (AMP) production and activate protein kinase A–dependent phosphorylation cascades (Austin, 1952; Puga Molina et al., 2018). These molecular events drive the development of hyperactivated motility and prepare the sperm for the acrosome reaction, both of which are essential for zona pellucida penetration. In humans, capacitation is tightly regulated to prevent premature acrosome exocytosis and ensure that fertilisation competence is achieved only in the appropriate anatomical location. Disruption of capacitation, whether due to seminal plasma abnormalities, oxidative stress, or reproductive tract pathology, is increasingly recognised as a contributor to male subfertility (Aitken, 2020; Puga Molina et al., 2018).

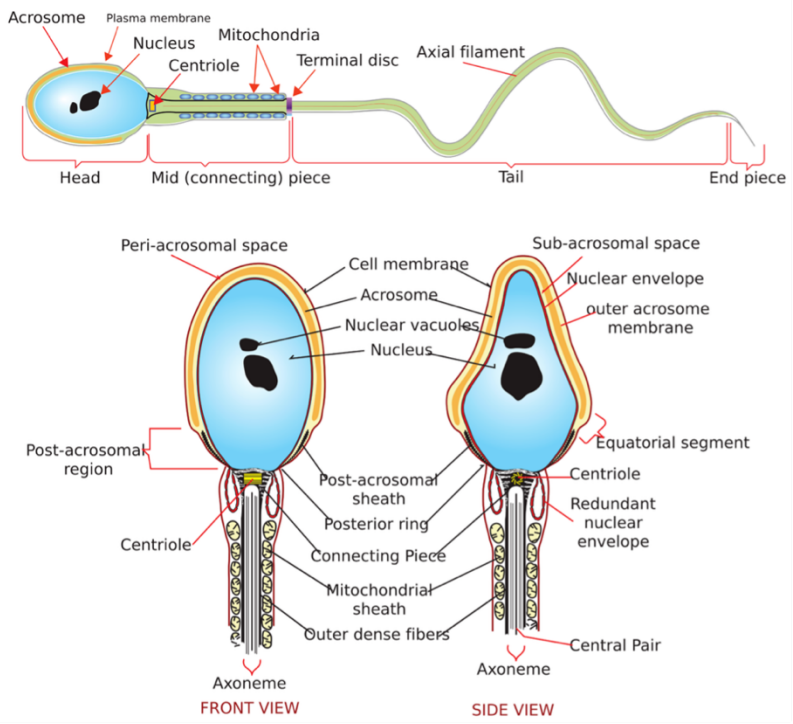

Figure 1.2. Complete Diagram of a Human Spermatozoon.

Image from LadyofHats, public domain, via Wikimedia Commons (LadyofHats, 2006).

1.3 Fertilisation and Preimplantation Embryo Development *In Vivo*

From ovulation through fertilisation, early development and implantation, the female reproductive tract provides a highly specialised and dynamic environment that supports the embryo in a stage-specific manner (Figure 1.3). Physical conditions such as pH, osmolarity, and ionic composition vary along the tract, forming physiological gradients rather than remaining static (Ng et al., 2017). These are complemented by a finely tuned microenvironment of nutrients, metabolites, cytokines, and growth factors secreted by the oviductal and uterine epithelium (Kane et al., 1997). Their synthesis is regulated with precise spatial and temporal control, driven predominantly by ovarian steroid hormones but also influenced by seminal plasma components and maternal systemic factors (Hardy & Spanos, 2002). Together, these cues orchestrate the viability, maturation, and developmental competence of the oocyte and early embryo, ensuring that each stage of pre-implantation development occurs in optimal conditions.

Understanding fertilisation and early embryo development *in vivo* relies heavily on insights gained from the mouse, which remains the principal model for studying mammalian development. Mouse embryos are readily available, inexpensive to maintain, and supported by robust *in vitro* culture systems and extensive transgenic resources, making them indispensable for dissecting the mechanisms governing cleavage, lineage specification, and pluripotency. By contrast, direct study of human embryos is limited by ethical constraints, restricted availability, and variability in the quality of *in vitro*–derived material, meaning that our knowledge of human development is comparatively fragmentary (Shahbazi & Zernicka-Goetz, 2018). As a result, most of what is known about cleavage dynamics, lineage specification, and the regulation of pluripotency derives from mouse embryos. Despite these limitations, both species share key developmental milestones: fertilisation produces a totipotent zygote, early cleavage generates morphologically similar blastomeres, and the first three lineages, trophectoderm (TE), epiblast (EPI), and primitive endoderm (PrE), are established by the late blastocyst stage (De Paepe et al., 2014). However, important species-specific differences exist. Human and mouse embryos differ in the timing of cleavage, the onset of zygotic genome activation, the dynamics of compaction, and the expression and localisation of lineage-specific transcription factors (Blakeley et al., 2015; Cauffman et al., 2009; Kimber et al., 2008) Even at fertilisation, subtle distinctions are evident: human sperm

oocyte interaction, zona pellucida composition, and signalling responses differ from those of the mouse, and *in vivo* blastocyst formation occurs on Day 4 in both species, despite the common misconception that human blastocysts form only on Day 5 *in vitro* (Hertig & Rock, 1973; Hertig et al., 1959). Together, these similarities and differences underscore the value of the mouse as a model while highlighting the need for caution when extrapolating findings to human embryogenesis.

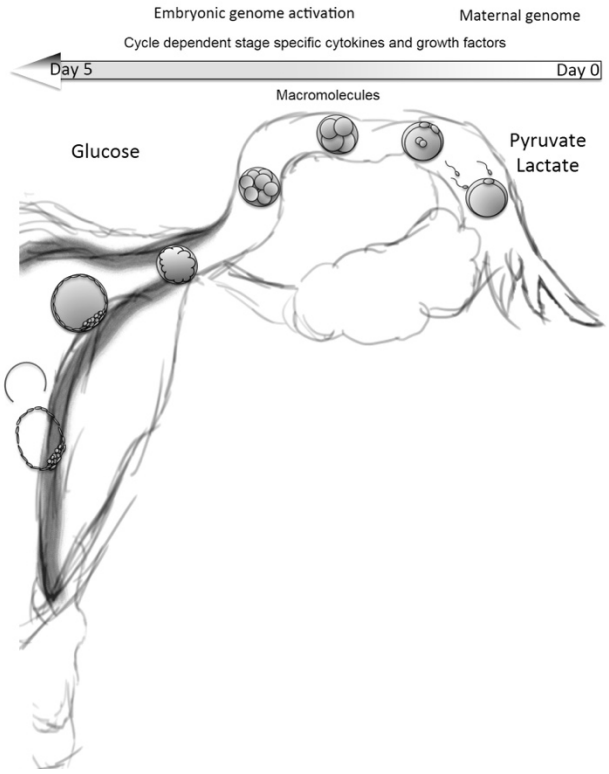

Figure 1.3 The female reproductive tract providing a cycle dependant, precise environment for the developing embryo, presenting specific metabolites, cytokines, growth factors and macromolecules in a gradient rather than static manner (illustration by Ellie Rawley, from (Sjoblom & Swearman, 2019).

1.3.1 Fertilisation

Fertilisation marks the union of a sperm cell with an oocyte, resulting in the formation of a zygote—the first stage of embryonic development (Tesarik, 1992). It involves a sequence of molecular interactions and cellular transformations that culminate in the fusion of the maternal and paternal genomes. Before fertilisation can occur, spermatozoa must undergo capacitation, a maturation process that renders them competent to penetrate the oocyte's

protective barriers. Capacitation involves biochemical and biophysical changes to the sperm plasma membrane, alterations in intracellular signalling pathways, and enhanced motility. These changes are triggered as sperm traverse the female reproductive tract, where they encounter specific ionic conditions, pH, temperature gradients, and reproductive tract proteins that promote membrane remodelling and functional activation (Breitbart & Grinshtein, 2023; Carrasquel Martínez et al., 2022).

Once capacitated, spermatozoa navigate towards the oocyte through a combination of thermotaxis and chemotaxis. Chemical cues released by the oocyte and surrounding cumulus cells guide sperm directionally towards the site of fertilisation. One such chemoattractant is stromal-derived factor-1 (SDF-1), which binds to the C-X-C chemokine receptor type 4 (CXCR4) receptor on spermatozoa, elevating intracellular calcium and supporting mitochondrial function essential for sustained motility (Zuccarello et al., 2011). Freshly ejaculated sperm are incapable of fertilisation until capacitation is complete, a process supported *in vivo* by the biochemical environment of the uterus and oviduct (Yanagimachi, 1994).

Fertilisation begins when spermatozoa reach the cumulus–oocyte complex. Progesterone secreted by cumulus cells activates the CatSper calcium channel on the sperm flagellum, triggering a rapid calcium influx that induces hyperactivation, a vigorous motility pattern required for penetration of the cumulus matrix (Squirrell et al., 2001; Strünker et al., 2011). The sperm then encounters the zona pellucida (ZP), a glycoprotein-rich extracellular matrix surrounding the oocyte. In humans, the ZP comprises four glycoproteins (ZP1–ZP4), with ZP3 and ZP4 acting as primary sperm receptors (Gupta, 2021). Binding to the ZP triggers the acrosome reaction, during which hydrolytic enzymes are released from the acrosomal vesicle to digest a path through the ZP. Enzymes such as hyaluronidases, serine proteases, and the 26S proteasome contribute to zona penetration (Kim et al., 2008; Rawe et al., 2008; Zimmerman & Sutovsky, 2009). Following acrosome exocytosis, the sperm binds secondarily to ZP2, enabling continued progression towards the oocyte plasma membrane.

Upon reaching the oolemma, the sperm binds and fuses with the egg plasma membrane. Although the molecular basis of gamete fusion is not fully elucidated, proposed mediators include integrins on the oocyte surface and the tetraspanin CD9, which is essential for

membrane fusion (Kaji et al., 2000). Fusion allows the sperm nucleus and associated structures to enter the oocyte cytoplasm (Noda et al., 2022). This event initiates egg activation, characterised by a series of intracellular calcium oscillations triggered by the sperm-specific phospholipase C zeta (PLCζ). PLCζ generates inositol 1,4,5-trisphosphate (IP3), which releases calcium from endoplasmic reticulum stores, driving completion of meiosis II, cortical granule exocytosis, and prevention of polyspermy (Nomikos et al., 2005; Saunders et al., 2002; Tomashov-Matar et al., 2008).

Following fusion, the paternal chromatin undergoes dramatic remodelling. The highly compacted protamine-bound DNA of the sperm nucleus is rapidly decondensed and replaced with maternal histones through the action of ooplasmic factors (McLay & Clarke, 2003; Noda et al., 2022). This remodelling is essential for paternal genome activation, failure results in embryonic arrest. Meanwhile, the sperm midpiece contributes the centrosome, which duplicates and forms the microtubule aster that guides pronuclear migration (Sathananthan et al., 1996). The male and female pronuclei then form, migrate towards one another, and undergo membrane breakdown as the parental chromosomes align on the first mitotic spindle, establishing the diploid zygote (Siu et al., 2021).

1.3.2 From Zygote to Blastocyst

The newly formed zygote rapidly initiates embryonic development. Cleavage divisions produce progressively smaller blastomeres without increasing overall embryo size, enabling compaction and subsequent blastocyst formation. During these early stages, global DNA demethylation occurs, with the paternal genome undergoing rapid active demethylation and the maternal genome demethylating more gradually during cleavage (Miller et al., 2010; Wu & Chu, 2008). These epigenetic transitions are essential for establishing totipotency and supporting normal pre-implantation development.

Pre-implantation embryo development spans the period from fertilisation to implantation and is characterised by three major events: the maternal–zygotic transition, blastomere polarisation at the 8-cell stage, and formation of the blastocyst. These stages involve dynamic morphological, physiological, and biochemical changes, with notable differences between mouse and human embryos. Comparative transcriptomic studies demonstrate that although

broad developmental milestones are conserved, species-specific differences exist in global gene expression and stage-specific regulatory pathways (Duranthon et al., 2008).

Following fertilisation, the mammalian zygote undergoes a series of mitotic cleavage divisions that increase cell number without increasing overall embryo size (Hillyear, 2022). Blastomeres progressively become smaller, and early embryos remain highly regulative, capable of tolerating the removal or addition of cells. By Day 2, embryos typically reach the 2- to 8-cell stage. Until this stage, in both mouse and human, the 1 cell embryo has been relying on maternal and paternal transcripts from the spermatozoon and oocyte. The activation of the embryos own genome when transcription shifts from maternally stored RNAs to the newly activated embryonic genome (Watson, 1992; Xue et al., 2013) occur in two stages. Minor embryonic genome activation (EGA) also referred to as minor zygote genome activation (ZGA) occur in the late S-phase of the one cell to the G1 phase of the two-cell embryo. (Hamatani et al., 2004; Xue et al., 2013). This is followed by the major EGA/major ZGA occurring in two-cell (mouse) or four-to-eight-cell (human) embryos (Asami & Perry, 2025; Braude et al., 1988; Hamatani et al., 2004; Xue et al., 2013). Blastomeres at this stage remain totipotent, as demonstrated by the ability of isolated mouse blastomeres to generate a complete organism (Tarkowski, 1959).

At the 8-cell stage, blastomeres undergo polarisation, establishing apical–basal domains and initiating the first cellular asymmetries. Compaction follows, during which blastomeres flatten and increase intercellular contact through adherens and tight junction formation (Ziomek & Johnson, 1980). Although maternal E-cadherin transcripts allow compaction to occur, embryos lacking zygotic E-cadherin fail to maintain adhesion at the blastocyst stage, highlighting the importance of embryonic gene expression for later development (Vestweber et al., 1987). In humans, compaction is more variable and may begin as early as the 4-cell stage or as late as the 16-cell stage (Cockburn & Rossant, 2010).

As cleavage continues, the embryo transitions to the morula stage (16–32 cells). The morula is characterised by tight cell-cell adhesion and a distinct outer layer of cells surrounding a central cavity. Within the morula, cells begin to differentiate, becoming increasingly specialised for specific roles in embryonic development (Sozen et al., 2014).

Two models describe how the first cell lineages, the TE and inner cell mass (ICM), are specified. The inside–outside model proposes that cell position determines fate, whereas the cell-polarity model proposes that polarity established at the 8-cell stage directs whether blastomeres divide symmetrically or asymmetrically, thereby generating inside and outside cell populations that seed the first lineage decisions (Handyside, 1981; Yamanaka et al., 2006). Around the 32-cell stage, the embryo forms a fluid-filled cavity, the blastocoel, through ion transport mediated by Na^+/K^+-ATPase in the TE and the establishment of tight junctions (Kidder & Watson, 2005). Blastocoel formation marks the transition to the blastocyst, comprising an outer TE layer that will form the placenta and an ICM that will generate the fetus. (Morris & Zernicka-Goetz, 2012; Piliszek et al., 2016).

Blastocyst hatching is a critical prerequisite for implantation in mammals, including humans, and failure of this process is a major cause of early embryonic loss and infertility. Before implantation can occur, the blastocyst must escape from the zona pellucida. As the blastocoel expands, aided by the influx of fluid to the cavity and trophectoderm cell mitosis, the mechanical pressure on the zona increases resulting in zona rupture (Ma et al., 2024). While the mechanical pressure is the major contributor to the process of hatching, it is further regulated by both cellular mechanisms, such as actin-based trophectodermal projections and a range of autocrine and paracrine cytokines and growth factors and proteases (Seshagiri et al., 2009).

Following hatching, the blastocyst is ready for implantation into the uterine lining. Implantation involves the attachment and invasion of the blastocyst into the endometrium, facilitated by specialised adhesion molecules and trophoblast cells within the trophectoderm.

1.3.3 Embryo Metabolism

As noted earlier, the female reproductive tract provides a precise milieu supporting the growth and development of the embryo as it transverses the tract (Fig.1.3). To meet the changing needs of the embryo, the tract is a gradient rather than static, with varying expression of cytokines, growth factors, macro molecules and metabolites. *In vivo*, mammalian embryos develop under hypoxic conditions, typically between 1% and 5%

oxygen—substantially lower than atmospheric levels. This environment promotes anaerobic metabolism and glycolysis, reducing reliance on mitochondrial oxygen consumption (Ng et al., 2017).

Lactate and pyruvate are the major substrates for the embryo pre compaction. Formation of lactate by the early embryo increases as the pyruvate concentration increases, while the pyruvate consumption depends on the lactate concentration (Lane & Gardner, 2000; Leese et al., 1993). High lactate concentrations increase viability of cleavage stage embryos, while the post compaction embryo is benefiting from a low concentration (Gardner & Sakkas, 1993).

During the earliest stages of development, glucose is used only minimally and can even be detrimental to embryos in culture, whereas pyruvate and lactate serve as the preferred energy substrates (Gardner & Leese, 1990). As the embryo approaches the morula stage, metabolic activity rises sharply and the ATP/adenosine diphosphate (ADP) ratio falls, reflecting increased energy demand associated with protein synthesis and ion transport for blastocoel formation. In the mouse and rat, pyruvate uptake declines markedly at this stage, while glucose consumption increases such that by the blastocyst stage it becomes the predominant exogenous energy source (Gardner & Harvey, 2015).

1.4 Intracytoplasmic Sperm Injection (ICSI) in Assisted Reproduction

ICSI is the most targeted laboratory method for achieving fertilisation in assisted reproduction and is now the predominant technique used to address male-factor infertility. Unlike conventional IVF, where sperm must undergo capacitation *in vitro* and penetrate the oocyte vestments within the fertilisation dish, ICSI bypasses these physiological requirements by delivering a single spermatozoon directly into the oocyte cytoplasm. Developed in the early 1990s, ICSI transformed clinical management of infertility by enabling fertilisation in cases where conventional IVF would otherwise fail, particularly in the presence of severely reduced sperm number, motility, or function (Palermo et al., 1992). By microinjecting an individual spermatozoon into the oocyte, ICSI overcomes barriers to natural gamete interaction and ensures that fertilisation can occur even when sperm quality is markedly compromised (Joris et al., 1998).

1.4.1 Clinical Applications and Indications for ICSI

ICSI has become an essential technique within assisted reproductive technology, particularly for the management of male-factor infertility. It is most commonly indicated in cases of oligozoospermia, asthenozoospermia, and teratozoospermia, where sperm number, motility, or morphology are insufficient to achieve fertilisation through conventional IVF. Prior to the development of ICSI, many of these men would have been considered functionally sterile, and the introduction of this technique has therefore transformed the clinical landscape by enabling fertilisation in situations where natural or *in vitro* sperm–oocyte interaction is unlikely to occur (O'Neill et al., 2018).

In addition to its central role in male-factor infertility, ICSI is also used in a range of other clinical scenarios. It is frequently employed following previous IVF cycles with low or failed fertilisation, where the underlying cause may be subtle defects in sperm–zona binding or oocyte activation (Mahutte & Arici, 2003). ICSI is also used in cases of unexplained infertility, where standard semen parameters appear normal, but fertilisation remains impaired. Furthermore, the technique is routinely combined with preimplantation genetic testing for PGT-A, as controlled fertilisation through ICSI reduces the risk of polyspermy and facilitates accurate chromosomal assessment of resulting embryos (Roque et al., 2019). Its use with surgically retrieved sperm, such as those obtained via percutaneous epididymal sperm aspiration (PESA) or testicular sperm aspiration (TESA) or extraction (TESE), has further expanded its clinical relevance, as these spermatozoa often exhibit limited motility and are unsuitable for conventional IVF (Gordon, 2002).

Through these applications, ICSI has become a versatile and widely adopted method within ART, offering a reliable means of achieving fertilisation across a broad spectrum of clinical indications.

1.4.2 Advantages of ICSI

ICSI offers several advantages over conventional IVF. Most notably, it circumvents the physiological barriers to fertilisation, ensuring that even sperm with markedly reduced

motility or abnormal morphology can successfully fertilise an oocyte. Because only a single viable spermatozoon is required, ICSI is particularly beneficial for men with extremely low sperm counts or those producing only a small number of motile sperm (Gordon, 2002).

There is great debate around the advantages of ICSI over conventional IVF in patients with normal or borderline sperm parameters (Berntsen et al., 2025). Advocates for ICSI argue that ICSI reduces the risk of fertilisation failure in couples with unexplained infertility or prior fertilisation failure using conventional IVF, however this has been proven wrong by numerous studies showing that ICSI does not result in higher fertilisation or live birth outcomes even in men with nonseverely decreased sperm quality (Berntsen et al., 2025; Wang et al., 2024).

1.4.3 Challenges, Limitations and Considerations

Despite its clinical advantages for couples with severe male infertility, ICSI presents several challenges. The procedure is technically demanding, requiring specialised equipment and highly trained embryologists, which increases treatment cost and may limit accessibility.

Concerns have also been raised regarding the long-term health of ICSI-conceived offspring. While most studies report no significant increase in congenital anomalies compared with naturally conceived children, some evidence suggests a slightly elevated risk of epigenetic alterations or chromosomal abnormalities (Ahmadi et al., 2023; Hoorsan et al., 2017). These risks may relate to the bypassing of natural sperm-selection mechanisms, potentially allowing sperm with compromised genomic integrity to contribute to the embryo. A recent study based on more than 850,000 children born from ART in New South Wales found a significant but small elevated risk of congenial malformation as a result of medically assisted fertility treatment. Importantly, they found that unnecessary laboratory manipulations, such as ICSI without clear medical indication, had a clear independent increased risk for congenital abnormalities in the offspring (Venetis et al., 2023).

Further, the microinjection procedure itself carries a risk of damaging intracellular structures, including the second metaphase spindle. Such disruption may lead to aneuploidy through non-disjunction during completion of meiosis II. Studies have shown that aneuploidy rates in embryos developing after ICSI are significantly higher compared to those from conventional

IVF (Swearman et al., 2018). It is suggested that this increase in aneuploidy could be the result of changes in pH during ICSI process, which in turn affects the meiotic spindle. Additionally, aspiration of cytoplasm to rupture the oolemma can cause cytoskeletal injury, particularly if excessive cytoplasmic volume is withdrawn. The unavoidable introduction of small amounts of culture medium or polyvinylpyrrolidone (PVP) during injection may also expose the oocyte to potentially harmful components (Dumoulin et al., 2001). Together, these observations highlight that although ICSI is highly effective, it is not biologically neutral and may influence early developmental events.

Ethical considerations also arise from the manipulation of human gametes and embryos (Delaunay et al., 2021). Ongoing debate surrounds the broader implications of creating embryos through direct micromanipulation, including potential long-term health effects and the psychosocial impact on individuals conceived through ICSI and other ART procedures (Hoorsan et al., 2017).

1.4.4 Laboratory Methodology of ICSI

For a couple undergoing an IVF cycle with ICSI, the first step is the retrieval of mature oocytes following controlled ovarian stimulation. Once collected, oocytes are denuded of their surrounding cumulus–corona complex, allowing accurate assessment of nuclear maturity and facilitating micromanipulation. In parallel, spermatozoa are prepared from ejaculated semen or, in cases of azoospermia, obtained surgically either by epididymal aspiration PESA or via testicular extraction techniques such as, TESA or TESE.

Microinjection is performed under an inverted microscope which is fitted with micromanipulators allowing for positioning and holding of the nude oocyte on one side, and selection, manipulation and aspiration of spermatozoa on the other.

A single motile spermatozoon is selected under high magnification, immobilised—typically by mechanically disrupting the tail—and aspirated into a fine injection pipette. During micromanipulation, the oocyte is stabilised with a holding pipette, and the injection pipette is advanced through the zona pellucida and oolemma to deposit the sperm directly into the

oocyte cytoplasm. This bypasses all extracellular barriers to fertilisation, including zona penetration and membrane fusion.

Following microinjection, oocytes are returned to culture in a controlled incubator environment. Fertilisation is assessed approximately 16–18 hours later, and normally fertilised zygotes are cultured to the blastocyst stage before transfer to the uterus or cryopreservation. This highly controlled sequence of laboratory steps ensures that fertilisation can occur even when sperm function is severely compromised. The methodology described is reflective of the practice at Westmead Fertility Centre, modified from previously published methodology (Joris et al., 1998; O'Neill et al., 2018)

1.5 Preimplantation Embryo Development *In Vitro*

A major factor limiting successful ART outcomes is the complexity around the manipulating and culturing of gametes and embryos *in vitro*. The *in vitro* environment stands in stark contrast to the *in vivo*, where from the time of ovulation through to fertilisation, development and implantation, the female reproductive tract provides an optimal environment supporting growth and development of the embryo in a time-stage specific manner (see section 1.3).

The culture of embryos *in vitro* is a sophisticated process that attempts to recapitulate the natural conditions of the female reproductive tract to reduce stress and improve embryos viability and offspring health. Technological advancements have resulted in the development of incubators with precise controlled culture conditions over temperature, gas composition, and humidity. Time-lapse imaging, a non-invasive monitoring technique, has transformed embryo selection protocols by providing continuous observation of embryos development while minimizing external disturbances and maintaining optimal culture conditions (Lundin & Park, 2020).

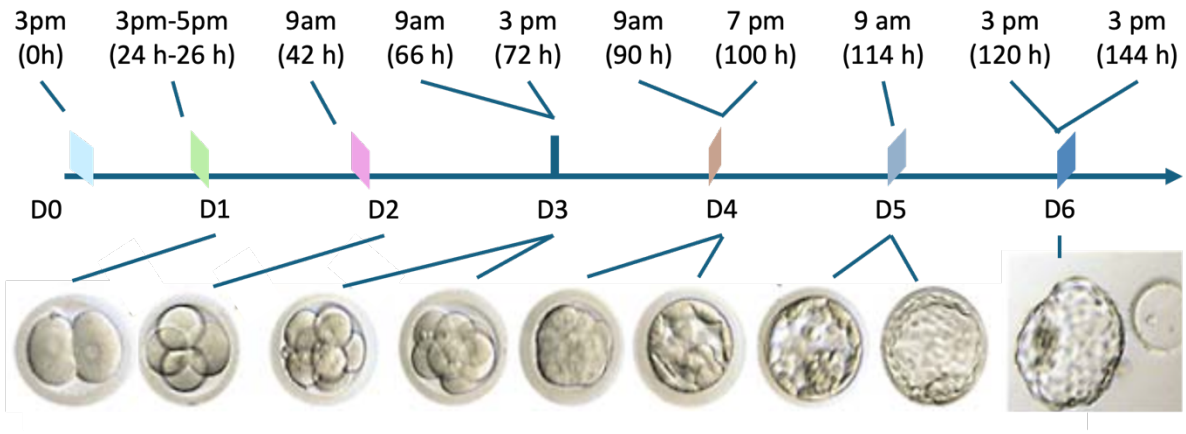

Figure 1.4. Timeline of in-vitro blastocyst development. Embryos reach the 2-cell stage at ~24–26 h post-insemination, the 4-cell stage by ~42 h (day 2), and the 8-cell stage by ~66 h (day 3), followed by compaction at ~72 h. Morula formation occurs around 90–100 h (day 4), with blastocyst formation on day 5 and hatching from ~120 h. Adapted from (Veeck & Zaninovic, 2003)

1.5.1 Culture Medium

Modern culture medium more closely approximates the *in vivo* reproductive tract, yet the static nature of *in vitro* culture introduces significant challenges. Culture medium therefore plays a pivotal role in supporting the changing metabolic requirements of the embryo at each developmental stage (Zmuidinaite et al., 2021). Extensive efforts have been made to mimic the oviductal and uterine environments, leading to the development of increasingly complex media formulations for ART (Johnson & Gardner, 2011). The transition from simple salt solutions to complex media containing amino acids, lipids, vitamins, and antioxidants has been instrumental in reducing cellular stress and improving embryo viability (Cappelaere et al., 2021).

Amino acids within the medium undergo spontaneous deamination, generating ammonium that accumulates alongside embryo-derived metabolic by-products (Gardner & Lane, 1993). Elevated ammonium disrupts embryo metabolism, intracellular pH regulation, gene expression, and imprinted methylation, ultimately impairing fetal growth (Lane & Gardner, 2003). To limit ammonium build-up, media are routinely replaced every 48 hours, and

unstable amino acids such as glutamine are substituted with more stable dipeptides like alanyl-glutamine (Biggers et al., 2004).

The shift towards extended culture to the blastocyst stage has further complicated optimisation of culture conditions. During this period, the embryo undergoes major physiological and metabolic transitions. Following compaction, it forms its first transporting epithelium and transitions from a cluster of relatively quiescent blastomeres to a structured blastocyst capable of regulating the microenvironment surrounding the inner cell mass (Gardner & Lane, 2005). This developmental progression is accompanied by a marked metabolic shift: pre-compaction embryos preferentially utilise pyruvate, whereas post-compaction embryos increasingly rely on glucose as their primary energy substrate (Gardner & Sakkas, 1993).

However, inappropriate media composition can have profound developmental consequences. In livestock species such as sheep and cattle, culture in serum-supplemented media is associated with large offspring syndrome (LOS), characterised by fetal overgrowth and abnormal organ development (Ceelen & Vermeiden, 2001; Thompson et al., 1995). These findings underscore the sensitivity of the pre-implantation embryo to its biochemical environment. Sequential media systems, designed to match the embryo's evolving metabolic needs from the zygote to the blastocyst stage, have significantly improved developmental outcomes and increased pregnancy rates following ART (Kleijkers et al., 2016; Zmuidinaite et al., 2021).

Despite continuous improvements, human embryo culture conditions remain suboptimal compared with the *in vivo* reproductive tract. As a result, embryo viability and developmental competence *in vitro* are believed to be compromised, contributing to the high rates of implantation failure observed in IVF. A major goal of current research is therefore to create culture systems that more closely replicate the dynamic biochemical and biophysical environment of the female reproductive tract, thereby supporting optimal development to the blastocyst stage.

Taking the gradient nature of the female reproductive tract into account, sequential media were developed on the principle that the embryo's metabolic requirements change markedly between the cleavage and blastocyst stages, necessitating stage-specific formulations that mimic the dynamic oviduct–uterine environment (Gardner & Lane, 1998). Cleavage stage medium is enriched in pyruvate and lactate to support pre-compaction embryos, whereas later formulations provide increased glucose, essential amino acids, and components required for blastocyst expansion. In contrast, single-step media are designed to contain all necessary substrates from fertilisation to blastocyst formation, allowing embryos to self-regulate nutrient uptake within a stable, uninterrupted environment (Biggers et al., 2005). Advocates of single-step systems argue that reduced handling and fewer media changes minimise stress and fluctuations in pH and temperature, while proponents of sequential media emphasise closer physiological alignment with *in vivo* metabolic transitions. Clinical outcomes appear broadly comparable, although subtle differences in embryo metabolism, gene expression, and blastocyst quality have been reported (Kleijkers et al., 2016; Zmuidinaite et al., 2021). Ultimately, both approaches can support high-quality blastocyst development, and the optimal choice may depend on laboratory workflow, culture system, and practitioner preference.

1.5.2 Culture Systems

Optimising embryo development *in vitro* requires far more than selecting an appropriate culture medium; it depends on rigorous control of the entire laboratory environment (Liperis & Sjöblom, 2017). Every physical and chemical parameter surrounding the embryo contributes to its developmental competence, and even minor deviations can have measurable consequences (Castillo et al., 2020). Incubators, where embryos spend the majority of their time, are central to this control. Continuous monitoring and maintenance are essential to ensure stable temperature, gas composition, and pH conditions that are critical for embryo viability (Moriyama et al., 2022). Small fluctuations in CO_2 concentration can significantly alter the bicarbonate buffering system, leading to shifts in culture-medium pH. Even subtle pH disturbances disrupt mitochondrial function and actin microfilament organisation, impairing cleavage and potentially resulting in abnormal development (Squirrell et al., 2001; Swain, 2010).

Temperature stability is equally important. All manipulation surfaces—including heated microscope stages, warming blocks, and laminar-flow hoods—must be precisely regulated. Brief exposure to suboptimal temperatures increases cellular stress, disrupts cytoskeletal organisation, and can arrest embryo development (Moriyama et al., 2022). Osmolarity is another critical parameter; deviations from physiological values impose osmotic stress, alter cell volume regulation, and compromise normal developmental progression.

Air quality within the embryology laboratory also plays a decisive role. Elevated concentrations of volatile organic compounds (VOCs), particulate matter, or other airborne contaminants negatively affect fertilisation, cleavage, and implantation rates (Khoudja et al., 2013). Modern laboratories therefore employ high-efficiency particulate air (HEPA) and activated-carbon filtration systems to maintain a clean, low-VOC environment

.

The overarching aim of *in vitro* culture is to support embryos capable of successful implantation and healthy development. However, factors such as oxygen tension, pH, temperature, media composition, and mechanical handling can influence epigenetic programming and alter developmental trajectories. For this reason, comprehensive quality-control systems are essential. These include routine calibration of equipment, environmental monitoring, validation of consumables, and strict adherence to standardised protocols. Together, these measures ensure consistency, minimise stress to the embryo, and improve clinical outcomes.

1.5.3 Time-Lapse Imaging During Embryo Culture

Time-lapse imaging allows continuous monitoring of embryonic development without removing embryos from the incubator environment. This approach provides detailed information on morphokinetic parameters, which have been shown to be reliable predictors of embryo quality (Meseguer et al., 2012). The application of time-lapse imaging in studying early embryogenesis began in the 1990s with early advancements in this field were demonstrated by Diana Payne and co-workers in Adelaide, Australia who used time-lapse techniques to record the initial phases of human fertilisation (Payne et al., 1997).

Advances in bioinformatics, culture media, and imaging technologies have collectively resulted in approximately a ten-fold improvement in the ability to maintain stable culture conditions while enabling more precise data analysis. When developing time-lapse monitoring systems, it is essential to account for the differing requirements of research-focused investigations and routine clinical practice. Research applications typically demand extended observation periods and advanced analytical software to generate large volumes of detailed data. In contrast, clinical settings are constrained by time limitations, making it necessary for the technologies used to be efficient, reliable, and straightforward to operate.

In time-lapse systems, the microscope is commonly integrated within a commercially available incubator (Pribenszky et al., 2017). One such system, the EmbryoScope, functions as a dedicated incubator that maintains the physiological conditions required for embryo viability throughout *in vitro* culture. A key advantage of the EmbryoScope is its high capacity, allowing simultaneous automated image capture of many individual embryos. Furthermore, the system incorporates image analysis software that presents embryo activity and cell division timing in in a clear and accessible format.

1.5.4 Embryo Morphokinetics

Morphokinetics refers to the use of time-lapse imaging systems to assess embryo development under *in vitro* conditions. Traditional morphological evaluation offers only static observations at specific time points, whereas morphokinetic analysis enables continuous monitoring of cell division dynamics. This allows for precise measurement of cleavage rates, the timing of developmental milestones, and simultaneous assessment of embryo morphology. Table 1.2 details the nomenclature of morphokinetic parameters agreed in good practice guidelines, outlining the parameters commonly used to describe post-fertilisation embryonic development (Coticchio et al., 2020).

Early morphokinetic events begin shortly after fertilisation with the formation of male and female pronuclei. Pronuclear appearance (tPNa) typically occurs between 6 and 8 hours post-insemination (hpi), while pronuclear fading (tPNf), which signals the onset of the first mitotic division, generally takes place between 18 and 22 hpi. The duration of the pronuclear stage is considered an early indicator of embryo competence, with specific time intervals being

associated with optimal developmental outcomes. The first cleavage division is particularly informative from a morphokinetic perspective. Initiation of the first cytokinesis (t2) usually occurs between 24 and 27 hours post-insemination, marking the division of the embryo into two blastomeres. Although these blastomeres remain adjacent for a short period following division, they subsequently undergo complete separation. Deviations in the timing of these processes especially unusually early or delayed first cleavage have been associated with diminished developmental potential and higher rates of aneuploidy (Del Carmen Nogales et al., 2017).

Subsequent cleavage events provide additional critical morphokinetic markers for embryo selection. The second cleavage to three cells (t3) generally occurs between 35 and 40 hpi, followed closely by the third cleavage to four cells (t4) between 37 and 42 hpi. The interval between t3 and t4 is considered particularly influential in embryo evaluation. Later cleavage stages, including progression to five (t5), six (t6), seven (t7), and eight cells (t8), also contribute valuable information regarding developmental progression during the early cleavage phase. A major transition occurs with compaction, during which individual blastomeres become indistinguishable as cell boundaries disappear and intercellular junctions are established. This process typically begins around day 3 or 4 of development (tComp) and is essential for establishing cell polarity and preparing the embryo for blastocyst formation. Both the timing and extent of compaction have been shown to correlate with subsequent developmental competence.

Blastocyst development introduces additional morphokinetic parameters of clinical significance. The onset of blastulation (tB), marked by the formation of the blastocoel cavity, usually occurs between 96- and 110-hours post-insemination. Further developmental milestones include the formation of an expanded blastocyst (tEB) and progression to a hatching blastocyst (tHB). The rate of blastocoel expansion and the timing of zona pellucida escape are strongly linked to implantation potential and pregnancy outcomes, making these parameters increasingly important in embryo transfer decision-making. Conversely, atypical morphokinetic patterns such as direct cleavage from one to three cells, multinucleation, unequal blastomere size, or developmental arrest are frequently associated with chromosomal abnormalities and reduced clinical success rates.

Table 1.2. Nomenclature of Morphokinetics Parameters

Parameter	Formula	Definition
Pntl		Time of pronuclei formation
NEBD		Nuclear envelopes break down
cytokiesis		First cytokinesis
t0		Time of insemination
tPB2		Time from insemination to appearance of second polar body
tPNa		Time from insemination to pronuclei appearance
tPNf		Time from insemination to pronuclei fading
t2 – t9		Time from insemination to corresponding divisions (two to nine)
tM		Time from insemination to compacting into the morula stage
tSB		Time from insemination to start of blastulation
tB		Time from insemination to blastocyst formation complete
tEB		Time from insemination to expanded blastocyst
tHB		Time from insemination to hatched blastocyst
ECC1	t2 – tPB2	The first-round cleavage
ECC2	t4 – t2	The second-round cleavage
ECC3	t8 – t4	The third-round cleavage
s1	t2 – t2	The first synchronization parameter, always equal to zero, parameter not used
s2	t4 – t3	The second synchronization parameter
s3	t8 – t5	The third synchronization parameter
t2_int	t3 – t2	The stage after first division, equal to c2
t4_int	t5 – t4	The stage after second division
t8_int	t9 – t8	The stage after third division

Adapted from (Coticchio et al., 2020)

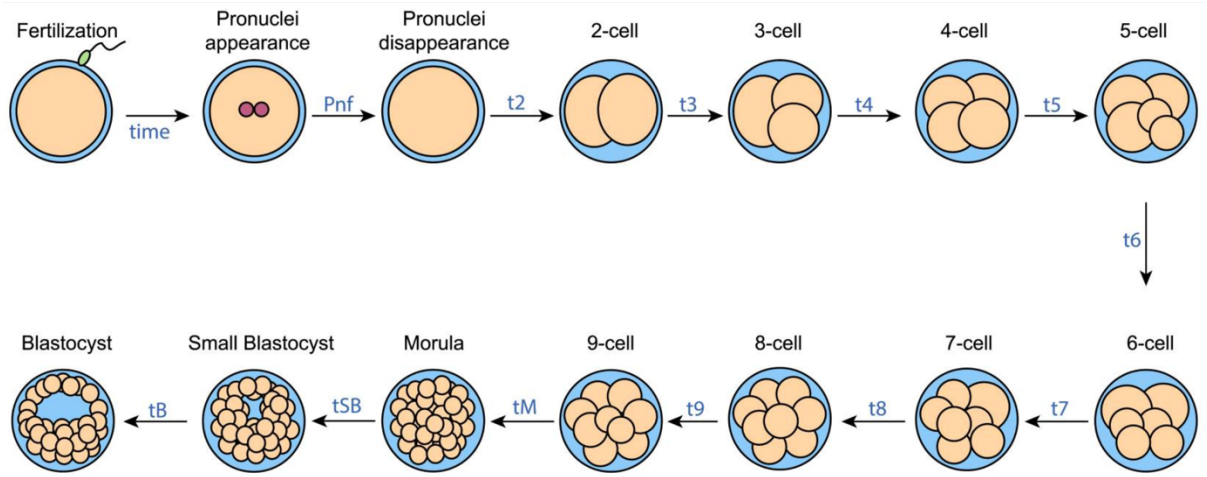

Figure 1.5. Embryo development following fertilisation and the corresponding morphokinetic parameters noted in Table 1.2. From (Yang et al., 2022).

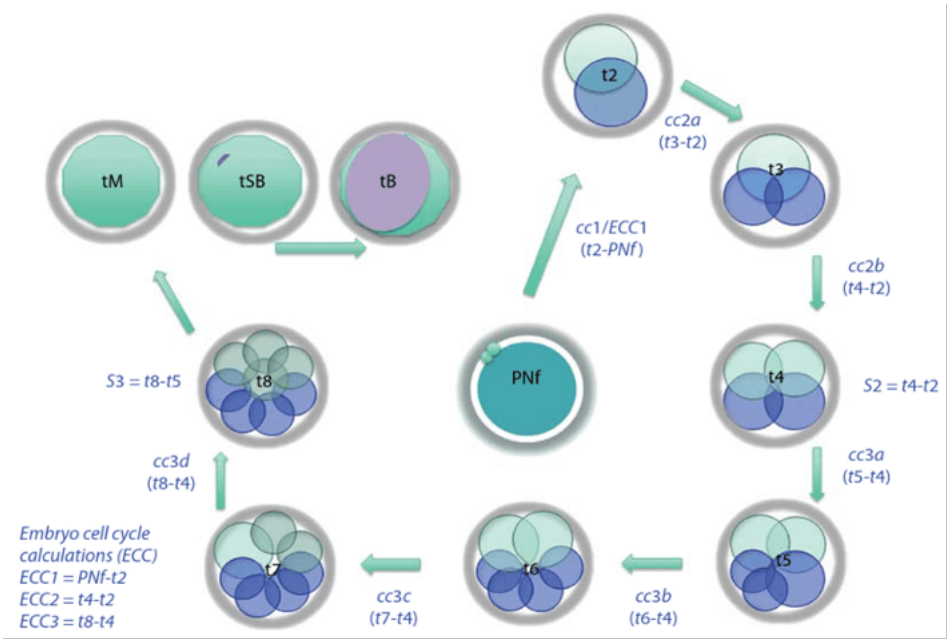

Figure 1.6. Schematic of blastomere cell-cycle durations (cc) and the corresponding embryo cell cycle (ECC) during the transition from the 2-cell to 4-cell stage (cc2a and cc2b) and the 4-cell to 8-cell stage (cc3a–cc3d). From (Campbell & Fishel, 2015)

1.6 Phosphodiesterase Inhibitors

Phosphodiesterases are enzymes that hydrolyse intracellular secondary messengers, such as cyclic AMP (cAMP), into AMP (Drobnis & Nangia, 2017). Non-specific phosphodiesterase (PDE) inhibitors including the methylxanthine compounds caffeine, pentoxifylline (PTX), and theophylline (THEO), act by inhibiting these enzymes, thereby allowing intracellular accumulation of cAMP (Sharpe et al., 2022). Elevated cAMP levels triggers a range of physiological effects, notably reduced erythrocyte deformability, decreased blood viscosity, and diminished platelet aggregation, all of which contribute to improved microcirculatory flow.

Pentoxifylline, is a synthetic compound characterised by its white, crystalline powder form, which is soluble in water and ethanol (Figure 1.7). Theophylline appears as a white, odourless crystalline powder that is sparingly soluble in water but readily soluble in alkaline solutions. It is naturally occurring in tea leaves, cocoa beans and coffee beans (IRAC et al., 1991).

Pentoxifylline and theophylline, through their methylxanthine-mediated inhibition of phosphodiesterases, not only elevate intracellular cAMP but also exert clinically relevant vasodilatory effects. This vasodilation arises from relaxation of vascular smooth muscle, improved microcirculatory flow, and reduced blood viscosity properties that have been exploited in the management of erectile dysfunction (ED). Oral administration of pentoxifylline in men with ED and/or male infertility has been shown to be a safe and effective option that can improve sperm quality (Dadgar et al., 2023; Lu et al., 2021). Pentoxifylline has also been used to improve endometrial thickness during ovarian stimulation for IVF, with the aim of enhancing embryo implantation, likely through increased uterine blood flow and associated improvements were found in oocyte maturity, embryo quality, and implantation rates (Vitale et al., 2022). However, the systemic therapeutic use of pentoxifylline and theophylline lies outside the scope of the present review. Here, the focus is specifically on their *in vitro* application as motility stimulants in ART, where their pharmacological actions on spermatozoa and their potential embryotoxicity are of primary relevance.

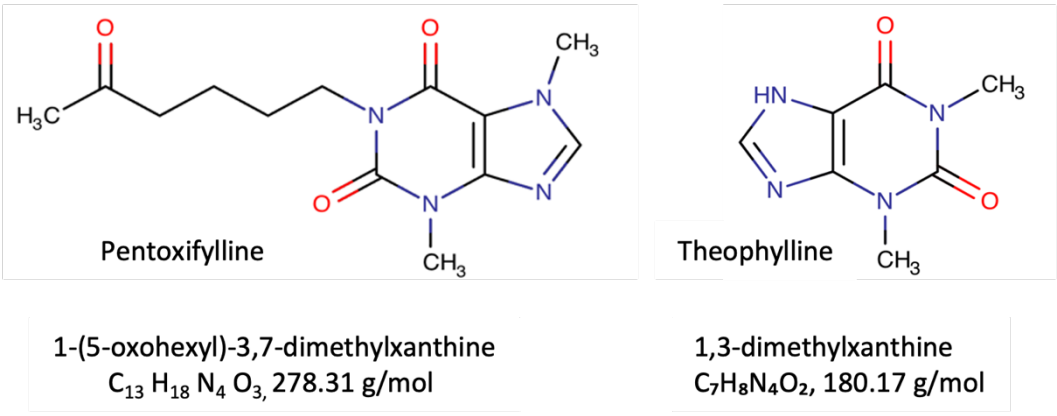

Figure 1.7. The Chemical Structure of Pentoxifylline and Theophylline. (IRAC et al., 1991).

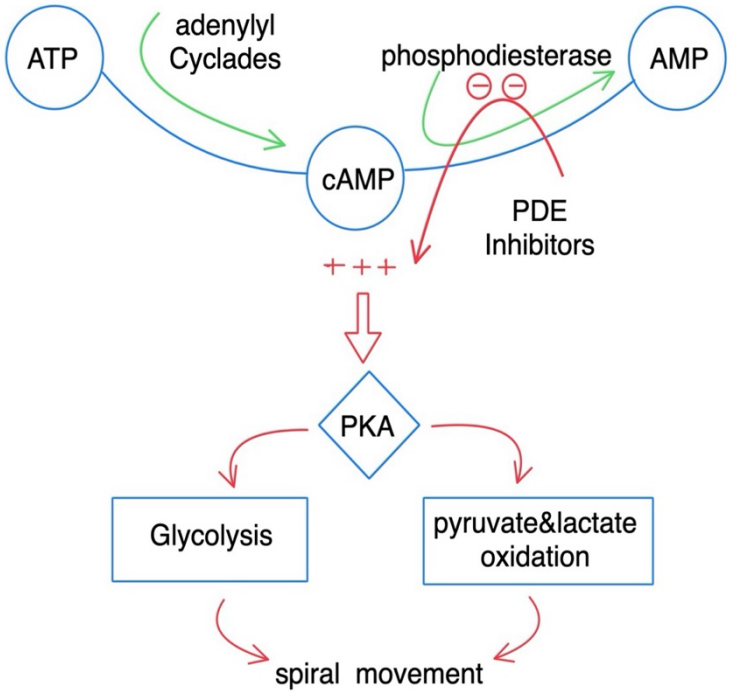

Figure 1.8. Schematic diagram indicating the PDE inhibitors mechanism of action to inhibit the phosphodiesterase enzyme which blocks the transformation of cAMP to AMP and preserve the cAMP concentration intracellular, and its role in activating PKA which in turn trigger glycolysis and pyruvate & lactate oxidation pathways leading to release more energy utilised by sperm cells towards activating the sperm spiral movement (Sharpe et al., 2022).

1.6.1 Phosphodiesterase Inhibitors as Sperm Motility Stimulants in ART

The role of cAMP in regulating sperm motility has long been established (Tash & Means, 1983). Spermatozoa generate adenosine triphosphate (ATP) and convert it to cAMP through the action of adenylyl cyclase. cAMP is subsequently hydrolysed by PDE enzymes to AMP (Azevedo et al., 2014). The addition of PDE inhibitors prevents the breakdown of cAMP to AMP, leading to an accumulation of intracellular cAMP. Elevated cAMP activates protein kinase A (PKA) signalling pathways, triggering downstream phosphorylation events that facilitate key metabolic processes, including glycolysis and the oxidation of pyruvate and lactate (Boswell-Smith et al., 2006). The stimulation of these metabolic pathways enhances flagellar activity, resulting in increased beat frequency and improved progressive motility (Figure 1.8) (Pereira et al., 2017; Sharpe et al., 2022).

PDE inhibitors, particularly pentoxifylline and theophylline, have become important adjuncts in ART due to their ability to stimulate motility in poorly motile or immotile spermatozoa (Ebner et al., 2014; Yovich et al., 1988) . In 1988, Yovich and colleagues in Western Australia reported the first clinical use of PTX during conventional IVF for severe male-factor infertility, achieving five pregnancies in a pronuclear-stage embryo transfer programme (Yovich et al., 1988). Their use is especially relevant in men with non-obstructive azoospermia (NOA), where TESA or TESE often yields only a small number of spermatozoa with minimal or absent motility (Ebner et al., 2011; Kovacic et al., 2006). Following initial processing of TESE/TESA samples, motility is often sparse, and fertilisation success in ICSI declines markedly when immotile spermatozoa are injected (Wu et al., 2005). Consequently, identifying viable sperm with restored motility is a critical step in the management of NOA. Similarly, in men with asthenozoospermia, a medical condition where decreased or no sperm motility is observed in ejaculated semen, the use of motility stimulants improve outcomes (Ebner et al., 2014). Moreover, studies using theophylline to improve motility in frozen thawed TESE samples demonstrated substantial improvements in motility and increased clinical pregnancy rates (Ebner et al., 2011). Table 1.3 summarises the clinical evidence on the use of phosphodiesterase inhibitors as motility stimulants, drawing together findings from multiple studies to illustrate their effectiveness and limitations within ART practice. Only studies with robust design and with medium to high participant numbers are included.

Table 1.3. Clinical Use of PTX and THEO in ICSI Cycles

Reference	Cycle Type	Findings
(Terriou et al., 2000)	ICSI fresh or frozen PESA / TESA 20 PTX vs 139 motile control	⇔ Fertilisation rates (45.2% vs 51.0% ns) ⇔ Embryo quality and cleavage stage at transfer ⇔ Pregnancy (30.0% per cycle vs 26.6% in controls, ns),
(Kovacic et al., 2006)	PTX-TESA/TESE ICSI 30 TESA/TESE ICSI (no PTX)	↑ Motility in 95.7% of the samples. ↑ Fertilization rate (66% vs. 50.9%; $p < 0.005$) ↑ Mean number of embryos per cycle (4.7 vs. 2.7 $p < 0.01$). ⇔ Clinical pregnancy rate per cycle (38.3% and 26.7, ns)
(Ebner et al., 2011)	65 Patients Sibling oocytes RCT THEO*-ICSI Frozen TESE ICSI-Frozen TESE	↑ Progressive motility. ↓ Time for selecting sperm ↑ Fertilization and blastulation rate (79.9% vs. 63.3% $p < 0.001$) ↑ Pregnancy rate. (53.9% vs. 23.8% $p < 0.05$)
(Mangoli et al., 2011)	25 PTX-TESA/TESE ICSI 25 TESA/TESE with HOS test	↑ Fertilization rate (62.0% vs. 41.1% $p < 0.05$) ↑ Clinical pregnancy rate (32% vs. 16% $p < 0.05$)
(Sandi-Monroy et al., 2019)	Ejaculated and TESE 113 THEO*-ICSI 702 ICSI (non-matched controls)	↓ Fertilisation (50.2 vs 59.3, $p<0.001$) ⇔ Clinical pregnancy rate(30.36 vs 31.91, ns) ⇔ Live birth ⇔ Birth outcomes including malformations and birthweight (ns)
(Dong et al., 2024)	240 PTX-TESA ICSI 101 TESA ICSI (no PTX) 5097 ICSI (ejaculated sperm) Matched PF-TESA ICSI and non-PF TESA ICSI, after propensity score matching (P>0.05)	⇔ Ectopic pregnancy, multiple gestation, miscarriage ⇔ Birth weight and low birth weight (P>0.05). ⇔ Multiple birth, preterm delivery and average of gestational age (P>0.05). ↑ Clinical pregnancy (54.17% vs 46.34%, $p<0.05$)) ↑ Implantation (40.10% vs 32.78%, $p<0.05$) ↑ Live birth 47.08% vs 38.41%,l $P<0.05$).

* indicates use of GM 501 SpemMobil; ⇔ no significant difference; ↑ significant increase; ↓ significant decrease

1.6.2 Potential Risks and Toxicity Associated with Phosphodiesterase Inhibitors

Since the introduction of PDE inhibitors and sperm motility stimulants into ART practice by Yovich et al. in 1988, its safety profile has remained a subject of debate, particularly regarding optimal dosing and the potential for adverse effects on gametes and early embryos. While pentoxifylline is well recognised for its ability to enhance sperm motility (Pereira et al., 2017), several studies have highlighted possible detrimental consequences for embryo development. Early work demonstrated that exposure to pentoxifylline and theophylline was associated with reduced embryo viability and impaired developmental progression (Fisher & Gunaga, 1975; Scott & Smith, 1995). A series of studies by Tournaye and colleagues (Tournaye et al., 1995; Tournaye et al., 1994a; Tournaye et al., 1994b) reported adverse effects of pentoxifylline on mouse embryos when oocytes or embryos were directly exposed to the compound.

As with many adjuvant treatments introduced into IVF, the widespread clinical use of pentoxifylline and theophylline has preceded robust confirmation of their safety in animal models. Early investigations examining the effects of PDE inhibitors on mouse oocytes and embryos reported negative outcomes; however, these studies were poorly designed by contemporary standards and do not meet the methodological requirements of modern mouse embryo assays (see Section 1.7.1). Consequently, a clear knowledge gap remains regarding the safety of motility stimulants in ART. This gap has been highlighted in reports noting a lack of consensus on the safety and efficacy of pentoxifylline, with authors emphasising the need for rigorous, large-scale studies to clarify its impact on embryo development, pregnancy outcomes, and any potential long-term risks to offspring (Navas et al., 2017).

1.7 The Mouse Embryo as a Model for Human Embryo Research

The mouse has been a central model in embryology since the nineteenth century, owing to its small size, resistance to infection, short gestation, and large litter size, all of which enable rapid, high-throughput experimentation. These practical advantages, combined with extensive genetic tools, have made the mouse indispensable for studying mammalian reproduction and early development.

The mouse remains the most widely used mammalian system for investigating pre-implantation development (Taft, 2008). As a spontaneous polyoestrous ovulator, it typically produces 8–12 oocytes per cycle, depending on strain. Ovulation occurs in a predictable four-day window, controlled by gonadotropins such as FSH and LH. As in humans, the LH surge triggers ovulation, after which 8 to 12 oocytes are typically released, depending on the strain of mouse. This hormonal regulation mirrors human reproductive biology, making mice an invaluable model for studying ovulatory mechanisms (Ménézo & Hérubel, 2002). Post-ovulation, the oocytes are transported to the infundibulum, the entry to the oviduct, by ciliary action, where fertilisation occurs in the ampulla, a process nearly identical to that in humans (Quinn & Horstman, 1998). This well-understood pathway of gamete transport and fertilisation in mice has provided critical insights into human reproductive health and has been instrumental in refining ART techniques.

Its high genomic homology with humans, approximately 99% of genes have identifiable human counterparts and broadly conserved imprinting patterns make it a powerful analogue for human development (Quinn & Horstman, 1998; Thompson et al., 2001). Importantly, the overall sequence of pre-implantation events is conserved between the two species, allowing mechanistic insights from mouse studies to inform human reproductive biology while avoiding the ethical constraints associated with human embryo research (see section 1.3). Although developmental timing differs between species, the morphological progression from zygote to blastocyst is broadly similar in mouse and human. In the mouse, EGA occurs at the 2-cell stage, whereas in humans it occurs between the 4- and 8-cell stages (Gardner & Lane, 2005). Fertilisation triggers extrusion of the second polar body within ~2 hours, pronuclear formation by 4–8 hours, and first cleavage at 18–22 hours (Howlett & Bolton, 1985).

Superovulation, achieved by sequential pregnant mare's serum gonadotrophin (PMSG) and human chorionic gonadotrophin (hCG) administration increases oocyte yield but may compromise oocyte quality (Fowler & Edwards, 1957). Because imprint establishment occurs during late oogenesis, accelerated maturation can disrupt methylation patterns, leading to imprinting errors (Lucifero et al., 2002; Young & Fairburn, 2000). Embryos from superovulated oocytes show approximately double the frequency of methylation abnormalities, particularly within the trophectoderm lineage (Fortier et al., 2008).

Mouse strains also vary in sensitivity to culture conditions (Fauque et al., 2010), and unlike laboratory mice, human ART patients often present with underlying infertility that may influence gamete and embryo competence (Gardner & Lane, 2005). For these reasons, the mouse is best viewed as a discovery platform rather than a direct surrogate for human development.

Considering all the above, the mouse model has proven indispensable in embryology research and the broader field of reproductive biology. Its physiological, metabolic, and genomic similarities to humans, combined with its practical advantages in the laboratory, make it an ideal model for studying reproductive functions and embryonic development. As a result, the mouse continues to play a pivotal role in advancing our understanding of human reproduction and improving ART, driving innovation and improving outcomes for individuals facing infertility.

1.7.1 Mouse Embryo Assay

The mouse model has also been crucial in the areas of quality control, quality assurance, and quality improvement within ART (Scott et al., 1993). Given the similarities in reproductive mechanisms between mice and humans, researchers often use mice to test new culture media, refine fertilisation techniques, and evaluate the safety and efficacy of various ART interventions. This not only ensures that the techniques developed are robust but also minimises the risk when translating these methods to human use. The Mouse Embryo Assay (MEA) is a long-established and highly sensitive bioassay used to evaluate the developmental safety of culture media, laboratory consumables, and micromanipulation procedures in ART. Its value lies in the remarkable sensitivity of the pre-implantation mouse embryo to subtle chemical, mechanical, and environmental perturbations, making it an indispensable tool for detecting embryotoxic contaminants that may not be identified through chemical analysis alone (Gardner & Lane, 2005; Thompson et al., 2001). MEA has therefore become a cornerstone of quality-control systems in IVF laboratories, ensuring that materials and procedures are capable of supporting normal embryo development before they are applied to human gametes.

Traditionally, MEA has been performed using one-cell or two-cell stage embryos, but increasing evidence indicates that assays beginning at the one-cell (2PN, zygote) stage are superior. One-cell embryos are more sensitive to environmental stressors because they have not yet undergone embryonic genome activation and rely entirely on maternally derived transcripts and proteins. This heightened vulnerability allows earlier detection of toxic effects that may be missed when the assay begins at the more robust two-cell stage (Davidson et al., 1988; Li et al., 2001). As a result, one-cell MEA is now considered the most stringent and informative version of the assay.

The choice of mouse strain also significantly influences assay sensitivity. Comparative studies using one-cell embryos from outbred (CF1), inbred (FVB), F1 hybrid (B6/CBA), and cryopreserved F2 hybrid (bcl/B6 × B6/bcl) lines have demonstrated that outbred CF1 embryos are the most sensitive to toxins, whereas inbred and hybrid strains show greater developmental resilience (Khan et al., 2013). The genetic diversity of outbred embryos appears to confer increased susceptibility to environmental insults, making them a more stringent biological indicator for detecting embryotoxicity. Consequently, outbred embryos provide an additional and valuable tool for effective quality-control testing, particularly when laboratories require high assay sensitivity to validate new media formulations or consumables.

MEA endpoints have also evolved over time. Early assays relied primarily on blastocyst formation rates, but this endpoint alone is now recognised as insufficiently sensitive. More refined measures such as hatching blastocyst rates, blastocyst total cell number, and ICM:TE allocation provide a more accurate assessment of subtle toxic effects (Fauque et al., 2010). The introduction of time-lapse imaging has further enhanced MEA sensitivity by enabling continuous monitoring of cleavage kinetics, compaction timing, blastocoel formation, and morphokinetic deviations. Time-lapse-based MEA has been shown to detect abnormalities that would not be apparent through static observation alone, offering a powerful refinement to laboratory quality-control systems (Morbeck, 2017). These developments reflect a broader shift in ART towards dynamic, physiology-based assessment of embryo health.

MEA has also been essential in evaluating the safety of laboratory plastics, oils, and culture systems. Early studies revealed that certain batches of mineral oil contained peroxides capable

of inhibiting blastocyst development, a discovery made possible only through MEA screening (Gardner & Lane, 1993). Similarly, the assay has been used to detect toxic residues in plasticware, pipettes, and micromanipulation tools, ensuring that manufacturing processes do not inadvertently compromise embryo viability. The assay's sensitivity to ammonium accumulation, pH instability, and oxidative stress has further driven improvements in media formulation, including the replacement of labile amino acids such as glutamine with more stable dipeptide forms (Biggers et al., 2004).

Despite species-specific differences in metabolism, imprinting, and developmental timing, MEA remains the most ethically acceptable and biologically relevant model for routine quality control in ART laboratories. Its predictive value is supported by decades of empirical evidence demonstrating that materials capable of supporting normal mouse development are overwhelmingly likely to be safe for human embryos. As human embryo culture increasingly extends to the blastocyst stage and relies on precise metabolic and epigenetic regulation, the role of MEA in safeguarding laboratory standards remains indispensable. While not a perfect analogue for human development, the mouse embryo provides a sensitive, practical, and scientifically validated system for detecting embryotoxicity, thereby contributing to the safety and reliability of modern IVF and ICSI procedures.

1.8 Thesis Hypothesis and Aims of the Thesis

In assisted reproductive technology (ART), phosphodiesterase inhibitors are widely used as motility stimulants, yet their direct effects on embryo development remain incompletely understood. This project aims to investigate both the potential benefits and risks of PDE inhibitors, with a particular focus on pentoxifylline (PTX) and theophylline (THEO), in the context of gamete manipulation and early embryo development.

PTX is commonly employed in ART to enhance sperm motility, particularly in cases of severe asthenozoospermia or when surgically retrieved spermatozoa exhibit limited movement. THEO is used in a similar manner, often as part of commercial preparations designed to transiently activate immotile but viable sperm. By inhibiting PDE activity and thereby increasing intracellular cAMP, these agents acutely stimulate flagellar motion and facilitate

fertilisation. However, concerns persist regarding potential toxic effects, including premature acrosome reactions, altered signalling pathways, and downstream consequences for embryo development. Balancing their clinical utility against these potential risks requires robust experimental and clinical evidence.

To address this, the experimental arm of the study will use the B6F1 mouse strain, known for its high sensitivity to culture conditions, as a model for human pre-implantation development. Zygotes harvested from superovulated mated females will be microinjected with defined concentrations and volumes of PTX or THEO using a technique that closely mimics intracytoplasmic sperm injection (ICSI). Injected zygotes will then be cultured *in vitro* under standardised conditions. Embryo development will be assessed through cleavage and blastocyst formation rates, alongside quantitative measures such as total cell number per blastocyst. These outcomes will be compared with multiple control groups (medium-injected and non-injected zygotes) to determine whether exposure to PTX or THEO alters developmental competence prior to implantation.

Additional analyses will employ time-lapse imaging to examine key morphokinetic events in injected zygotes, enabling detection of subtle abnormalities in cleavage dynamics and developmental milestones that would not be apparent through static observation alone.

Complementing the laboratory work, a retrospective cohort study of ICSI cycles in which PTX and/or THEO were used during sperm preparation will be undertaken. The primary outcome will be live birth, with secondary outcomes including fertilisation rate, blastocyst formation, embryo utilisation, and miscarriage rates. Together, the experimental mouse model and clinical cohort analysis will provide an integrated evaluation of the safety and functional impact of PTX and THEO in ART, informing evidence-based use of these agents in routine practice.

1.8.1 Hypothesis

Given the absence of robust functional mouse embryo assay data, and recognising that previous studies relied on simple in-culture exposure rather than microinjection, we hypothesised that a functional mouse embryo assay simulating ICSI, achieved through direct

microinjection of clinically relevant concentrations of PTX and THEO into zygotes, would provide a rigorous means of determining whether these agents compromise pre-implantation development and of confirming whether their clinical use as motility stimulants affects ART outcomes.

1.8.2 Objective and Aims

The objective of this research project is to increase our understanding of the effect of phosphodiesterase inhibitors PTX and THEO on gametes and embryos with the overarching aim to improve ART outcomes.

The specific aims were:

1. To examine the effect of phosphodiesterase inhibitors by injecting PTX and THEO into mouse zygotes and evaluating their ability to form good quality blastocysts following *in vitro* culture compared to control groups not injected with phosphodiesterase inhibitors.
   This work is detailed in Chapter 2.

2. To assess and compare the developmental competence of the cultured mouse blastocysts from experimental and control groups by quantifying total cell number following propidium iodine staining.
   This work is detailed in Chapter 2

3. To further evaluate the safety of PTX and THEO by analysing morphokinetic developmental patterns in embryos cultured following zygote injection of PTX and THEO experimental and control groups.
   This work is detailed in Chapter 3.

4. To retrospectively evaluate clinical outcomes in MAR treatment cycles where advanced sperm preparation techniques, including the use of PTX and THEO, were employed.
   This work is detailed in Chapter 4.

Chapter 2

Developmental Outcomes Following ICSI-Mimicking Microinjection of Phosphodiesterase Inhibitors in Mouse Zygotes

2.0 Introduction

The use of phosphodiesterase (PDE) inhibitors as motility stimulants is well established in assisted reproductive technology, yet their direct effects on early embryo development remain poorly defined. Much of the existing evidence has been generated from studies in which one-cell embryos were simply exposed to these agents in culture. Although such approaches have raised concerns about potential toxicity, they do not reflect the way these compounds are used clinically, nor do they provide a functional assessment of developmental competence. A critical gap therefore remains in determining whether clinically relevant concentrations of pentoxifylline (PTX) and theophylline (THEO) pose any risk to the embryo when introduced in a manner that mirrors real-world practice.

To address this gap, the present study employs a functional mouse embryo assay designed to simulate intracytoplasmic sperm injection (ICSI), in which defined volumes of PTX or THEO are microinjected directly into zygotes. A carefully structured control system underpins this approach. First, zygotes injected with polyvinylpyrrolidone (PVP) serve as a clinically relevant comparator, as viscous PVP is routinely used during ICSI to slow sperm movement, facilitate morphological assessment, enable controlled tail softening, and stabilise the injection pipette. Second, a medium-only injection control isolates the effect of the injection procedure itself, independent of PVP or PDE inhibitors. Finally, a non-injected negative control provides a baseline for normal development. Together, these controls allow us to distinguish effects arising from the injection process from those attributable specifically to PTX or THEO.

By assessing cleavage progression, blastocyst formation, and quantitative measures of cell composition, this chapter aims to determine whether PDE inhibitor exposure compromises pre-implantation development in a sensitive and physiologically relevant model. Through this functional assessment, we seek to generate robust evidence regarding the safety of PTX and

THEO at the point of gamete manipulation, thereby informing their continued use as motility stimulants in ART.

2.1 Aims

Taken together, this experimental design, including the structured control system and the ICSI-mimicking microinjection approach, provides a rigorous framework for determining whether transient exposure to PTX and THEO affects early developmental competence in the mouse model, and it is within this context that the following aims were established.

1. To examine the effect of phosphodiesterase inhibitors by injecting PTX and THEO into mouse zygotes and evaluating their ability to form good quality blastocysts following *in vitro* culture compared to control groups not injected with phosphodiesterase inhibitors.

2. To assess and compare the developmental competence of the cultured mouse blastocysts from experimental and control groups by quantifying total cell number following propidium iodine staining.

2.2 Materials & Methods

2.2.1 Experimental Design

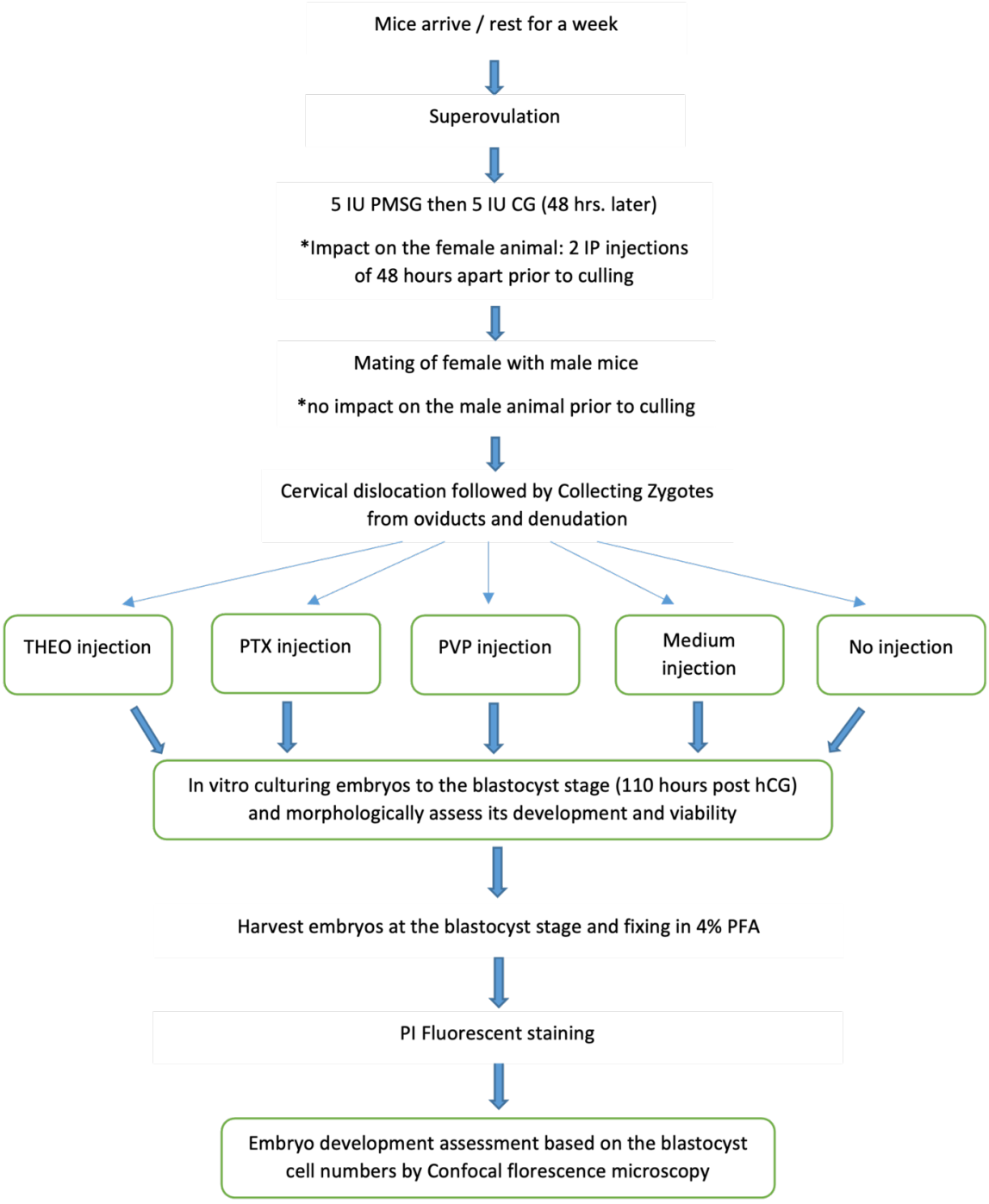

Figure 2.1. Overview of the experimental workflow for the functional mouse embryo assay. Schematic outlining the sequence from superovulation and mating to zygote collection, microinjection treatments, in-vitro culture, and blastocyst assessment.

2.2.2 Ethics

Ethical approval for animal research was obtained from the Western Sydney Local Health District (WSLHD) Animal Ethics Committee (AEC), Project Number 4358.12.21, titled “Effect of phosphodiesterase inhibitors injection on the development and viability of mouse Embryos”. The research was conducted in compliance with applicable legislation and code for care ("Animal Research Act 1985," 1985; "Australian Code for the Care and Use of Animals for Scientific Purposes," 2013) and the conditions of AEC approval.

2.2.3 Laboratory Quality Control

Process validation is important to assure the consistency and validity of processes and experiments in both clinical and research laboratories. To minimise variations all key environmental parameters were monitored daily with respect to incubator CO_2 concentration and temperature, room temperature, temperature of the refrigerator where culture media are stored, temperature of devices and microscope heated stages. All heating devices were adjusted to ensure a culture medium temperature of 37°C ± 0.2°C, verified using a Testo 950 temperature instrument coupled with a 905-T2 probe (Testo, West Chester, PA, USA). Incubator CO_2 concentration and temperature was logged and recorded daily using an InControl 1050 (Labotect Labor-Technik-Göttingen GmbH, Göttingen, Germany).

The pH of all series of culture media used was tested at the start of each experiment using a blood gas analyser (Epoc, Siemens Healthineers, Ottawa, Ontario, Canada).

2.2.4 Culture Media and Laboratory Reagents

Embryos were handled and cultured in media supplied by Vitrolife AB (Västra Frölunda, Sweden). Although the exact formulations of these stage-specific media are proprietary, they are derived from the Growth Medium Series (Barnes et al., 1995; Gardner, 1994). The medium used for cleavage-stage embryos contains amino acids, lactate, pyruvate, and a low concentration of glucose. In contrast, the post-compaction culture medium is enriched with both essential and non-essential amino acids and contains higher levels of glucose. All media which is supplemented with 5 mg/ml Human Serum Albumin (HSA) at the time of manufacturing is indicated by the ‘Plus’ suffix.

Media used for culture (G-1™ Plus, and G-2™ Plus) are carbonate-buffered and require an atmosphere of 6% CO_2 to maintain physiological pH. Media intended for handling and cryopreservation are buffered with MOPS (3-N-morpholino-propanesulphonic acid).

Across all experiments, G-MOPS™ supplemented with 5% HSA in-house was used as the collection and handling medium (HSA-solution™, Vitrolife AB). This medium is denoted throughout as G-MOPS™+HSA. Cleavage-stage pre-implantation mouse embryos were cultured in G-1™ Plus until reaching the 6–8-cell stage on day 3 of development. From this stage onwards, embryos were transferred to the blastocyst culture medium G-2™ Plus and maintained until the blastocyst stage 117 hours post zygote injection. Culture was performed in drops of medium over-layered with Ovoil™ mineral oil. All culture dishes were pre-equilibrated for a minimum of 2 hours to ensure appropriate pH and temperature conditions (at 37.0 °C in 6% CO_2, 7% O_2 and 87% N_2). Further details of the culture medium are provided in Appendix 2.1.

The experiments involved two phosphodiesterase (PDE) inhibitors: THEO and PTX. GM501 SpermMobil (Gynemed GmbH Co. KG, Sierksdorf, Germany) is the only THEO containing product approved by the Therapeutic Goods Administration for human use in Australia (TGA; ARTG ID 390549). It consists of a N-2-hydroxyethylpiperazine-N'-2-ethanesulfonic acid (HEPES)-buffered, HSA-free medium with a low bicarbonate concentration and is intended to enhance sperm motility, particularly in necrozoospermic ejaculates and immotile spermatozoa retrieved from testicular tissue. For the present experiments, SpermMobil was diluted 1:20 in G-MOPS™+HSA in accordance with the manufacturer's instructions (denoted THEO throughout experiments). The exact concentration of THEO in the formulation is withheld by the manufacturer for commercial reasons; however, functional concentrations of PDE inhibitors reported in the literature typically fall within the 1–5 mM range (Ebner et al., 2011; Loughlin & Agarwal, 1992; Yoshioka et al., 2003).

PTX was used in the form of Trentoximal (Alex Co. for Pharmaceutical Industries, Alexandria, Egypt) and diluted to a final concentration of 5 mM in G-MOPS™+HSA (denoted PTX in all experiments).

All laboratory chemicals and reagents used across experiments were purchased from Sigma-Aldrich / Merck (Bayswater, VIC, Australia) unless otherwise specified.

2.2.5 Animals

Female and male outbred Swiss mice (SwissTacAusb; Australian BioResources Ltd, Moss Vale, NSW, Australia) were used for initial zygote injection method development, optimisation and validation.

Female and male inbred C57BL/6J × DBA/2J (B6D2F1) mice were used for all embryo experiments and were purchased from Ozgene (Perth, WA, Australia).

All mice were maintained at the Westmead Bioresources Facility (WBF), Westmead precinct, NSW, Australia, and housed in individually ventilated cages on a 12-hour light–dark cycle with food and water available *ad libitum*. Male mice were housed individually, whereas female mice were housed in groups of three to four. On arrival at WBF, mice were allowed one week rest before any experimental intervention.

2.2.6 Ovulation Induction

To induce superovulation, 3–4-week-old pre-pubertal female mice received an intraperitoneal (i.p.) injection at midday of 5 IU (0.1 ml) pregnant mare's serum gonadotrophin (PMSG; Folligon, MSD Animal Health, Bendigo, VIC, Australia). After 48 hours, they were given a second i.p. injection of 5 IU human chorionic gonadotrophin (hCG; Chorulon, MSD Animal Health, Bendigo, VIC, Australia) and then placed singly or in pairs in a cage with an 8–10-week-old male and left over night. Mating was confirmed the following morning by the presence of a vaginal copulation plug (designated Day 1 after fertilisation).

2.2.7 Zygote Collection

All dissections, zygote retrievals, and embryo handling performed outside the incubator were conducted under strictly controlled temperature conditions at 37 °C on a heated microscope stage (LEC Instruments, Wantirna, VIC, Australia), ensuring optimal preservation of embryo viability and preventing thermal stress that could compromise developmental potential (Yeung et al., 2004).

Superovulated female mice were humanely sacrificed by cervical dislocation 21 hours after hCG administration (Day 1 after fertilisation), following standard institutional guidelines for animal welfare. Immediately following euthanasia, the mice were prepared for dissection. The skin surface was disinfected with 70% ethanol to minimise the risk of contamination. A horizontal incision was made across the abdominal wall using surgical scissors, providing access to the internal organs. The skin was retracted to expose the underlying musculature and peritoneum, which were subsequently incised to reveal the visceral cavity. To prevent damage to the reproductive structures, the gastrointestinal tract was gently displaced, exposing the reproductive tract, including the ovaries, oviducts, and bicornuate uterus.

The reproductive tract was carefully dissected free from the mesometrium—the connective tissue supporting the uterus—using fine forceps (Figure 2.2). Particular care was taken to preserve the integrity of the oviduct, which contains the developing zygotes. The oviduct was then severed at two points: proximally at its junction with the ovary, and distally where it enters the uterus (details see Appendix 2.2).

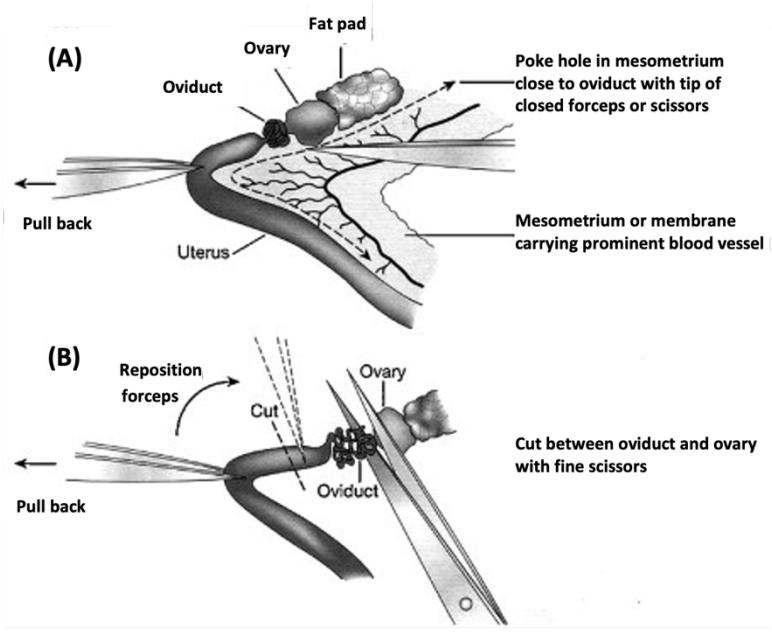

Figure 2.2. Dissection of the oviduct. (A) The ovary, oviduct, and uterine horn are separated from the mesometrium using the closed tips of fine forceps. (B) A cut is made between the oviduct and the ovary, and after repositioning the forceps, a second cut separates the oviduct from the uterus. Adapted from *Manipulating the Mouse Embryo: A Laboratory Manual*. (Nagy et al., 2003).

Oviducts were dissected under a stereomicroscope (SMZ-2B; Nikon, Tokyo, Japan) on an LEC heated stage in 1 ml G-MOPS™+HSA handling medium in a 60 mm Falcon organ centre well dish (Falcon, Corning Life Sciences, Tewksbury MA, USA; Cat. No. 353037). Pronucleate oocytes at the 1-cell stage (zygotes) are typically located within the swollen infundibulum, the funnel-shaped region at the proximal end of the oviduct. The infundibulum was carefully opened using fine forceps, and the embryos were gently flushed from the oviduct into the medium. They were then transferred using a glass handling pipette with an inner diameter of 190–210 µm (Vitrolife AB; Product ref. 15530) into a fresh, pre-equilibrated centre well dish (Vitrolife AB; Product ref. 16005) containing 1 ml of G-MOPS™+HSA medium in preparation for denudation.

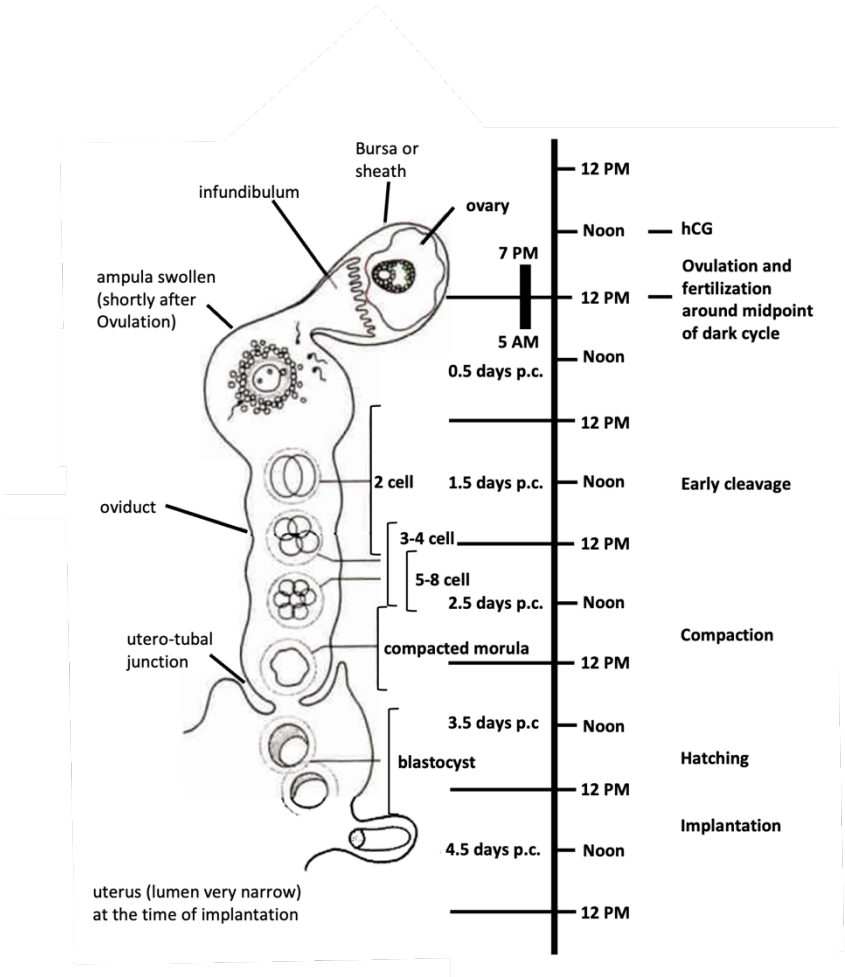

Figure 2.3. *In vivo* mouse reproductive tract showing the swollen ampulla, where fertilised eggs are located shortly after ovulation and remain until blastocyst formation. Adapted from Manipulating the *Mouse Embryo: A Laboratory Manual* (Behringer et al., 2014)

Initial denudation to remove the majority of cumulus cells surrounding the collected zygotes was carried out in a pre-equilibrated centre-well dish containing 80 IU hyaluronidase (0.1 ml HYASE-10X™ (Vitrolife AB) diluted in 1 ml G-MOPS™+HSA), using a glass handling pipette with an inner diameter of 156–190 µm (Vitrolife AB; Product ref. 15535). The zygotes were then transferred to a 60 mm Falcon culture dish (Cat. No. 353002) containing 100 µl drops of G-MOPS™+HSA overlaid with 8 ml Ovoil™ for further fine denudation. This step was performed using a narrower glass handling pipette with an inner diameter of 130–133 µm (Vitrolife AB; Product ref. 15532) to ensure complete removal of all remaining cumulus cells.

The denuded zygotes were examined for the presence of pronuclei. Pronucleate zygotes were then randomly allocated into 20 µl drops of G-1™ Plus, overlaid with Ovoil™, in a 60 mm holding dish and maintained in an incubator set to 6% CO_2 and 7% O_2 prior to microinjection.

2.2.8 Zygote Injection

To replicate the clinical process—in which spermatozoa are exposed to PDE inhibitors to enhance motility prior to the selection and injection of a motile sperm into an oocyte—the PDE inhibitors THEO and PTX were injected directly into zygotes using a controlled experimental design. All micro manipulation was done using a Nikon Ti eclipse inverted microscope fitted with Narishige MTK-1 Takanome Micromanipulators (Narishige Group, Tokyo Japan) and a heated stage (Thermo Plate, Tokai Hit, Shizuoka-ken, Japan). Holding and injection pipettes (Vitrolife AB; Product Ref. 15305 and 15430) were attached and precisely aligned (details see Appendix 2.3).

A consistent injection volume was maintained across all experiments by aspirating a microbead into the injection pipette to act as a displacement marker. The volume aspirated and subsequently delivered into each zygote was quantified by measuring the movement of the microbead using an eyepiece micrometer. The displacement distance corresponded to approximately 50–55 µm, comparable to the length of a spermatozoon. The injected volume was calculated by treating the fluid column within the pipette as a cylinder, using the measured column height (50–55 µm) and the injection pipette inner diameter of 5 µm (radius 2.5 µm). This yielded injection volumes of approximately 981.7–1080.0 μm^3, equivalent to 0.98–1.08 pl (picolitres).

An injection dish (ICSI Dish, Vitrolife AB; Product Ref. 16006) was prepared containing several 10 μl drops of G-MOPS™+HSA, overlaid with 6 ml Ovoil™, to contain zygotes and microbeads during injection. Further the dish contained 10 μl four experimental drops of i) 5mM THEO in G-MOPS™+HSA, ii) 5mM PTX in G-MOPS™+HSA, iii) PVP (ICSI™, Vitrolife AB) and iv) G-MOPS™+HSA only (Fig.2.4). The dish was pre-incubated in a warming incubator without gas, at 37 °C for one hour before use.

Table 2.1. Experimental Group Identifiers, Treatment Descriptions, and Rationale

Experimental Identifier	Treatment Description and Rationale
iTHEO	Zygotes injected with 5mM THEO in G-MOPS™+HSA to test the effect of PDE inhibitors in line with the aim of the project
iPTX	Zygotes injected with 5mM PTX in G-MOPS™+HSA to test the effect of PDE inhibitors in line with the aim of the project
iPVP	Zygotes injected with PVP (ICSI™, Vitrolife AB) to mimic the standard conditions during clinical application of ICSI
iCON	Zygotes injected with G-MOPS™+HSA only to serve as an injected control
CON	No Injection to serve as a negative control

The table outlines the identifiers assigned to each experimental group, together with a brief description of the injected solution (where applicable) and the rationale for its inclusion in the study. The “i” prefix denotes groups that underwent microinjection, while “CON” represents the non-injected control.

Zygotes were randomised into five groups: the four experimental groups and one control group that was not exposed to injection as described in Table 2.1.

Randomisation was performed using a computer-generated sequence. Embryos were assigned a random number using the RAND() function in Microsoft Excel, and the list was sorted in ascending order. Allocation proceeded sequentially according to the predefined prioritisation strategy, with embryos first assigned to the priority groups (iTHEO, iPTX and iCON) followed by random allocation to groups iPVP and CON. This method ensured unbiased allocation while achieving the required sample sizes for the primary comparison groups.

After pre-equilibration of the injection dish (Figure 2.4), the zygotes were transferred from the holding dish into the injection dish's G-MOPS™+HSA drops using a 156-190 µm glass handling pipette.

For microinjection, the injection dish was placed on the micromanipulation stage, and the injection needle was introduced into the dish and allowed to stabilise. The needle was then positioned in a microbead-containing drop, from which a single bead was aspirated to serve as a visual marker. The pipette was subsequently moved to one of the experimental drops, where a defined volume of solution was aspirated, with the aspirated volume determined by the displacement of the microbead.

Each zygote was positioned using the holding pipette, ensuring the polar body was oriented at either the 12 or 6 o'clock position. The injection pipette was lowered into the medium and advanced to penetrate the zona pellucida and cytoplasm. Following penetration, a precise volume of the pipette experimental contents (THEO, PTX, PVP or G-MOPS™+HSA) was expelled, again quantified by microbead displacement, after which the injection pipette was withdrawn. This procedure was repeated for all remaining zygotes, ensuring that each received an equivalent injection volume across all experimental conditions. To prevent cross-contamination between experimental solutions, the injection pipette was emptied and flushed with G-MOPS™+HSA medium between treatments, then reloaded with oil and a new microbead before aspirating the next experimental solution.

After injection, each group of zygotes was transferred together into a fresh 40 mm culture dish (Culture Dish 40 mm; Vitrolife AB) in 20 µl drops of G-1™ Plus, overlaid with Ovoil™.

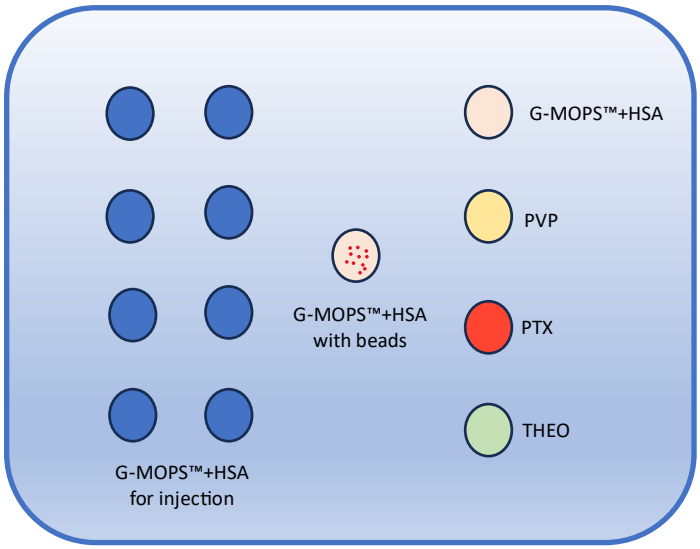

Figure 2.4. Illustration of the injection-dish Setup. The drops on the left are used for placing zygotes prior to injection, while the drops on the right contain the different injection solutions used in the experiment. The central drop is a G-MOPS™ + HSA drop containing the microbeads used to calibrate the injected volume for all solutions. All drops were clearly labelled to prevent cross-contamination.

2.2.9 Embryo Culture

Injected zygotes and subsequent embryos were cultured in 40 mm culture dishes in groups of five to six, in 20 µl drops of G-1™ Plus overlaid with 5.0 ml Ovoil™ for 48 hours. On Day 3 of development, at the 6–8-cell stage, embryos were transferred into 20 µl drops of G-2™ Plus and cultured until 96 hours post zygote injection at the blastocyst stage. All culture dishes were prepared on the morning of use and equilibrated for at least 2 hours prior to embryo allocation. Culture was carried out at 37.0 °C in an atmosphere of 6% CO_2, 7% O_2 and 87% N_2 (K-MINC-1000, Cook IVF, QLD, Australia).

2.2.10 Embryo Morphology

Embryo morphology and development were assessed using a Nikon Ti Eclipse inverted microscope at 48, 72, 96 and 114 hours post hCG injection (24, 48 and 96 hours post zygote injection, see timeline Fig.2.6). Normally fertilised oocytes were identified by the presence of

two pronuclei (2PN) or by extrusion of the second polar body at the time of zygote collection (Figure 2.5.A). At 48 post hCG, cleavage-stage embryos were assessed by recording the number of blastomeres (Figure 2.5.B), and at 72 hours the cell number or degree of compaction was noted (Figure 2.5.C). At 114 hours post hCG, successful blastocyst formation was recorded (Figure 2.5.D), and blastocysts were graded using the Gardner and Schoolcraft scoring system (Gardner & Schoolcraft, 1999). Briefly, blastocysts were assessed for the degree of expansion, with early blastocysts assigned a score of 1 or 2. Blastocysts with a clearly defined cavity were graded as 3 or 4, those initiating hatching were graded as 5, and fully hatched blastocysts were graded as 6. The quality of the inner cell mass (ICM) and trophectoderm (TE) was graded as A, B or C, with A representing the highest quality and C the lowest.

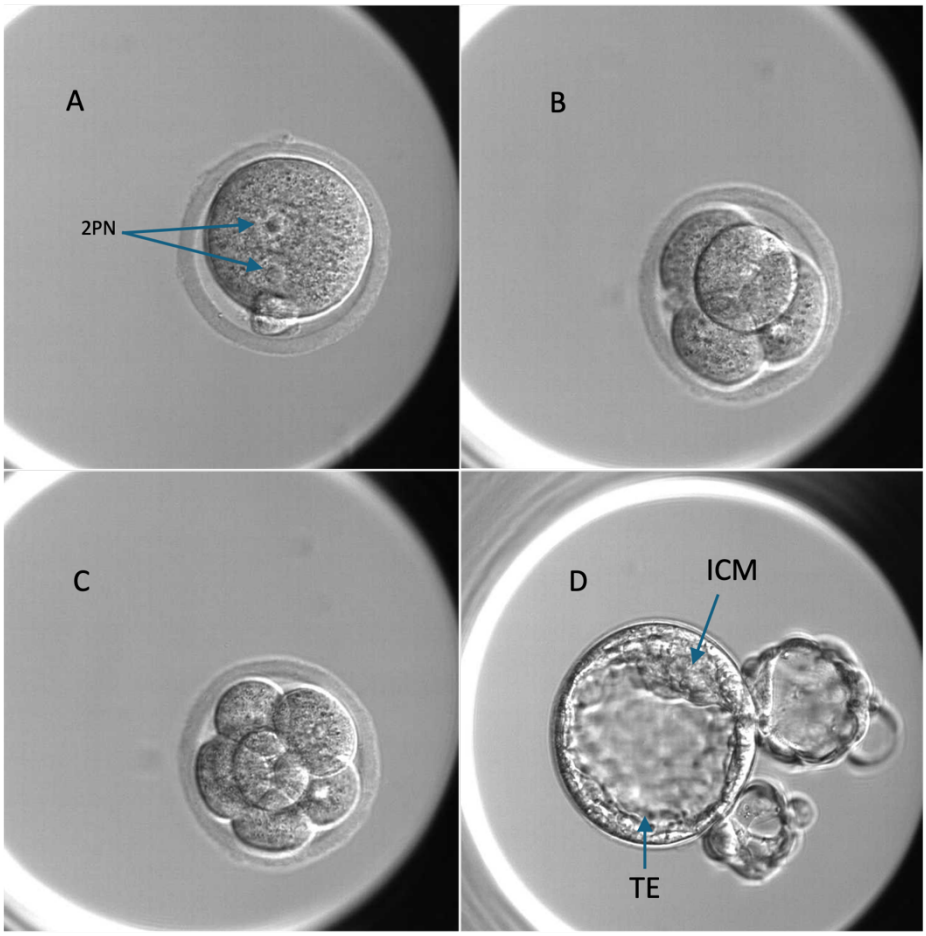

Figure 2.5. Representative Images of Embryo Morphology at Key Developmental Stages. Images Showing Fertilisation, Cleavage, Compaction, and Blastocyst Formation.

2.2.11 Blastocyst Harvest and Tissue Fixation

Blastocysts were harvested and fixed at 96 hours post zygote injection. Blastocysts from the same experimental group were transferred together using a glass handling pipette with an inner diameter of 156–190 µm (Vitrolife AB; product ref. 15537) from the culture dish into a centre-well dish containing 1 mg/mL PVP in PBS (PVP–PBS). They were left for 5 minutes and then washed through three consecutive dishes containing PVP–PBS to ensure complete removal of all components from the culture medium. The blastocysts were subsequently transferred into a 20 µL drop of 4% paraformaldehyde (PFA; Boster Biological Technology, Pleasanton, CA, USA) under oil in a clearly labelled 40 mm culture dish and kept overnight at 4 °C to allow fixation.

2.2.12 Staining and Total Cell Count

For the purpose of determining cell numbers in blastocysts derived from each experimental group, propidium iodide (PI) nuclear staining was employed. PI is a fluorescent intercalating agent that inserts itself between the base pairs of double-stranded DNA, thereby enabling visualisation of cell nuclei. As PI also binds to RNA, RNase was used to prevent background staining from cytoplasmic RNA (details see Appendix 2.4).

Following fixation, blastocysts were transferred using a 190–210 µm handling pipette into a Nunc 4-well dish (Thermo Fisher Scientific, Waltham, MA, USA) containing 1 mL PVP–PBS and washed through four consecutive wells. The embryos were then permeabilised by incubation in a centre-well dish containing 0.5% Triton X-100 in PBS for 60 minutes at 37 °C. Blastocysts were washed a further four times in PVP–PBS and transferred into a centre-well dish containing a 1:1 mixture of 50 µg/mL RNase A in PBS and 50 µg/mL PI in PBS, followed by incubation in the dark for 60 minutes at room temperature. After incubation, the blastocysts were washed four times in PVP–PBS before mounting on microscope slides.

Blastocysts were mounted individually in a 20 µL drop of 20% glycerol on a clean glass slide, after which a 20 × 20 mm glass coverslip was gently positioned over the sample. Light pressure was applied to flatten the embryo while ensuring the blastocyst remained intact. The coverslip was sealed with nail varnish, and the position of the blastocyst was marked on the underside of the slide with a fine permanent marker to facilitate identification during confocal

fluorescence microscopy. This procedure was repeated for all blastocysts from each experimental group. To avoid bias, slide labels were randomly coded to allow blinded assessment of cell numbers.

Imaging was performed using a Leica Stellaris 5 confocal microscope (Leica Microsystems GmbH, Wetzlar, Germany), and images were processed using ImageCompass software (Leica Microsystems GmbH). An excitation wavelength of 493 nm was selected, corresponding to the illumination range of PI (491–495 nm), and fluorescence emission was collected between 495 and 650 nm. A Z-stack acquisition was used to ensure complete imaging of each embryo, covering a depth of 60 µm with 0.4 µm step intervals. Laser gain and intensity were adjusted to avoid over-saturation and minimise image noise, thereby producing high-contrast images. A three-dimensional reconstruction was generated using ImageCompass software, and total cell numbers were counted twice for each embryo, with an image saved for reference.

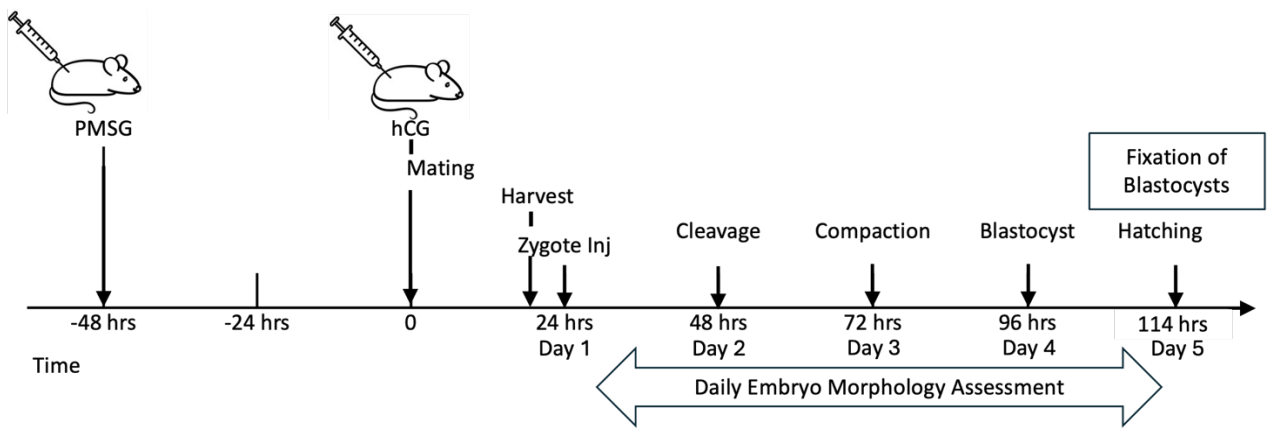

Figure 2.6. Overview of the Experimental Timeline.

Sequence of Injections Followed by a 114-hour Interval Before Tissue Collection.

2.2.13 Statistical Analysis

Randomisation of zygotes was performed using the RAND() function in Microsoft Excel (Microsoft Corporation, Redmond, Washington, USA).

Developmental outcomes were summarised as the percentage of embryos reaching each morphological stage at the specified time points, with Wilson–Brown 95% confidence intervals calculated for all proportions. Pairwise comparisons between treatment and control groups were performed using two-tailed Fisher's exact tests. To account for multiple testing, raw p-values were adjusted using the Benjamini–Hochberg false discovery rate (FDR) procedure, and adjusted q-values < 0.05 were considered statistically significant.

Total cell numbers obtained from propidium-iodide-stained blastocysts were analysed using both parametric and non-parametric approaches. Group means ± SD were compared using one-way ANOVA with Tukey's post-hoc test, and in parallel, medians and interquartile ranges (IQR) were compared using the Kruskal–Wallis test followed by Dunn's post-hoc test with FDR correction. This dual-analysis strategy was used to ensure robustness given the modest sample sizes and potential deviations from normality. Full pairwise statistical outputs are provided in Appendix 2.5 Tables S1–S4.

All statistical analyses and graph generation were performed in GraphPad Prism 10 (GraphPad Software, San Diego, California, USA). A significance threshold of $p < 0.05$ (or $q < 0.05$ for FDR-adjusted comparisons) was applied throughout.

2.3 Results

2.3.1 Zygote Injection: Method Development, Optimisation and Validation

At the outset of this project, it was essential to establish a highly controlled and technically robust zygote injection process. Microinjection at the one-cell stage is an exceptionally delicate procedure that demands considerable technical skill, as even minor variations in pipette positioning, injection pressure, or volume delivery can compromise embryo viability.

To support this optimisation phase, embryos from an outbred Swiss mouse strain (SwissTacAusb) were used, as they are more robust and tolerant of manipulation than the inbred strain employed in the main experiments. A substantial amount of preliminary work was therefore dedicated to determining a method for delivering an exact, standardised injection volume and ensuring that the procedure itself did not introduce artefacts. This optimisation phase involved iterative refinement of micromanipulation parameters and close monitoring of embryo survival and developmental progression. Only once the injection process consistently produced embryos that developed normally and were indistinguishable from uninjected controls was the protocol considered validated and adopted for experimental use.

Across the optimisation period, blastocyst development was monitored solely to confirm that the injection procedure supported normal developmental competence. Initial practice injections were performed using PVP, as it is routinely available in the laboratory and is introduced into oocytes during clinical ICSI alongside the sperm. In this group, 19 of 43 zygotes (44.2%) reached the blastocyst stage. Subsequent optimisation involved injections with the experimental compounds, during which 53 of 64 zygotes injected with THEO (82.8%) and 39 of 56 zygotes injected with PTX (69.6%) formed blastocysts. The non-injected control group produced 26 blastocysts from 47 embryos (55.3%). As these groups were generated at different times during method development, they were not intended for direct comparison. Instead, the key requirement was simply that injected embryos demonstrated robust developmental potential and achieved blastocyst formation at rates exceeding those of the non-injected control. This criterion was met, supporting the conclusion that the optimised injection protocol did not impair embryo viability.

2.3.2 Effect of PDE Inhibitor Microinjection on Blastocyst Formation

A total of 204 zygotes were harvested 18 hours (h) post-hCG from 30 superovulated B6F1 female mice and randomly allocated to one of five groups: the 5 mM Theophylline injection group (iTHEO; n = 48), the 5 mM Pentoxifylline injection group (iPTX; n = 52), the PVP injection control (iPVP; n = 35), the media injection control (iCON; n = 46), and a non-injected negative control (CON; n = 23). Following manipulation, all embryos were cultured under identical conditions for five days. Cleavage was assessed at 48 h post-hCG, and blastocyst development and morphology were assessed at 96 h and 114 h, including inner cell mass integrity, trophectoderm organisation, and the degree of blastocyst expansion and hatching.

Cleavage rates did not differ significantly between groups (Table 2.2; Fig. 2.7.A). Two-tailed Fisher's exact tests showed no evidence of pairwise differences (all raw $p > 0.13$), and no comparisons remained significant after Benjamini–Hochberg false discovery rate (FDR) correction (all adjusted $p > 0.65$). Cleavage proportions ranged from 71.4% in the iPVP group to 87.0% in both the CON and iCON groups, indicating that microinjection with the various solutions did not impair early embryo viability or the ability to cleave.

Similarly, blastocyst formation at 96 h did not differ significantly between groups (Fig. 2.7.B). The highest blastocyst rate was observed in the non-injected CON group (87.0%), whereas the injected groups (iTHEO, iPTX, iPVP) showed modestly lower rates (62.5–71.2%). Although iTHEO embryos exhibited a lower blastocyst rate compared with CON (62.5% vs 87.0%), this difference did not reach statistical significance (raw $p = 0.051$), and all other pairwise comparisons were non-significant.

All embryos that cleaved in each experimental group progressed to the blastocyst stage, meaning that the overall blastulation rate at 114 h was identical to the cleavage rates shown in Table 2.2.

Hatching rates at 114 h were also not significantly different between groups (Fig. 2.7.C). The iCON group showed the lowest hatching rate (45.7%), whereas iPTX exhibited the highest (71.2%). However, no pairwise comparisons remained significant after FDR correction.

In contrast, the proportion of embryos reaching the highest morphological grade (5AA) varied markedly between groups (21.7–71.2%, Fig 2.7.D). Embryos in the iCON group showed the lowest rate of 5AA formation. Fisher's exact tests confirmed significant differences between iCON and each of the other groups (raw $p \leq 0.0009$), and all four comparisons remained significant after FDR correction (adjusted $p < 0.003$). No other pairwise comparisons were significant (adjusted $p > 0.15$).

Across developmental endpoints, cleavage and 96 h blastocyst formation were broadly comparable between groups. Divergence emerged at 114 h, where hatching and 5AA grading revealed a consistent deficit in the iCON group relative to all other treatments. These findings indicate that while early development was unaffected, later-stage blastocyst expansion and morphological quality were significantly impaired in the iCON condition.

Table 2.2. Developmental Progression of Mouse Embryos Following Microinjection Across Experimental Groups.

Group	Zygotes Injected (*n*)	Cleaved 2-4 cells 48 h (%) (95% CI)	Blastocysts 96 h (%) (95% CI)	Hatching Blastocysts 114 h (%) (95% CI)	Grade 5AA Blastocysts 114 h (%) (95% CI)
iTHEO	48	79.2% (65.7-88.3)	62.5% (48.4–74.8)	64.6% (50.4-76.6)	60.4% (46.3-73.0)*
iPTX	52	86.5% (74.7-93.3)	80.8% (68.1–89.2)	71.2% (57.7-81.7)	71.2% (57.7-81.7)*
iPVP	35	71.4% (54.7-83.7)	65.7% (49.2–79.2)	54.3% (38.2-69.5)	51.4% (35.6-67.0)*
iCON	46	87.0% (74.3-93.9)	69.6% (55.2–80.9)	45.7% (32.2-59.8)	21.7% (12.3-35.6)
CON	23	87.0% (67.9-95.5)	87.0% (67.9–95.5)	65.2% (44.9-81.2)	60.9% (40.8-77.8)*

Values represent the percentage of embryos achieving each developmental stage at the specified time points, presented with Wilson–Brown 95% confidence intervals. Pairwise comparisons were performed using two-tailed Fisher's exact tests, with multiple comparisons corrected using the Benjamini–Hochberg false discovery rate (FDR) procedure.* Significantly different from iCON after FDR correction ($p<0.01$).

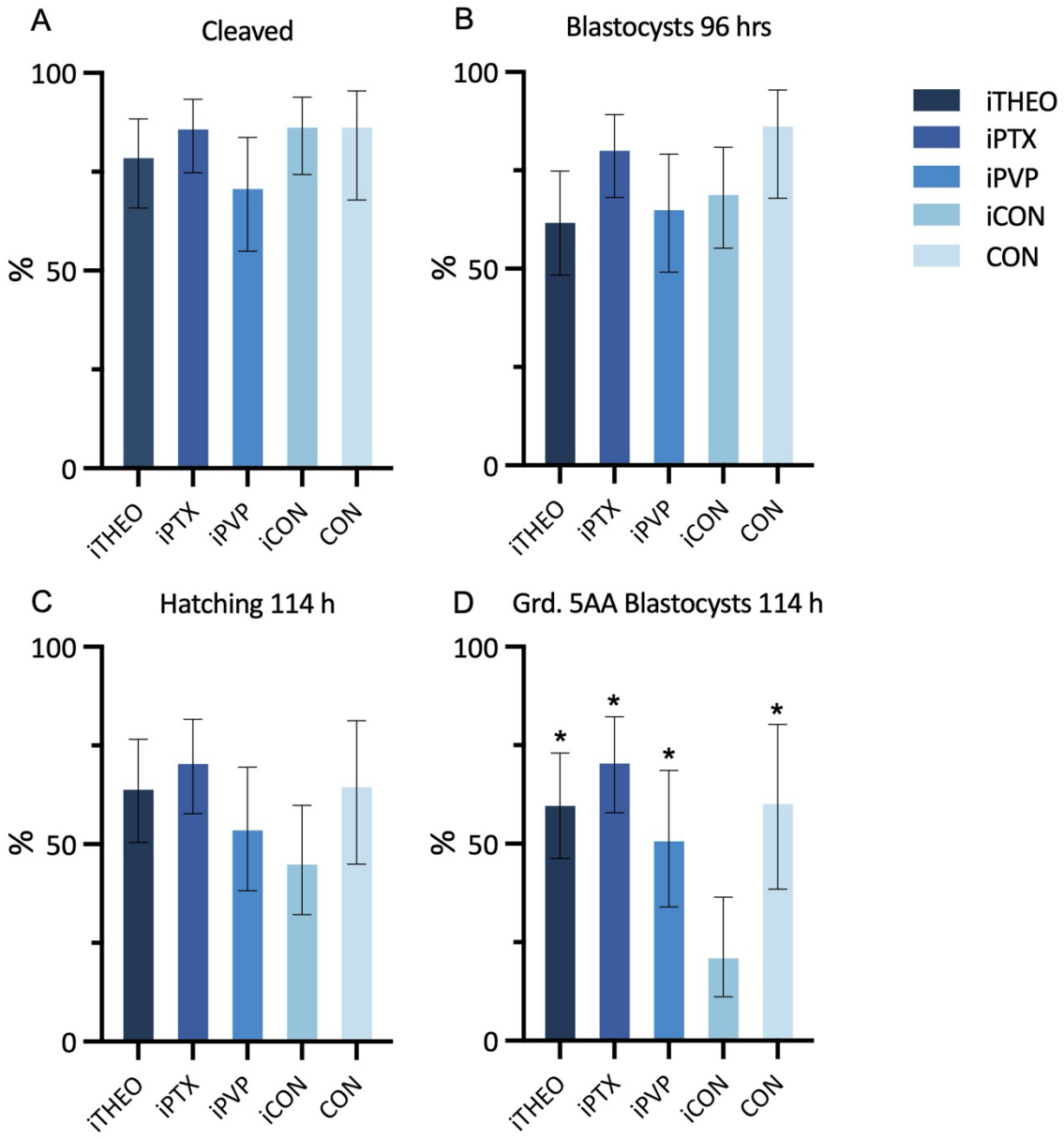

Figure 2.7. Developmental outcomes following microinjection across experimental groups. Bar graphs showing (A) cleavage at 48 h, (B) blastocyst formation at 96 h, (C) hatching at 114 h, and (D) and grade 5AA blastocysts at 114 h for embryos allocated to the five experimental groups (iTHEO, iPTX, iPVP, iCON, CON). Values represent the percentage of injected zygotes reaching each developmental stage, displayed with Wilson-Brown 95% confidence intervals. Pairwise comparisons were performed using Fisher's exact tests with Benjamini–Hochberg false discovery rate (FDR) correction. * Significantly different from iCON after FDR correction (p<0.01).

2.3.3 Effect of PDE Inhibitor Microinjection on Blastocyst Total Cell Number

Cell number provides a sensitive indicator of proliferative capacity and overall embryo quality (Brison & Schultz, 1997; Lane & Gardner, 1997; Scott et al., 1993). Blastocysts generated in each experimental group were therefore assessed by determining their total cell count. Blastomere nuclei were stained with propidium iodide (PI) and imaged using confocal fluorescence microscopy (Fig.2.9). Cell numbers were first recorded from two-dimensional (2D) projections. Extended depth of focus was then achieved using Z-stack acquisition to visualise all nuclei within the three-dimensional (3D) structure of the embryo. For accurate 3D quantification, each Z-stack was examined twice using the imaging software, allowing rotation of the embryo and inspection of each optical plane to ensure that all nuclei across the full depth of the blastocyst were counted.

2D total cell counts

Total cell counts obtained from 2D projections differed significantly between groups (one-way ANOVA, $p < 0.001$; Kruskal–Wallis, $p < 0.001$; Table 2.3, Fig. 2.8.A). Post-hoc testing revealed a clear divergence between the PDE inhibitor groups: iPTX embryos exhibited significantly reduced 2D cell numbers, whereas iTHEO embryos did not differ from the non-injected CON baseline. The clinical analogue control (iPVP) also showed cell numbers equivalent to CON, indicating that the injection procedure itself does not impair development when PVP is used, as in the clinical setting. In contrast, the media-only injection control (iCON) exhibited significantly lower 2D cell numbers than CON, demonstrating that microinjection with medium alone is sufficient to reduce proliferative capacity. No other pairwise comparisons reached significance. Thus, both parametric and non-parametric analyses identified iPTX and iCON as the only groups with reduced 2D cell numbers relative to the physiological baseline.

3D total cell counts

A similar pattern was observed in the 3D reconstructions (Table 2.3, Fig. 2.8.B). Total cell counts again differed significantly between groups (one-way ANOVA, $p \approx 0.0002$; Kruskal–Wallis, $p \approx 0.0004$). As in the 2D analysis, iTHEO embryos exhibited 3D cell numbers comparable to CON, whereas iPTX embryos showed significantly reduced counts. The iPVP group did not differ from CON, confirming that the clinical-analogue injection procedure does not adversely affect cell number. The media-only injection control (iCON) again showed

significantly lower 3D cell numbers than CON. Dunn's FDR-corrected comparisons supported these findings, identifying iTHEO and CON as significantly higher than iPTX, with iTHEO also exceeding iCON. No other pairwise differences were significant. These results demonstrate that only PTX injection and media-only injection reduced total cell number, whereas THEO and PVP injections did not.

Comparison of 2D and 3D counting modalities

Although absolute cell numbers were higher in 2D projections than in 3D reconstructions, the relative differences between experimental groups were highly consistent across both counting methods. Paired analysis within the same embryos confirmed that 2D counts were systematically higher than 3D counts (paired t-test, $p < 0.0001$), reflecting the expected inflation caused by nuclear overlap in 2D projections. Despite this offset, 2D and 3D counts were strongly correlated ($r \approx 0.9$), and the magnitude of the 2D–3D difference did not vary meaningfully between groups. Importantly, both modalities identified the same biological pattern: iPTX and iCON embryos exhibited reduced total cell numbers relative to the non-injected CON group, whereas iTHEO and iPVP embryos developed with cell numbers indistinguishable from unmanipulated controls. This concordance indicates that the observed group differences reflect genuine biological effects of the treatments rather than artefacts of the imaging modality. Full statistical outputs for all pairwise comparisons, including Tukey's post-hoc tests following one-way ANOVA and Dunn's FDR-corrected tests following Kruskal–Wallis, are provided in Appendix 2.5 Tables S1–S4.

Together, these analyses indicate that iPTX consistently suppresses total cell number relative to the other treatment groups, whereas iTHEO and iPVP maintain cell counts comparable to untreated controls, highlighting a clear divergence in how these interventions influence early embryo growth.

Table 2.3. Total Cell Counts of Blastocysts Across Experimental Groups.

Group	n	Total Cell Number 2D Mean ± SD	Total Cell Number 3D Mean ± SD	Significance vs CON (2D)	Significance vs CON (3D)
iTHEO	22	187 ± 31	171 ± 27	ns	ns
iPTX	25	147 ± 26	145 ± 25	$p < 0.05$	$p < 0.05$
iPVP	13	181 ± 17	167 ± 15	ns	ns
iCON	16	147 ± 24	143 ± 27	$p < 0.05$	$p < 0.05$
CON	12	181 ± 19	168 ± 37	-	-

Mean ± SD total cell numbers for each treatment group derived from 2D projections and 3D Z-stack reconstructions. Group differences were analysed using one-way ANOVA with Tukey's post-hoc test and Kruskal–Wallis with Dunn's FDR-corrected comparisons.

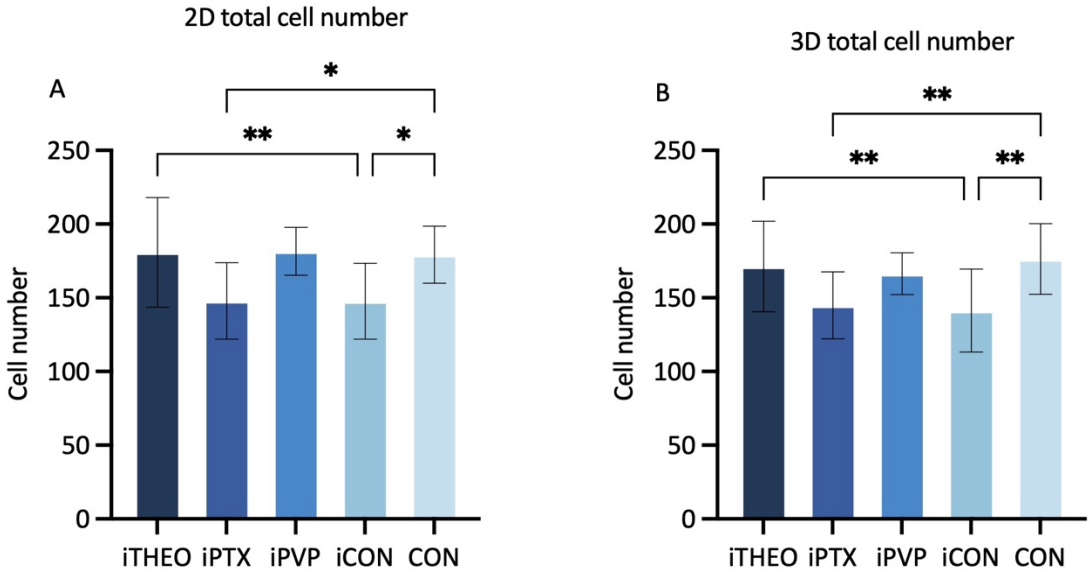

Figure 2.8. Total cell number of blastocysts across experimental groups.

(A) 2D total cell numbers from confocal projections. (B) 3D total cell numbers from Z-stack reconstructions. Bars show mean ± SD. Group differences were assessed using one-way ANOVA with Tukey's post-hoc test.relative to the non-injected CON baseline, whereas iTHEO and iPVP embryos did not differ from controls.

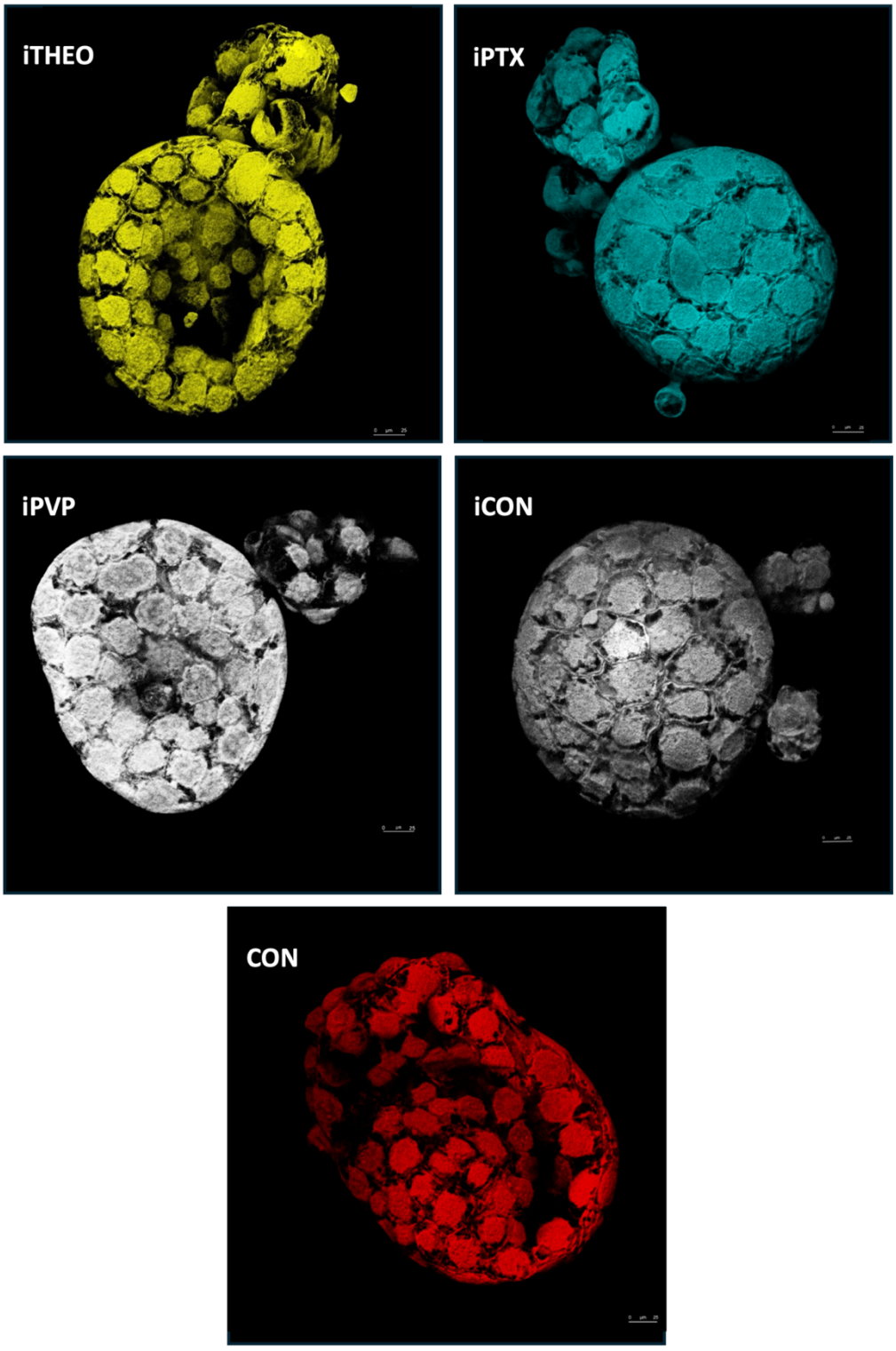

Figure 2.8. Blastocysts stained for cell number. Images are representative for the morphological appearance of expanded blastocysts under fluorescence microscope following PI staining for each of the experimental groups; iTHEO, iPTX, iPVP, iCON, CON.

2.4 Chapter Summary

This chapter established a validated and technically consistent microinjection protocol suitable for assessing the developmental effects of PTX and THEO in the mouse zygote model. The optimisation phase demonstrated that once injection parameters were standardised, embryos tolerated the procedure well and progressed to the blastocyst stage at rates comparable to, or exceeding, non-injected controls. This provided a necessary foundation for the subsequent experimental work.

Across the main study groups, early developmental milestones, including cleavage and blastocyst formation at 96 h, were broadly similar, indicating that neither injection of PTX nor THEO impaired early viability. Divergence emerged only at later stages, where the media-only injection control (iCON) consistently underperformed, particularly in hatching and top quality 5AA grading. This pattern suggests that the act of injecting medium alone introduces a detrimental mechanical or osmotic effect not observed when PVP, THEO, or PTX are present. Importantly, the clinical analogue control (iPVP) performed equivalently to non-injected embryos, supporting the safety of the standard ICSI injection environment.

Total cell-number analyses further refined these observations. The counting of cells in both 2D and 3D identified reduced cell numbers in iPTX and iCON embryos, whereas iTHEO and iPVP embryos were indistinguishable from untreated controls. The concordance between counting methods strengthens the conclusion that PTX, but not THEO, exerts a measurable suppressive effect on proliferative capacity at the blastocyst stage.

Together, these findings demonstrate that the optimised microinjection procedure is developmentally permissive, that injection of THEO and PVP do not adversely affect pre-implantation development, and that injection of PTX and medium-only injection each introduce specific deficits detectable at the blastocyst stage. These results provide a clear rationale for the more sensitive morphokinetic analyses undertaken in Chapter 3.

Chapter 3

Morphokinetic Consequences of ICSI-Mediated Phosphodiesterase Inhibitor Exposure in Preimplantation Mouse Embryos

3.0 Introduction

In this chapter, we extend our evaluation of phosphodiesterase inhibitor safety by examining whether transient exposure to pentoxifylline (PTX) and theophylline (THEO) during ICSI-mimicking microinjection affects the tempo and pattern of early embryo development. Using the same mouse embryo model described in Chapter 2, zygotes collected from naturally cycling or hormonally stimulated females were microinjected with PTX, THEO, or control solutions and cultured under continuous time-lapse imaging to capture their morphokinetic profiles.

While end-point measures such as blastocyst formation and total cell number provide important indicators of embryo viability, they do not capture the dynamic processes that shape early development. Cleavage timing, synchrony, and the duration of individual cell cycles are highly sensitive markers of embryo health, and deviations from established developmental trajectories have been associated with impaired competence. Time-lapse culture systems now allow these events to be monitored continuously, offering a detailed morphokinetic profile that complements traditional morphological assessment.

Early embryo development follows a geometric cleavage pattern (1→2→4→8 cells: Fig. 3.1 and Fig. 3.2), and the duration of each cell cycle, whether measured at the level of individual blastomeres or as whole-embryo embryo cell cycles (ECCs), is considered predictive of viability. Cell-cycle length reflects the time taken for DNA repair and cellular rearrangements before division. From time-lapse annotations, the second blastomere cycles (cc2a and cc2b) span from t2 to t3 or t4, while the corresponding embryo-level cycle (ECC2) spans from t2 to t4. The same logic applies to the third cycle, where four blastomeres divide between t4 and t8 (cc3a–d), and the embryo-level ECC3 is defined as t8–t4. Because these systems can be

complex, synchronisation metrics provide a simplified alternative: s2 (t4–t3) reflects how tightly the two blastomeres divide during the second cycle, and s3 (t8–t5) captures the spread of cleavage timings across the four blastomeres in the third cycle. These parameters offer a sensitive readout of subtle perturbations in cell-cycle regulation.

Building on the microinjection model established in Chapter 2, this chapter evaluates whether transient exposure to PTX or THEO alters these morphokinetic patterns. Using the same structured control system—PVP-injected, medium-injected, and non-injected embryos—zygotes were cultured in a time-lapse incubator to capture cleavage events from the first division through compaction and blastocyst formation. This design enables us to distinguish effects arising from the injection procedure itself from those attributable specifically to PDE inhibitor exposure.

Through detailed analysis of cleavage timings, ECC2 and ECC3 durations, and synchronisation parameters s2 and s3, this chapter provides a sensitive and physiologically relevant assessment of whether PTX and THEO disrupt normal developmental kinetics following zygote microinjection.

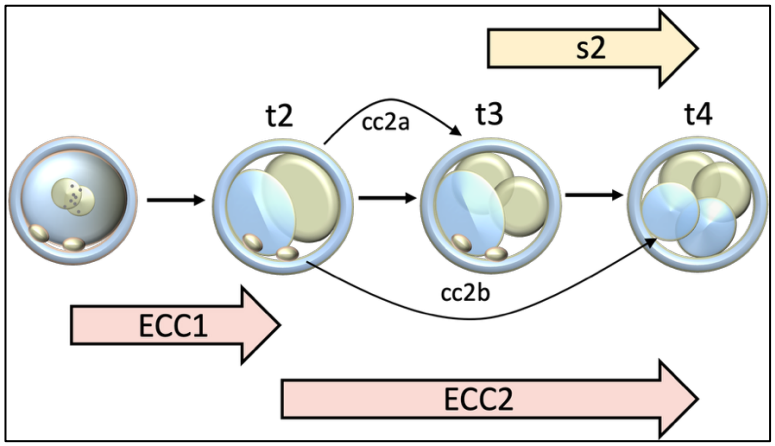

Figure 3.1. Schematic of ECC2 and the synchronisation parameter s2.
Diagram illustrating the transition from the 1-cell to the 4-cell stage, showing the individual blastomere cell-cycle durations (cc2a and cc2b) and the corresponding embryo-level cell cycle (ECC1 = t2-t2PNf, ECC2 = t4–t2). Synchronisation of the second cell cycle (s2) is defined as the interval between the first and second blastomere cleavages (s2 = t4–t3), reflecting how tightly

sister blastomeres divide. This schematic provides a visual guide to the calculation of ECC2 and s2 from time-lapse annotations (adapted from(Ciray et al., 2014).

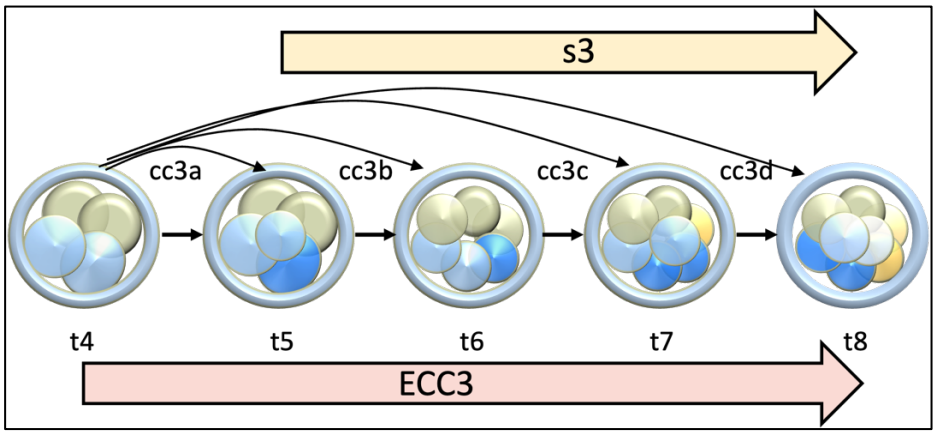

Figure 3.2. Schematic of ECC3 and the synchronisation parameter s3.

Diagram illustrating the transition from the 4-cell to the 8-cell stage, showing the four individual blastomere cell-cycle durations (cc3a–cc3d) and the corresponding embryo-level cell cycle (ECC3 = t8–t4). Synchronisation of the third cell cycle (s3) is defined as the interval between the first and last blastomere divisions within this cycle (s3 = t8–t5), providing a measure of how synchronously the four blastomeres cleave. This schematic supports the methodological description of ECC3 and s3 derived from time-lapse annotation (adapted from (Ciray et al., 2014).

3.1 Aim

Against this background, the aim of the current chapter was:

3. To further evaluate the safety of PTX and THEO by analysing morphokinetic developmental patterns in embryos cultured following zygote injection of PTX and THEO experimental and control groups.

3.2 Materials & Methods

3.2.1 Experimental Design

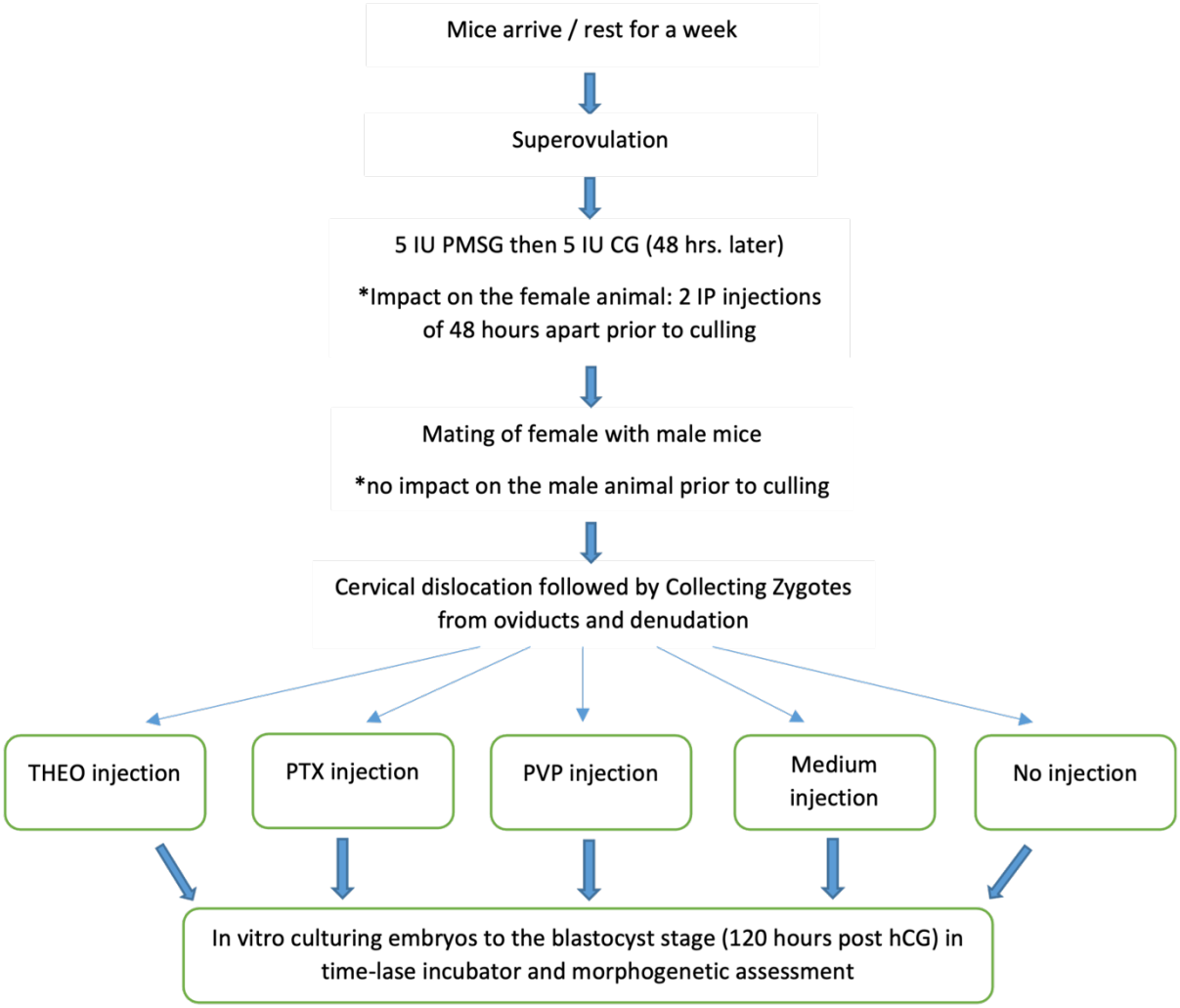

Figure 3.3. Overview of the experimental workflow for the functional mouse embryo assay. Schematic outlining the sequence from superovulation and mating to zygote collection, microinjection treatments, in-vitro culture, and blastocyst assessment.

3.2.2 Ethics

Ethical approval for animal research was obtained from the Western Sydney Local Health District (WSLHD) Animal Ethics Committee (AEC), Project Number 4358.12.21, titled “Effect of phosphodiesterase inhibitors injection on the development and viability of mouse Embryos”. The research was conducted in compliance with applicable legislation and code for care ("Animal Research Act 1985," 1985; "Australian Code for the Care and Use of Animals for Scientific Purposes," 2013) and the conditions of AEC approval.

3.2.3 Laboratory Quality Control

Process validation and quality control (QC) are essential to ensure the consistency and reliability of procedures and results in both clinical and research laboratories. To minimise variation, key environmental parameters were monitored daily, including incubator CO_2 concentration and the temperatures of critical equipment. Detailed QC procedures are described in Chapter 2, Section 2.2.3.

3.2.4 Culture Media and Laboratory Reagents

Embryos were handled and cultured in media supplied by Vitrolife AB (Västra Frölunda, Sweden) as detailed in Chapter 2, Section 2.2.4 and Appendix 2.1. Briefly, G-MOPS™ supplemented with 5% HSA was used as the collection and handling medium, denoted throughout as G-MOPS™+HSA. Cleavage-stage pre-implantation mouse embryos were cultured in G-1™ Plus until day 3 of development, when medium was changed to G-2™ Plus and maintained until the blastocyst stage 96 hours post zygote injection.

The experiments involved two phosphodiesterase (PDE) inhibitors: Theophylline (THEO; GM501 SpermMobil; Gynemed GmbH Co. KG, Sierksdorf, Germany) diluted 1:20 in G-MOPS™+HSA in accordance with the manufacturer’s instructions (denoted THEO throughout experiments) and PTX (Trentoximal; Alex Co. for Pharmaceutical Industries, Alexandria, Egypt) diluted to a final concentration of 5 mM in G-MOPS™+HSA (denoted PTX in all experiments).

All laboratory chemicals and reagents used across experiments were purchased from Sigma-Aldrich / Merck (Bayswater, VIC, Australia) unless otherwise specified.

3.2.5 Animals

Female and male inbred C57BL/6J × DBA/2J (B6D2F1) mice were used for all embryo experiments and were sourced from Ozgene (Perth, WA, Australia) and housed at Westmead Bioresources Facility (WBF), Westmead precinct, NSW, Australia. Mice were held in individually ventilated cages on a 12-hour light–dark cycle with food and water available *ad libitum*. Male mice were housed individually, whereas female mice were housed in groups of three to four. On arrival at WBF, mice were allowed one week rest before any experimental intervention.

3.2.6 Ovulation Induction and Zygote Collection

Superovulation and zygote collection was performed as outlined in Section 2.2.6 and 2.2.7 of Chapter 2. Briefly, female 3–4-week-old mice were superovulated by an i.p. injection of 5 IU pregnant mare's serum gonadotrophin (PMSG; Folligon, MSD Animal Health, Bendigo, VIC, Australia) followed by an i.p. injection of 5 IU human chorionic gonadotrophin (hCG; Chorulon, MSD Animal Health) 48 hours later. Superovulated females were mated overnight singly or in pairs in a cage with an 8–10-week-old male as confirmed by the presence of a vaginal copulation plug the morning after (designated Day 1 of pregnancy).

Mice were humanely sacrificed by cervical dislocation and oviducts were dissected under a stereomicroscope (SMZ-2B; Nikon, Tokyo, Japan) on an LEC heated stage in G-MOPS™+HSA handling medium. Pronucleate oocytes at the 1 cell stage (zygotes) were recovered from the infundibulum region of each oviduct and transferred into G-MOPS™+HSA medium in preparation for denudation. Cumulus cells were removed in 0.1 ml HYASE-10X™ (Vitrolife AB) diluted in 1 ml G-MOPS™+HSA), using progressively narrower glass handling pipettes (Vitrolife AB; Product ref. 15535 and 15532). The zygotes were then transferred to a 60 mm Falcon culture dish (Cat. No. 353002) containing 100 µl drops of G-MOPS™+HSA overlaid with 8 ml Ovoil™ for further fine denudation. Zygotes were then randomly allocated into 20 µl drops of G-1™ Plus, overlaid with Ovoil™, and placed in the incubator prior to microinjection (37.0 °C in 6% CO_2, 7% O_2 and 87% N_2; K-MINC-1000, Cook IVF, QLD, Australia).

3.2.7 Zygote Injection

To model the clinical exposure of spermatozoa to PDE inhibitors prior to selection and injection, zygotes were microinjected with THEO or PTX. All micromanipulation procedures were performed on a Nikon Ti Eclipse inverted microscope equipped with Narishige MTK-1 micromanipulators (Narishige Group, Tokyo, Japan) and a heated stage (Thermo Plate, Tokai Hit, Shizuoka-ken, Japan). Holding and injection pipettes (Vitrolife AB; product refs. 15305 and 15430) were aligned and calibrated prior to use.

Zygotes were randomised into four experimental drops of i) 5mM THEO in G-MOPS™+HSA, ii) 5mM PTX in G-MOPS™+HSA, iii) PVP (ICSI™, Vitrolife AB) and iv) G-MOPS™+HSA only and one control group that was not exposed to injection (Table 3.1). Randomisation was performed using a stratified allocation approach in which groups iTHEO and iPTX were assigned higher priority to ensure adequate sample sizes for key comparisons. Embryos were first assigned to these priority groups using a computer-generated random sequence, after which the remaining embryos were randomly distributed to groups iPVP, iCON and CON.

Table 3.1 Experimental Group Identifiers, Treatment Descriptions, and Rationale

Experimental Identifier	Treatment Description and Rationale
iTHEO	Zygotes injected with 5mM THEO in G-MOPS™+HSA to test the effect of PDE inhibitors in line with the aim of the project
iPTX	Zygotes injected with 5mM PTX in G-MOPS™+HSA to test the effect of PDE inhibitors in line with the aim of the project
iPVP	Zygotes injected with PVP (ICSI™, Vitrolife AB) to mimic the standard conditions during clinical application of ICSI
iCON	Zygotes injected with G-MOPS™+HSA only to serve as an injected control
CON	No Injection to serve as a negative control

The table outlines the identifiers assigned to each experimental group, together with a brief description of the injected solution (where applicable) and the rationale for its inclusion in the study. The “i” prefix denotes groups that underwent microinjection, while “CON” represents the non-injected control.

After pre-equilibration of the injection dish, the zygotes were transferred from the holding dish into the injection dish's G-MOPS™+HSA drops using a 156-190 µm glass handling pipette. Injection volumes were standardised using a microbead displacement method, with the bead serving as a visual marker to ensure consistent aspiration and delivery of approximately 1 picolitre (pl) across all treatments. Preparation of the injection dish, composition of experimental drops, randomisation of zygotes into treatment groups, and all steps relating to aspiration, injection, flushing, and prevention of cross-contamination followed the validated protocol described in Chapter 2, Section 2.2.8.

3.2.8 Embryo Culture

Following injection, zygotes from each group were transferred into an EmbryoSlide+® culture dish (Vitrolife AB; product ref. 16450). Each slide contains 16 microwells arranged in two partitions, each holding 180 µL of G-1™ Plus culture medium, together with four larger 30 µL washing wells. All wells were overlaid with 1.8 mL Ovoil™. Slides were pre-equilibrated for two hours in a 6% CO_2, 7% O_2 incubator (Heraeus BBD 6220; Thermo Fisher Scientific, Waltham, MA, USA) before one injected zygote was placed into each microwell, giving a total of 16 zygotes per slide. Wells were labelled to distinguish the different injection groups. The EmbryoSlide+® was then placed into an EmbryoScope+ time-lapse incubator (Vitrolife AB) for continued culture.

After 48 hours (Day 3 of development), the slide was removed from the EmbryoScope+ and embryos were transferred individually into the washing well of a pre-equilibrated EmbryoSlide+® containing G-2™ Plus medium overlaid with Ovoil™. Each embryo was washed twice in G-2™ Plus to remove all G-1™ Plus medium and then returned to the corresponding microwell in the new slide to maintain continuity of developmental history and allow uninterrupted imaging of the same embryo.

3.2.9 Morphokinetic Event Definitions and Time-Lapse Annotation Procedures

Embryo development was monitored using the EmbryoScope+ system which is operated using EmbryoViewer software (Version 7, Vitrolife), which provides the interface for continuous time-lapse monitoring. Embryo tracking of morphokinetic events is enabled by automated image acquisition every 10 minutes across multiple focal planes secure storage and playback of time-lapse sequences.

All morphokinetic annotations were performed manually using EmbryoViewer's built-in annotation tools, following the standardised definitions recommended by the ESHRE Time-Lapse Working Group (Coticchio et al., 2020). The time of mouse hCG injection was noted as starting time (t0) and annotated events included time to pronuclear fading (tPNf), 2-cell (t2), 3-cell (t3), 4-cell (t4), 5-cell (t5), 6-cell (t6), 7-cell (t7), and 8-cell (t8) stages, as well as the onset of compaction (tSC), morula formation (tM), and blastocyst formation (tSB). These parameters were compared across culture groups to identify differences in cleavage dynamics, developmental timing, and overall morphokinetic profiles. The mouse oocytes were fertilised *in vivo* and to minimise the influence of biological variation in the timing of mating, all developmental events were subsequently also normalised to tPNf.

The duration of embryo cell cycles (ECC) and synchronisation (s) of cell cleavage events were calculated; ECC2 = t4-t2, ECC3 = t8-t4, s2 = t4–t3, and s3 = t8–t5.

3.2.10 Statistical Analysis

Randomisation of zygotes was performed using the RAND() function in Microsoft Excel (Microsoft Corporation, Redmond, Washington, USA). Morphokinetic timings were non-normally distributed and right-skewed; therefore, they were summarised using medians and interquartile ranges (IQR). Time-to-event parameters were compared using the Kruskal–Wallis test followed by Dunn's post-hoc tests with built-in multiple-comparison correction. GraphPad Prism 10 (GraphPad Software, San Diego, California, USA) was used for all statistical analyses and graph generation. P values < 0.05 were considered as significant.

3.3 Results

3.3.1 Effect of PDE Inhibitor Injection on Morphokinetic Developmental Outcomes

To investigate the effect of PDE inhibitor microinjection on morphokinetic developmental outcomes, a total of 89 zygotes were harvested 18 hours (h) post-hCG from 18 superovulated B6F1 female mice and randomly allocated to one of five groups: the 5 mM Theophylline injection group (iTHEO; n = 24), the 5 mM Pentoxifylline injection group (iPTX; n = 19), the PVP injection control (iPVP; n = 17), the media injection control (iCON; n = 16), and a non-injected negative control (CON; n = 13). Extra zygotes were added to the iTHEO group due to some technical challenges during the injection. Following manipulation, all embryos were cultured under identical conditions in the EmbryoScope+ for five days to allow for morphokinetic assessment of each embryo. Key developmental milestones were annotated for the fading of the pronuclei (tPNf), cleavage to 2 cells (t2), 3cells (t3), 4 cells (t4), 5 cells (t5), 6 cells t6, 7 cells (t7), 8cells (t8), start of compaction (tSC), full compacted morula formation (tM), initiation of blastocoel cavity formation (blastulation, tSB) and hatching (tHBN).

Cleavage at 48 h post hCG injection was comparable with the outcomes from experiments in Chapter 2. 75.0 % of injected zygotes cleaved after injection group iTHEO, and 76.0% and 93.8% in iPTX and iCON respectively. All injected zygotes cleaved in the iPTX and CON groups.

Analysis of morphokinetic parameters revealed several significant differences between groups across early cleavage, compaction and blastocyst-stage events (Table 3.2, Fig. 3.4; 3.5; 3.6). Pairwise comparisons indicated that zygotes injected with medium (iCON) and the non-injected zygote control (CON) differed at multiple time points, with additional differences observed between iPTX and iCON, and between iTHEO or iPVP and iCON for selected parameters.

Table 3.2. Time-Lapse Morphokinetic Parameters Across Experimental and Control Groups

Time-Event	iTHEO Median (IQR)	iPTX Median (IQR)	iPVP Median (IQR)	iCON Median (IQR)	CON Median (IQR)
tPNf	30.9 (29.7–32.0)	30.8 (29.0–32.8)[a]	30.5 (29.0–33.0)	32.4 (32.1–33.4)[ab]	30.3 (28.9–32.0)[b]
t2	32.9 (31.4–33.6)	33.0 (31.3–34.5)[c]	32.5 (31.0–34.2)[d]	34.5 (33.5–35.1)[bcd]	31.4 (30.5–33.5)[b]
t3	51.8 (50.7–52.2)[c]	52.2 (49.8–53.1)[a]	52.3 (50.3–52.8)	53.7 (52.9–54.5)[abc]	51.5 (49.1–52.3)[b]
t4	52.0 (51.5–54.0)	52.8 (50.9–53.8)	53.0 (50.6–53.8)	54.2 (53.1–55.0)[b]	51.5 (49.7–53.0)[b]
t5	61.3 (59.58–62.1)[C]	61.8 (60.0–62.9)	62.3 (59.8–63.5)	63.5 (61.6–64.2)[bc]	59.9 (58.7–62.0)[b]
t6	61.7 (60.2–63.5)	62.1 (60.5–62.9)	62.7 (59.8–63.7)	63.7 (62.8–64.3)[b]	60.4 (59.4–62.5)[b]
t7	62.3 (60.6–64.0)[c]	62.6 (60.7–64.3)	63.4 (60.5–64.1)	64.8 (63.7–65.8)[bc]	61.0 (59.9–62.9)[b]
t8	62.9 (61.6–64.3)	62.9 (61.5–64.8)	63.7 (60.7–64.1)	64.8 (63.7–65.8)[b]	61.3 (60.6–62.7)[b]
tSC	72.5 (68.3–75.6)	72.7 (67.8–76.3)	68.8 (66.8–70.9)	73.8 (72.6–74.6)[b]	68.2 (67.4–70.7)[b]
tM	77.4 (73.2–80.9)	80.1 (74.1–85.5)[a]	75.6 (72.6–77.5)	78.1 (76.9–81.0)[ab]	74.6 (72.1–76.3)[b]
tSB	91.0 (88.8–96.0)	91.3 (87.0–93.8)	92.9 (89.0–95.2)	93.8 (92.0–94.9)	91.0 (88.8–93.5)
tHN	103.0 (98.2–106.5)	101.3 (98.2–107.2)	102.0 (99.8–104.4)	102.9 (101.7–104.4)	100.0 (97.8–102.7)

Values are presented as median with interquartile range (IQR). Timings represent absolute hours from fertilisation to each developmental event. Group differences were assessed using the Kruskal–Wallis test with Dunn's post-hoc correction. Superscripts indicate statistically significant pairwise comparisons. I [a]iPTX vs. iCON tPNf, t3, tM $p<0.05$, [b]iCON vs. CON tPNf, tM $p<0.05$, t2, t3, t4, t5, t6, t7, tSC $p< 0.01$, t8 <0.001, [c]iTHEO vs. iCON t2, t5, t7 $p<0.05$, t3 $p<0.01$, [d]iPVP vs. iCON t2 $p<0.05$

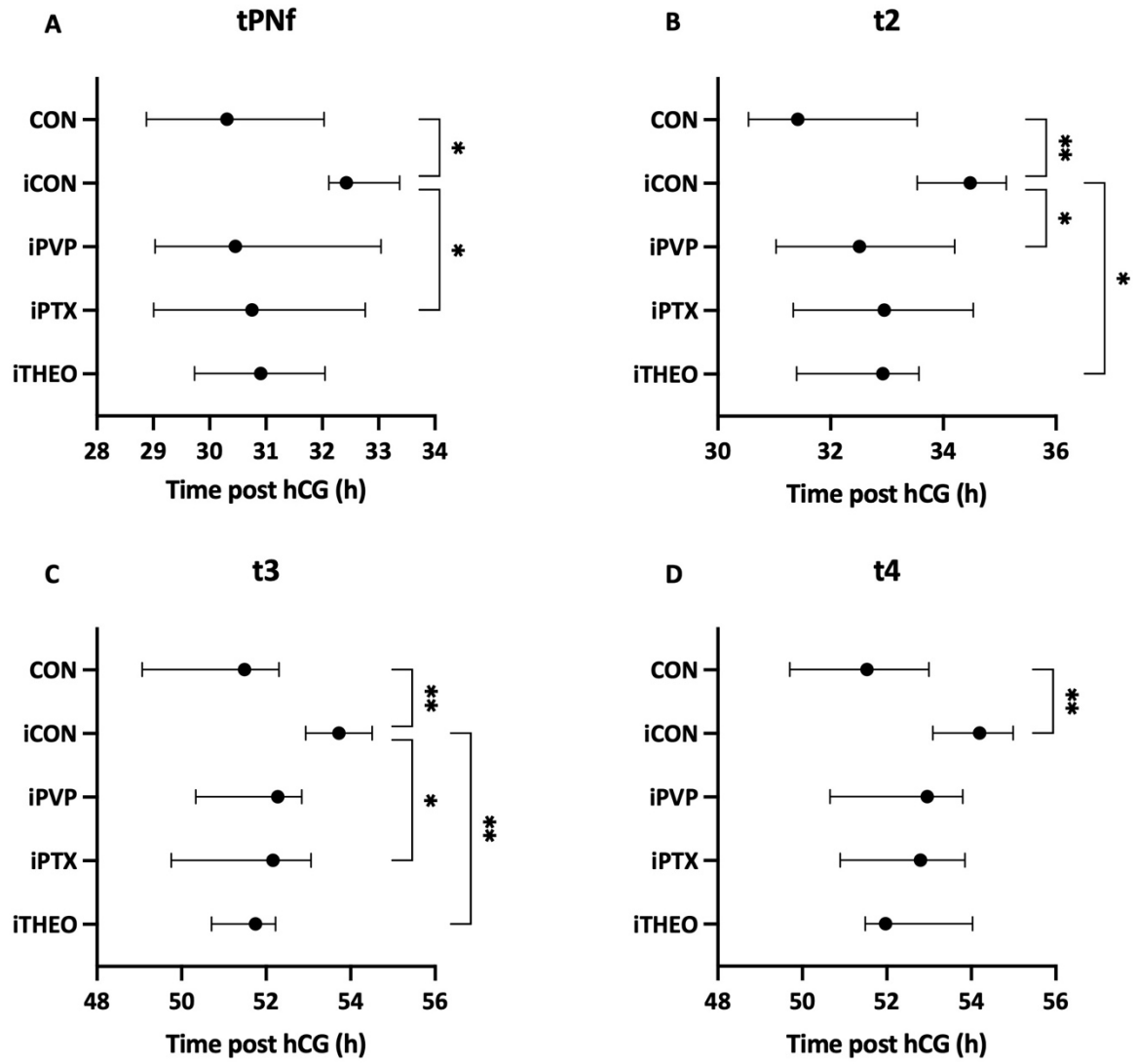

Figure 3.4. Early cleavage-stage morphokinetic timings across experimental groups

Median timings (with IQR) for pronuclear fading (tPNf), first cleavage (t2), second cleavage (t3), and third cleavage (t4) across the five groups (iTHEO, iPTX, iPVP, iCON, CON). Each point represents the group median with horizontal IQR bars. Timings represent absolute hours post hCG injection. Group differences were assessed using the Kruskal–Wallis test with Dunn's post-hoc correction. Superscripts indicate statistically significant pairwise comparisons *$p < 0.05$; **$p < 0.01$.

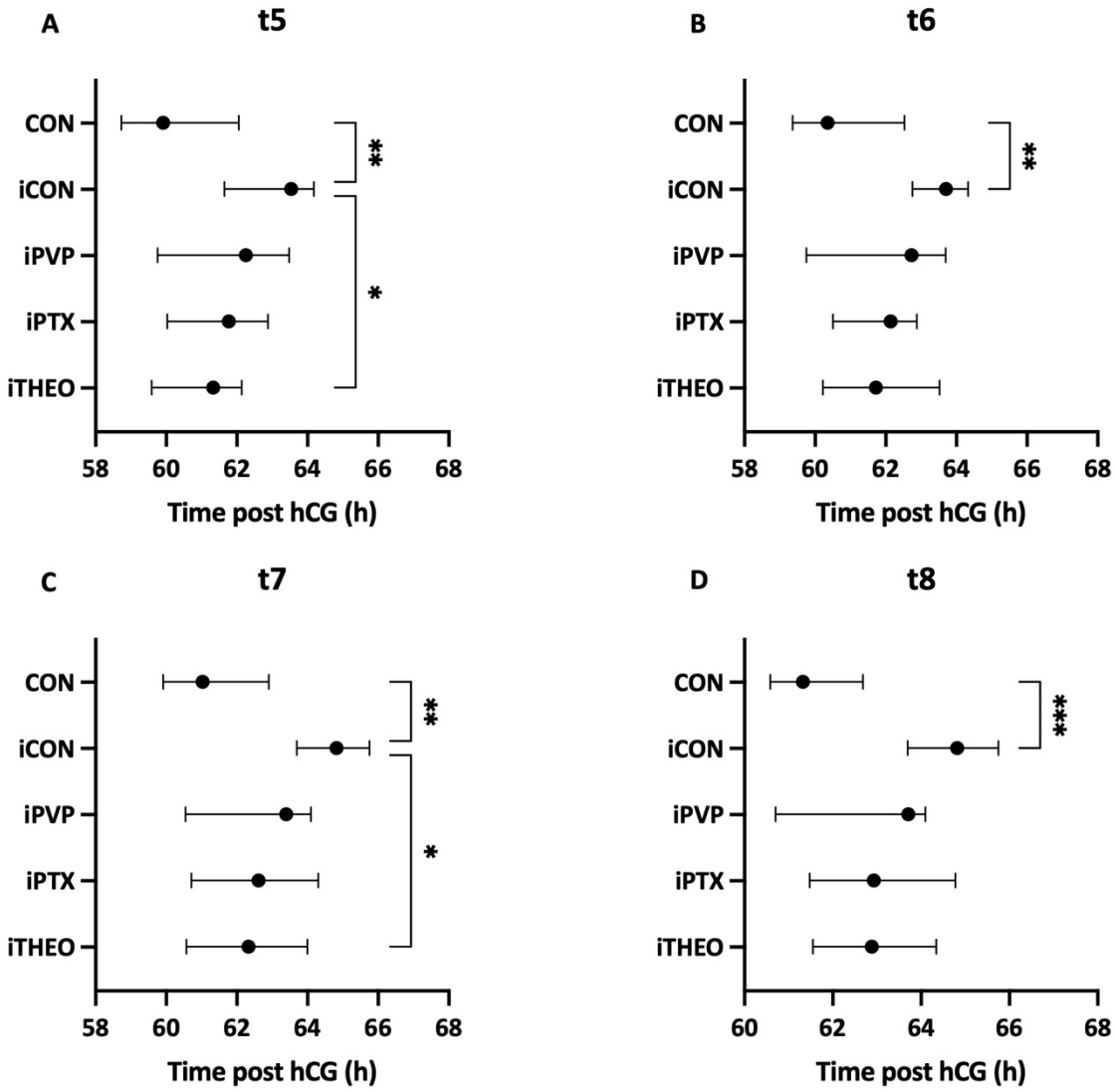

Figure 3.5. Mid-cleavage morphokinetic timings across experimental and control groups. Median timings (with IQR) for cleavage to 5–8 cells (t5, t6, t7, t8) across the five groups. Each point represents the group median with horizontal IQR bars. Timings represent absolute hours from fertilisation. Group differences were assessed using the Kruskal–Wallis test with Dunn's post-hoc correction. Superscripts denote significant pairwise comparisons *$p < 0.05$; **$p < 0.01$; ***$p < 0.001$.

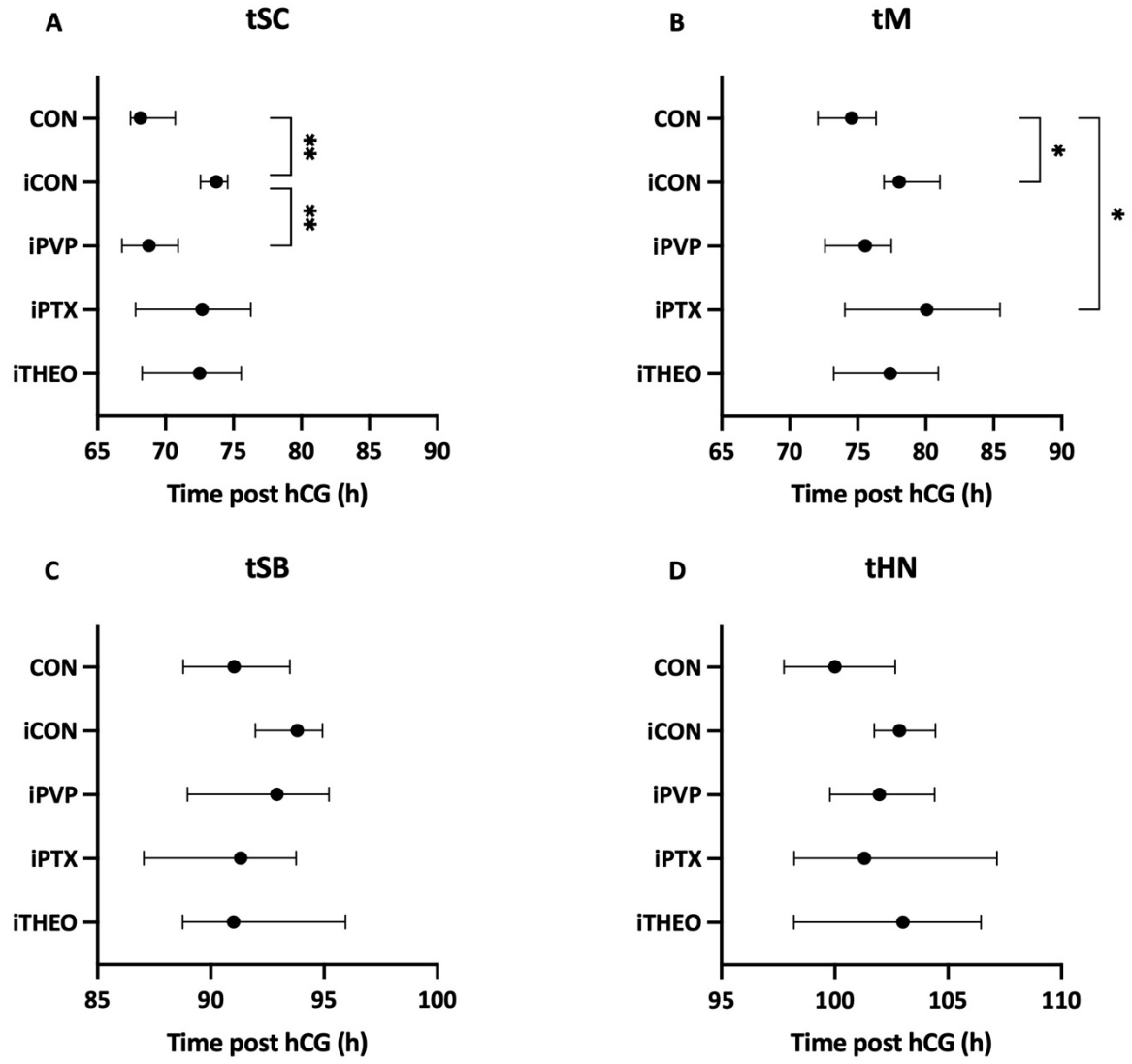

Figure 3.6. Late preimplantation morphokinetic timings across experimental groups.
Median timings (with IQR) for onset of compaction (tSC), morula formation (tM), initiation of blastulation (tSB), and hatching/expanded blastocyst (tHN) across the five groups. Points represent group median with horizontal IQR bars. Timings are absolute hours from fertilisation. Data was assessed using the Kruskal–Wallis test with Dunn's post-hoc correction. Superscripts indicate significant pairwise comparisons *$p < 0.05$; **$p < 0.01$.

To minimise the influence of biological variation in mating and injection timing, all developmental events were subsequently normalised to tPNf. Following normalisation, the majority of between-group differences were no longer evident. Only the timing to morula formation (tM) remained significantly different, with CON embryos reaching this stage significantly earlier than embryos developing after iPTX ($p = 0.0311$). All other normalised

parameters showed no significant differences between groups (Table 3.3, Fig. 3.7: 3.8; 3.9), indicating that differences in the morphokinetic timings post hCG could be attributable to variation in the timing of mating or that the effect of zygote injection has its most significant effect at the early syngamy stages rather than intrinsic post syngamy developmental kinetics.

Table 3.3. Embryo Developmental Timings Normalised to tPNf Across

Time-Event	iTHEO Median (IQR)	iPTX Median (IQR)	iPVP Median (IQR)	iCON Median (IQR)	CON Median (IQR)
t2	1.7 (1.6–2.1)	1.6 (1.4–1.9)	1.74 (1.5–2.1)	1.9 (1.4–2.1)	1.583 (1.1–2.0)
t3	20.86 (19.9–21.7)	20.51 (19.9–21.6)	20.72 (20.2–21.5)	21.14 (20.0–21.6)	20.65 (19.5–20.9)
t4	21.6 (20.8–22.2)	21.9 (20.6–23.0)	21.4 (20.9–21.8)	21.6 (20.5–22.3)	20.7 (20.0–21.7)
t5	30.0 (29.4–31.1)	30.6 (29.6–31.3)	30.7 (29.9–32.1)	30.6 (29.2–31.3)	29.8 (29.3–30.4)
t6	30.8 (29.7–31.6)	30.8 (30.1–32.0)	30.7 (29.9–32.3)	31.0 (30.3–31.4)	30.1 (29.6–31.1)
t7	31.2 (30.2–32.1)	31.4 (30.7–33.6)	31.2 (30.7–32.4)	31.6 (31.4–32.5)	31.0 (30.4–32.0)
t8	31.9 (30.4–32.7)	32 (31.1–33.6)	31.5 (30.8–32.4)	32.1 (31.4–32.5)	31.5 (30.2–32.4)
tSC	41.2 (37.7–44.8)	41.2 (37.9–44.1)	38.3 (36.3–39.5)	41.5 (38.7–42.4)	38.4 (36.4–40.2)
tM	45.8 (43.6–49.1)	47.9 (44.5–52.5)[a]	44.6 (42.7–47.6)	45.5 (44.5–47.8)	43.5 (42.2–44.7)[a]
tSB	60.3 (58.1–65.7)	59.3 (57.0–62.6)	61.4 (57.7–64.4)	61.7 (58.6–63.1)	60.9 (58.0–62.5)
tHN	70.7 (68.2–74.1)	68.9 (65.7–75.2)	70.0 (68.2–73.9)	70.4 (68.8–71.4)	70.0 (68.3–72.2)

Values are presented as median with interquartile range (IQR). Timings represent hours post-tPNf. Group differences were assessed using the Kruskal–Wallis test with Dunn's post-hoc correction. Superscripts indicate statistically significant pairwise comparisons. [a]iPTX vs. CON tM $p<0.05$

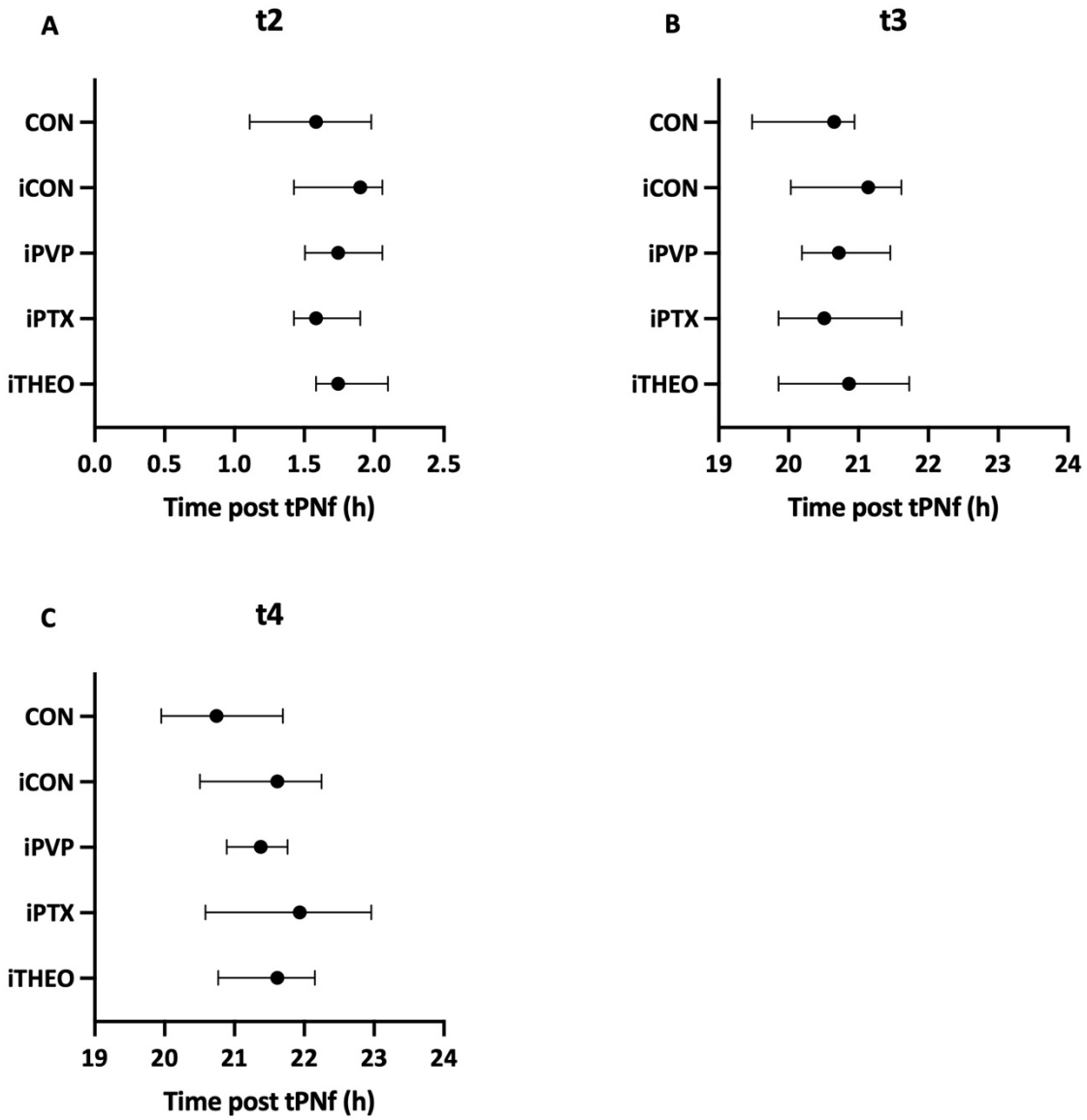

Figure 3.7. Early cleavage-stage morphokinetic timings normalised to tPNf.
Median timings (with IQR) for (A) t2, (B) t3, and (C) t4 expressed as hours post-tPNf across the five groups (iTHEO, iPTX, iPVP, iCON, CON). Each point represents the group median with horizontal IQR bars. Group differences were assessed using the Kruskal–Wallis test with Dunn's post-hoc correction; no significant differences were detected.

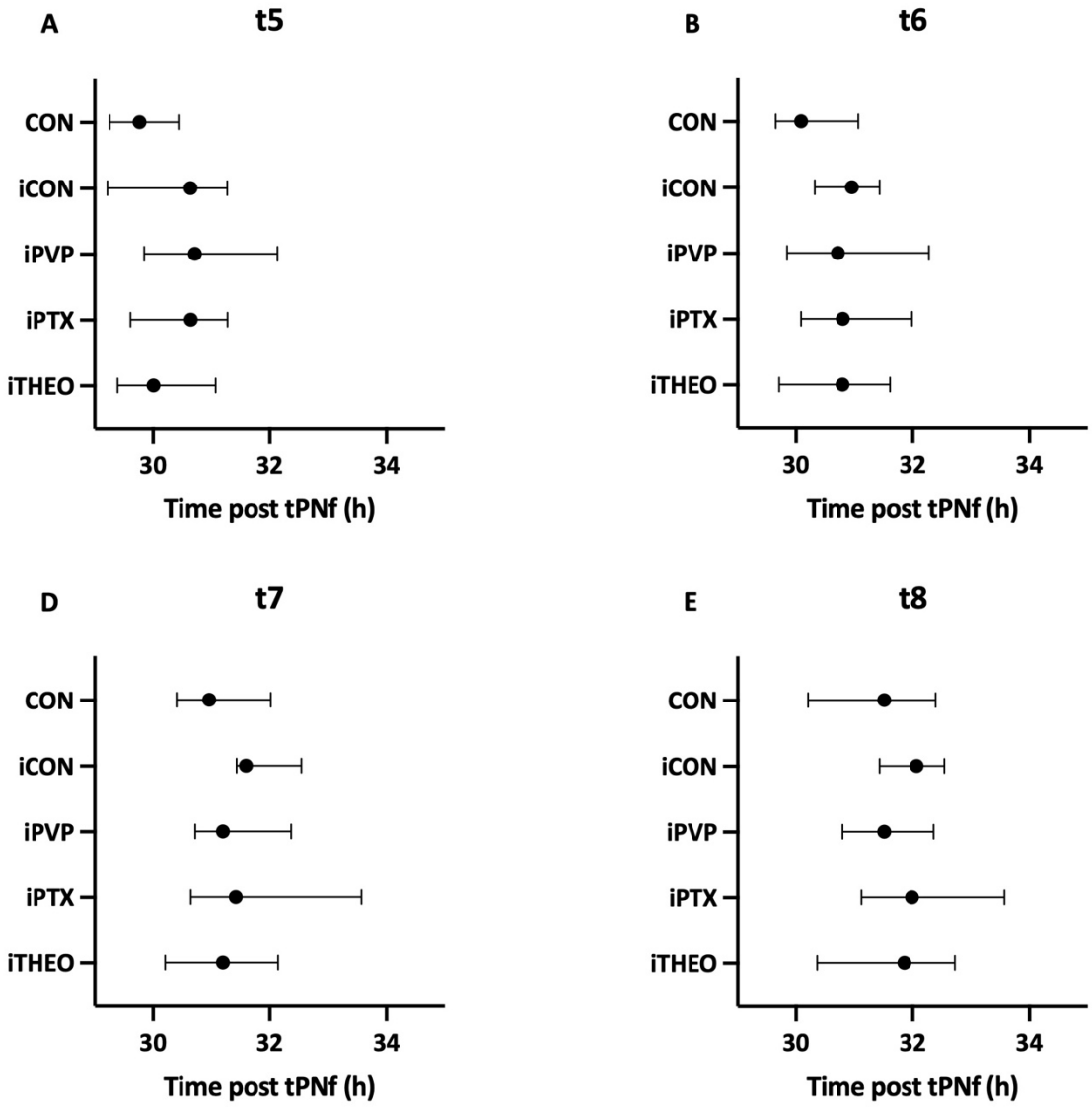

Figure 3.8. Mid-cleavage morphokinetic timings normalised to tPNf.

Median timings (with IQR) for (A) t5, (B) t6, (C) t7, and (D) t8 expressed as hours post-tPNf across the five groups. Each point represents the group median with horizontal IQR bars. Group differences were assessed using the Kruskal–Wallis test with Dunn's post-hoc correction; no significant differences were detected.

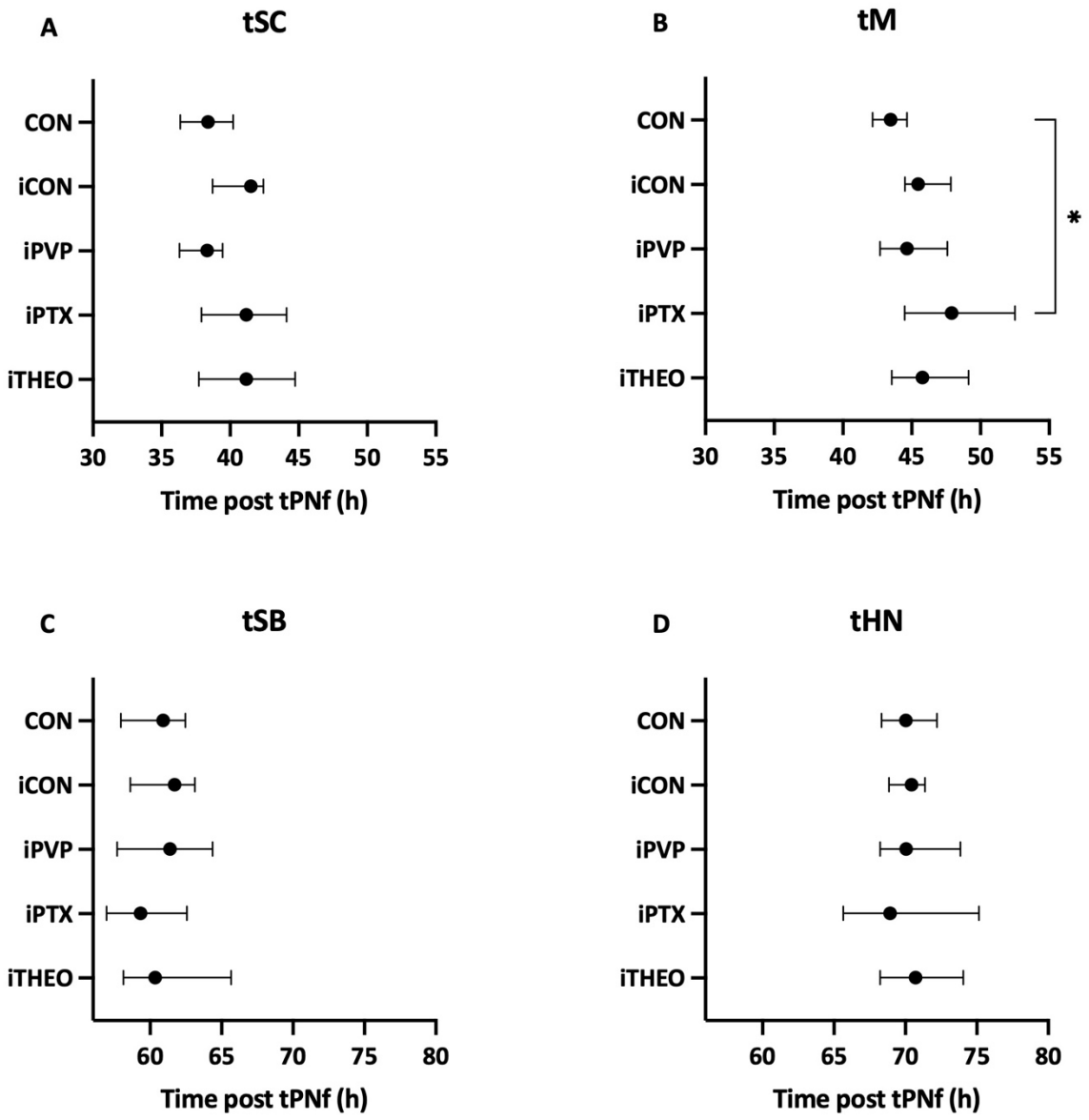

Figure 3.9. Late preimplantation morphokinetic timings normalised to tPNf.
Median timings (with IQR) for (A) tSC, (B) tM, (C) tSB, and (D) tHN expressed as hours post-tPNf across the five groups. Each point represents the group median with horizontal IQR bars. Group differences were assessed using the Kruskal–Wallis test with Dunn's post-hoc correction. Superscripts indicate statistically significant pairwise comparisons *$p < 0.05$; *$p < 0.01$; *$p < 0.001$.

3.3.2 Effect of PDE Inhibitor Injection on Duration of Events Related to Dynamics of Early Preimplantation Period

Early embryo development follows a geometric cleavage pattern (Figure 3.2 and Figure 3.3), and the duration of each cell cycle measured at the level of embryo cell cycles (ECCs) is considered highly predictive of viability. Cell-cycle length was calculated from time-lapse annotations for embryo-level cycle (ECC2) spans from t2 to t4 (t4-t2) and t4 to t8 (ECC3, t8-t4). Synchronisation demonstrated by how tightly sister blastomeres divide was calculated s2 = t4–t3 for the second cycle, and s3 = t8–t5 for the third. There were no significant differences in the synchronisation time s2 and s3 between the experimental groups (Fig 3.10 panel A and B) and the time for ECC2 and ECC3 was comparable across all injections and control (Fig 3.10 panel C and D).

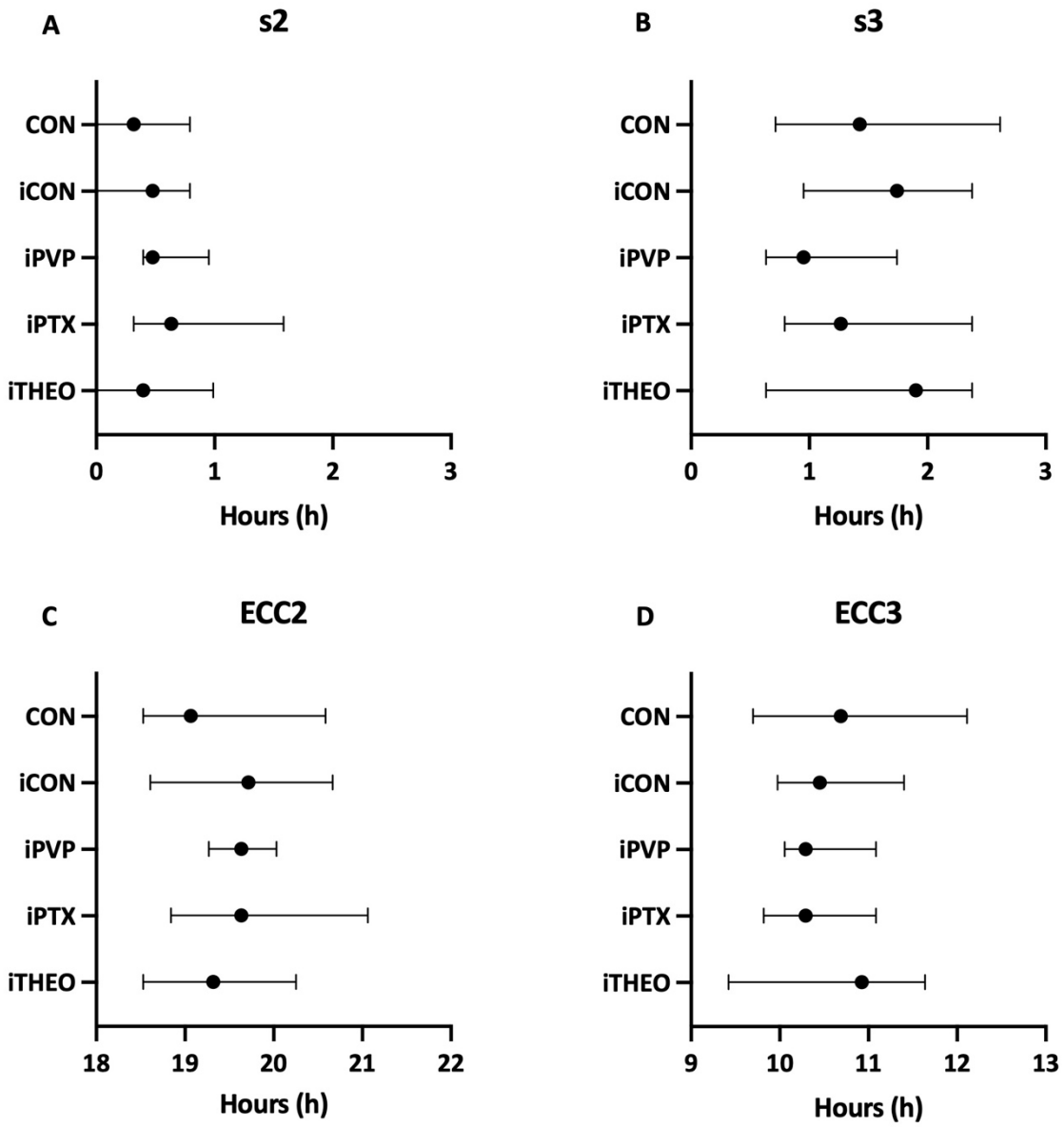

Figure 3.10. Embryo-level cell-cycle durations and synchronisation parameters across experimental groups.

Median time (with IQR) for (A) synchronisation of the second cell cycle (s2 = t4–t3), (B) synchronisation of the third cell cycle (s3 = t8–t5), (C) embryo cell-cycle 2 (ECC2 = t4–t2), and (D) embryo cell-cycle 3 (ECC3 = t8–t4) across the five groups (iTHEO, iPTX, iPVP, iCON, CON). Each point represents the group median with horizontal IQR bars. Group differences were assessed using the Kruskal–Wallis test with Dunn's post-hoc correction; no significant differences were detected for any parameter.

3.4 Chapter Summary

This chapter examined whether microinjection of PTX or THEO alters the morphokinetic profile of pre-implantation mouse embryos. Overall, the findings indicate that the timing and coordination of early developmental events were largely preserved across all treatment groups. Although several differences were initially observed when events were referenced to hCG, these disparities were no longer evident once timings were normalised to pronuclear fading (tPNf), suggesting that variation in mating or fertilisation timing contributed more to the observed differences than the microinjection treatments themselves.

Importantly, the key morphokinetic indicators of embryo health, ECC2, ECC3, and the synchronisation parameters s2 and s3, were comparable across all groups. Neither PTX nor THEO disrupted cleavage-cycle duration or the synchrony of blastomere division, and both performed similarly to the clinical analogue control (iPVP) and the non-injected baseline. The only remaining difference after normalisation was a modest delay in morula formation in iPTX relative to CON, but this did not extend into later developmental stages or affect subsequent synchronisation metrics.

Taken together, these results show that while PTX and THEO differ in their effects on blastocyst cell number (as demonstrated in Chapter 2), neither compound exerts a measurable impact on the intrinsic timing or coordination of early cleavage events. This supports the conclusion that PDE inhibitor exposure during zygote microinjection does not disrupt the fundamental kinetic architecture of pre-implantation development. These findings provide an important complement to the morphological and cell-number analyses and help contextualise the broader safety assessment explored in Chapter 5.

Chapter 4

Evaluation of Different Sperm Preparation Methods and their Impact on Fertility Treatment Outcomes; a Retrospective Cohort Study

4.0 Introduction

The refinement of sperm preparation techniques has been central to the evolution of assisted reproductive technologies (ART). Since the introduction of intracytoplasmic sperm injection (ICSI) more than three decades ago, the use of epididymal and testicular spermatozoa has enabled men with obstructive and non-obstructive azoospermia to achieve biological parenthood. These samples, however, vary widely in quality, cellular composition, and the presence or absence of motile spermatozoa, making laboratory preparation a critical determinant of downstream fertilisation and embryo development. The effectiveness of processing these tissues can directly influence ICSI outcomes, and ongoing efforts aim to optimise laboratory strategies to improve the likelihood of identifying viable sperm in a timely and reliable manner.

Advanced preparation methods, including the use of phosphodiesterase inhibitors such as pentoxifylline (PTX) and theophylline (THEO), have been adopted in many centres to enhance motility and facilitate sperm selection. Sharing and evaluating these approaches across the embryology community is essential for refining best practice and improving clinical outcomes. As ART continues to expand, there is increasing emphasis on ensuring that laboratory procedures not only maximise fertilisation and blastocyst development but also support the long-term health of children conceived through these technologies. Suboptimal processes may have consequences that extend beyond early development, contributing to risks such as preterm birth, congenital anomalies, or imprinting disorders. This underscores the need for continual reassessment of laboratory methods and for aligning *in vitro* practices as closely as possible with physiological conditions.

Within this context, the present chapter examines clinical outcomes associated with different sperm washing and preparation techniques used in medical assisted reproduction (MAR) cycles, including those employing PTX and THEO. By retrospectively analysing fertilisation, embryo development, utilisation, pregnancy, and live-birth outcomes, this work aims to identify preparation strategies that best support successful treatment and healthy offspring.

4.1 Aim

Accordingly, the aim of Chapter 4 was:

4. To retrospectively evaluate clinical outcomes in MAR treatment cycles where advanced sperm preparation techniques, including the use of PTX and THEO, were employed.

4.2 Materials & Methods

4.2.1 Ethics

The project was submitted via the Human Research Ethics Application (HREA) system for review by a Human Research Ethics Committee (HREC):

2025/ETH00130 – Evaluation of different sperm preparation methods and their impact on fertility treatment outcomes.

The application was assessed under the *low or negligible risk* review pathway and was initially considered by the Western Sydney Local Health District Human Research Ethics Committee. The project was determined to meet the requirements of the *National Statement on Ethical Conduct in Human Research (2023)* and was **approved**.

Date of decision notification: **4 June 2025**.

Due to circumstances outside the control of the student and the Principal Investigators/Supervisors, site-specific approval (SSA) was not granted. As a result, the project could not proceed, and no retrospective cohort data were able to be evaluated or reported.

4.2.2 Clinical Setting

Westmead Fertility Centre (WFC), fully owned by the University of Sydney, have been offering fertility treatment for more than 40 years helping thousands of couples achieve their goal to have a healthy child. The centre is embedded in Westmead Hospital, and the clinical work is driven by the latest developments in *In Vitro* Fertilisation (IVF), fertility technologies and methodologies to give patients the best chance of success. Tightly connected to the clinical work, the centre's aim of improving reproductive care with exceptional research is rooted in the University of Sydney and the Reproduction and Perinatal Centre (RPC) with the mission to provide the highest quality of research-based evidence to improve long-term health outcomes and clinical care for women, families and babies before conception, through to pregnancy and after birth.

Clinical procedures were performed by a team of trained embryologists, including the author.

4.2.3 Patient Population

The study was designed as a retrospective cohort study including patients undergoing treatment for infertility at WFC between 2016 to date with the following inclusion and exclusion criteria:

Inclusion Criteria

- Collection of one or more mature oocytes
- Ejaculated or testicular sperm (fresh or frozen)
- ICSI as mode of fertilisation
- Female age <43 years at the time of oocyte collection

Exclusion Criteria

- Patients having conventional IVF as mode of fertilisation
- Fertility preservation cycles
- Patients enrolled in the donor programme

4.2.4 Culture Medium

Culture medium used in the human embryology laboratory at WFC was supplied by Vitrolife AB (Västra Frölunda, Sweden). Although the precise formulations of these stage-specific media are proprietary, they are based on the G-series system originally developed at Monash University (Barnes et al., 1995; Gardner, 1994). This sequential culture system provides media tailored to the metabolic requirements of each developmental stage. Media designed to support oocytes, fertilisation, and cleavage-stage embryos contain amino acids, lactate, pyruvate, and a low concentration of glucose (G-IVF™ for oocytes and conventional IVF fertilisation, and G-1™). EDTA is included to suppress early glycolysis. In contrast, the post-compaction medium G-2™ contains both essential and non-essential amino acids and higher concentrations of glucose. As EDTA is omitted and glucose is increased to meet the metabolic needs of post-compaction embryos, it is essential that embryos are thoroughly washed in G-2™ at the time of medium change to remove all traces of EDTA.

Media supplemented with 5 mg/ml Human Serum Albumin (HSA) at manufacture are denoted by the suffix ‘Plus’. G-IVF™ Plus contains 10 mg/ml HSA to support sperm capacitation during

fertilisation. G-MOPS™ was supplemented with 5% or 10% HSA in-house (HSA-solution™, Vitrolife AB), denoted G-MOPS™+5% HSA and G-MOPS™+10% HSA throughout this chapter.

G-IVF™ Plus, G-1™ Plus, and G-2™ Plus are carbonate-buffered and therefore require an atmosphere of 6% CO_2 to maintain physiological pH. *In vivo*, mammalian embryos develop under hypoxic conditions, typically between 1% and 5% oxygen—substantially lower than atmospheric levels. This environment promotes anaerobic metabolism and glycolysis, reducing reliance on mitochondrial oxygen consumption. Accordingly, all media were pre-equilibrated for a minimum of two hours, and all embryo culture was performed at 37.0 °C in 6% CO_2, 7% O_2, and 87% N_2. These conditions are referred to as "incubation" or "in the incubator" throughout this chapter. Culture was conducted in drops of medium overlaid with Ovoil™ mineral oil.

G-MOPS™, used for handling and cryopreservation procedures, is buffered with MOPS (3-N-morpholino-propanesulphonic acid), enabling manipulation of gametes and embryos outside the incubator while maintaining optimal pH at 37.0 °C under atmospheric conditions.

Further details of the culture media are provided in Appendix 2.1.

4.2.5 Laboratory Quality Control

Oocyte and embryo handling, manipulation, and culture were performed in the embryology laboratory, while semen samples were assessed and prepared in the andrology laboratory at WFC. In accordance with clinic licensing requirements and mandatory compliance with the Reproductive Technology Accreditation Committee (RTAC) Code of Practice (Reproductive Technology Accreditation Committee, 2021), both laboratories operate under strict quality control (QC) standards and procedures. These include, but are not limited to, continuous monitoring of key laboratory equipment and environmental conditions, particularly incubator temperature and gas composition.

4.2.6 Semen Analysis

Semen samples were collected by masturbation into a sterile container within a designated collection room following 2–5 days of abstinence. All samples were allowed to liquefy at room

temperature and were analysed within 45 minutes of production. Semen analysis was performed by a trained embryologist in accordance with the World Health Organisation (WHO) Laboratory Manual for the Examination and Processing of Human (World Health Organisation, 2021). And WHO 2016 for the period prior to 2021. The parameters assessed were sperm concentration, motility, and morphology.

An initial assessment of sperm concentration was performed using a Makler chamber. A sterile glass Pasteur pipette (230 mm, non-plugged; referred to as 'Pasteur pipette' throughout this chapter; Sigma-Aldrich Pty Ltd, Bayswater, VIC, Australia) was used to place a drop of semen onto the counting grid, and the Makler coverslip was placed on top. Counting was performed at 20× magnification using an upright transmitted-light compound microscope (Nikon CH-2, Nikon Corporation, Tokyo, Japan). The number of sperm in ten squares was recorded as the pre-preparation concentration.

Then two drops of semen were placed onto a clean glass slide and gently covered with coverslips. Motility assessment was performed at 20× magnification twice, with the number of progressively motile and non-progressively motile sperm recorded out of 100 sperm under each coverslip (total 200 perm). the average was calculated and recorded as the initial motility.

Morphology assessment was performed by placing a single drop of semen onto a CellVu Prestained Morphology slide (Millenium Sciences, Inc., New York, United States) and applying a coverslip. After 10 minutes, 200 sperm were evaluated for normal morphology according to WHO criteria. Abnormal forms were not subclassified by head, mid-piece, or cytoplasmic defects; assessment was limited to categorisation as normal or abnormal.

The following parameters were considered normal at initial assessment: concentration ≥15 M/ml; progressive motility ≥30%; morphology ≥4% normal forms.

4.2.7 Sperm Preparation

After the initial assessment, the remaining semen sample was prepared. A Pasteur pipette was used to transfer up to 2 ml of the sample from the collection container into a pre-prepared density-gradient tube. The gradient was prepared by adding 1 ml of 80% PureSperm (Nidacon

International AB, Göteborg, Sweden) to a 15 ml centrifuge tube (Vitrolife AB; product ref. 16105), followed by carefully layering 1 ml of 40% PureSperm over the top using a Pasteur pipette. The semen sample was then gently layered onto the gradient, and the tube was centrifuged at 0.3 RCF for 20 minutes.

Following centrifugation, the sperm pellet at the bottom of the tube was carefully aspirated using a Pasteur pipette and transferred into a separate 15 ml tube containing 2 ml of G-MOPS™+10% HSA, pre-warmed to room temperature. This tube was centrifuged at 0.3 relative centrifugal force (RCF) for 5 minutes. The resulting pellet was then transferred into a second wash tube containing 2 ml of G-MOPS™+10% HSA and centrifuged again at 0.3 RCF for 5 minutes.

Depending on the size of the pellet (with the entire pellet taken if small or not visible, and only a portion taken if large), a Pasteur pipette was used to transfer the pellet into a 15 ml tube containing 1 ml (or less, if the pellet was not visible) of G-IVF™ Plus + 5% HSA. The pellet was resuspended by gentle mixing with the Pasteur pipette.

4.2.8 Preparation for ICSI of Poor Sperm and PESA/ TESA/ MICRO TESE Samples

Semen ejaculates of very poor quality, as well as testicular or epididymal aspirates, were prepared according to the quality and parameters of each sample.

For men with azoospermia, where no sperm are present in the ejaculate, spermatozoa were retrieved either by passing a needle through the scrotal skin into the head of the epididymis and aspirating fluid (percutaneous epididymal sperm aspiration, PESA), by aspirating seminiferous tubules directly from the testis (testicular sperm aspiration, TESA), or by microscope-guided dissection to identify sperm-producing tubules (microsurgical testicular sperm extraction, micro-TESE). Aspirates were collected into a sample tube (Vitrolife AB; product ref. 16103) or a 40 mm culture dish (Vitrolife AB) containing 3–5 ml G-MOPS™. Tubules containing red blood cells were washed in 40 mm dishes of G-MOPS™ before being gently teased apart and milked under a stereomicroscope (SMZ 1200; Nikon).

Depending on sample quality, aspirates were processed using one of the following approaches: i) wash only; ii) mini-gradient preparation; iii) erythrocyte lysis buffer (ELB) treatment; or iv) addition of a phosphodiesterase inhibitor.

Wash-only preparation

The sample was placed in a 15 ml tube containing 2 ml G-MOPS™+10% HSA, pre-warmed to room temperature, and centrifuged at 0.3 RCF for 5 minutes. The pellet was then aspirated using a Pasteur pipette and transferred into a 15 ml tube containing 1 ml (or less if the pellet was not visible) of G-IVF™ + 5% HSA.

Mini-gradient preparation

Samples suitable for a mini-gradient were layered over 0.5 ml of warm 80% PureSperm in a 1.5 ml Safe-Lock® microcentrifuge tube (embryo-tested; Eppendorf SE, Hamburg, Germany) and centrifuged for 10 minutes at 500 g. The supernatant was removed, and the pellet was washed in 1 ml G-MOPS™+10% HSA by centrifugation for 5 minutes at 500 g. The final pellet was resuspended in 0.1 ml G-MOPS™+10% HSA.

Erythrocyte lysis buffer (ELB) treatment

Samples with a high proportion of red blood cells were placed in a 15 ml tube containing 2 ml G-MOPS™+10% HSA and centrifuged at 0.5 RCF for 10 minutes. The supernatant was removed, and the pellet was resuspended in 0.5 ml ELB (Red Blood Cell Lysis Buffer; Roche Diagnostics GmbH, Mannheim, Germany) and incubated at room temperature for 5 minutes. Following incubation, 2 ml G-MOPS™+10% HSA was added and the sample centrifuged again at 0.5 RCF for 10 minutes. The supernatant was removed, and the pellet resuspended in 0.1 ml G-MOPS™+10% HSA.

Phosphodiesterase inhibitor treatment

Samples containing non-motile or poorly motile spermatozoa after preparation were treated with GM501 SpermMobil (Gynemed GmbH Co. KG, Sierksdorf, Germany), the only phosphodiesterase inhibitor-containing product approved by the Therapeutic Goods Administration (TGA; ARTG ID 390549) for human use in Australia. GM501 SpermMobil is a HEPES-buffered, HSA-free medium with low bicarbonate concentration, designed to enhance

sperm motility, particularly in necrozoospermic ejaculates and immotile spermatozoa retrieved from testicular tissue. A volume of 3–4 µl GM501 SpermMobil was added to the sperm-containing drop in the ICSI dish (see section 4.2.10; approximately 30–40 µl, diluted 1:10) and incubated in a warming incubator without gas at 37 °C for 10 minutes to facilitate sperm activation prior to ICSI.

4.2.9 Ovulation Induction and Oocyte Collection

Patients underwent ovarian hyperstimulation to optimise the number of oocytes available for treatment. The specific protocol and dose of follicle-stimulating hormone (FSH) were determined by the patient's fertility specialist. Most patients were managed using a GnRH antagonist protocol, in which the ovaries were stimulated with daily injections of recombinant FSH (rFSH; Gonal-F, Merck, Darmstadt, Germany, or Puregon, MSD, NJ, USA) from day 1 or 2 of the menstrual cycle. Down-regulation was achieved with daily GnRH antagonist injections commencing on day 5–7 of the cycle (Cetrotide, Merck, or Orgalutran, MSD).

A smaller group of patients underwent a long down-regulation protocol, receiving daily injections of a GnRH agonist from day 21 of the cycle (Lucrin; leuprorelin acetate; AbbVie Pty Ltd, North Ryde, NSW, Australia, or Decapeptyl; triptorelin; Ipsen Pty Ltd, Sydney, NSW, Australia). Daily rFSH injections (Gonal-F, or Puregon) commenced once full ovarian suppression had been achieved, confirmed by the onset of menstruation and ultrasound examination. In approximately half of patients, rFSH stimulation was supplemented with daily recombinant luteinising hormone (rLH; Luveris or Pergoveris, Merck).

Follicular development was monitored by serum oestradiol measurement and transvaginal ultrasound. When three or more follicles reached a diameter of ≥17 mm, final oocyte maturation was induced with a trigger injection of human chorionic gonadotrophin (hCG; Ovidrel 250 µg, Merck) or, in applicable GnRH antagonist cycles, a GnRH agonist (Lucrin or Decapeptyl).

Oocytes were retrieved 36–38 hours after the trigger injection by transvaginal ultrasound-guided follicle aspiration (oocyte pick-up, OPU). Cumulus–oocyte complexes

(COCs) were identified in the follicular fluid, washed in G-MOPS™+5% HSA, transferred into pre-equilibrated G-IVF™ Plus, and maintained at 37 °C in 6% CO_2 until denudation.

4.2.10 Denudation and Intracytoplasmic Sperm Injection (ICSI)

Patients included in this study had a male-factor component to their infertility diagnosis, characterised by poor semen parameters. As a result, all patients required ICSI to achieve fertilisation.

Cumulus cells were removed from all COCs through a process known as denudation. COCs were transferred into a denudation dish containing 80 IU hyaluronidase (0.1 ml HYASE-10X™ (Vitrolife AB) diluted in 1 ml G-MOPS™+5% HSA) in a centre-well dish (Vitrolife AB; product ref. 16005). Initial denudation to remove the majority of cumulus cells was performed using an embryo-tested glass Pasteur pipette (229 mm; ORIGIO®, CooperSurgical, Trumbull, CT, USA). The oocytes were then transferred to a 40 mm culture dish containing drops of G-MOPS™+5% HSA under Ovoil™ for further fine denudation using a glass handling pipette with an inner diameter of 190–210 µm (Vitrolife AB; product ref. 15537). This step was repeated in a fresh drop using a narrower glass handling pipette with an inner diameter of 127–129 µm (Vitrolife AB; product ref. 15531) to ensure complete removal of all remaining cumulus cells. Denuded oocytes were then placed into 1 ml G-1™ Plus in a centre-well dish and maintained in a gassed incubator prior to ICSI.

ICSI was performed 39–40 hours after the hCG trigger injection by a trained embryologist. All micromanipulation was carried out using a Nikon Ti Eclipse inverted microscope fitted with either (i) Narishige micromanipulators (Narishige Group, Tokyo, Japan), (ii) Narishige MTK-1 Takanome micromanipulators, or (iii) an RI Integra 3™ micromanipulator, together with a heated stage (Thermo Plate, Tokai Hit, Shizuoka-ken, Japan). Holding and injection pipettes (Vitrolife AB; product refs. 15305 and 15430) were attached and precisely aligned.

Microinjection was performed in 10 µl drops of pre-equilibrated G-MOPS™+5%HSA under Ovoil™, with each oocyte positioned on the holding pipette such that the polar body positioned at either 12 or 6 o'clock. PVP (ICSI™; Vitrolife) was used to slow sperm motility and facilitate immobilisation and capacitation. A single spermatozoon was aspirated into the

injection pipette and gently introduced into the oocyte cytoplasm head-first. Membrane rupture and oocyte activation were achieved by gentle aspiration and expulsion of the oolemma.

Following microinjection, oocytes were transferred to a pre-equilibrated dish containing G-1™ Plus under Ovoil™ and returned to the incubator overnight (see Section 4.2.12 for details of embryo culture set-up).

4.2.11 Fertilisation Assessment

Fertilisation was assessed 16–18 hours after microinjection (designated as Day 1) and confirmed by the presence of two pronuclei (2PN). For patients scheduled for a fresh embryo transfer (ET), culture was continued as described in Section 4.2.12. Patients assigned to a freeze-all embryos (FAE) cycle had all fertilised oocytes cryopreserved at this time.

4.2.12 Embryo Culture

Following injection, oocytes were transferred into one of two culture systems used in the WFC embryology laboratory.

For culture in the EmbryoScope+ time-lapse incubator (Vitrolife), an EmbryoSlide+® culture dish (Vitrolife AB; product ref. 16450) was used. Each slide contains 16 microwells arranged in two partitions, each holding 180 µl of G-1™ Plus culture medium, together with four larger 30 µl washing wells (also containing G-1™ Plus). All wells were overlaid with 1.8 ml Ovoil™. Slides were pre-equilibrated for two hours in a 6% CO_2, 7% O_2 incubator (Heraeus BBD 6220; Thermo Fisher Scientific, Waltham, MA, USA) before one injected oocyte was placed into each microwell, giving a total of 16 injected oocytes per slide. The EmbryoSlide+® was then placed into the EmbryoScope+ for continued culture.

For culture in the CulturePro incubator (Vitrolife), a CulturePro® culture dish (Vitrolife AB; product ref. 16352) was used. Each dish contains four culture wells holding 50 µl of G-1™ Plus, with each well subdivided into four compartments by a cross-shaped fence, creating a well-of-wells (WOW) configuration. Four larger 100 µl washing wells (also containing G-1™ Plus) are positioned at the base. All wells were overlaid with 1.6 ml Ovoil™. Dishes were

pre-equilibrated as above, and one injected oocyte was placed into each WOW, giving a total of 16 injected oocytes per dish. The CulturePro® dish was then placed into the CulturePro incubator for continued culture. As this incubator is not fitted with a time-lapse imaging system, dishes were removed for fertilisation and embryo assessment.

On Day 3 of development, the slide or dish was removed from the incubator and embryos were transferred individually into the washing well of a pre-equilibrated EmbryoSlide+® or CulturePro® dish containing G-2™ Plus medium overlaid with Ovoil™. Each embryo was washed twice in G-2™ Plus to remove all traces of G-1™ Plus and then returned to the corresponding microwell in the new slide or dish to maintain continuity of developmental history and, where applicable, to allow uninterrupted time-lapse imaging.

Embryo development in the EmbryoScope+ time-lapse incubator was monitored by automated image capture every 10 minutes. This system enables continuous, undisturbed culture under stable environmental conditions, allowing precise annotation of preimplantation developmental events. Time-lapse recordings were used to document key morphokinetic parameters from fertilisation to blastocyst formation.

Embryo development in the CulturePro incubator was assessed manually using an inverted microscope, and observations were recorded in the patient's laboratory notes.

4.2.13 Assessment of Embryo Morphology

Embryo morphology and development were assessed using a Nikon Ti Eclipse inverted microscope prior to embryo transfer on Day 2, Day 3, or Day 5. Cleavage-stage embryos were evaluated by recording the number of blastomeres, the degree of fragmentation, blastomere symmetry, and the presence of visible nuclei. Embryos were classified as follows:

A — no fragmentation, regular blastomeres, and nuclei visible in most cells;

B — some fragmentation, blastomere irregularity, and no visible nuclei;

C — highly fragmented, irregular, poor-quality embryos.

Blastocysts were graded according to the Gardner and Schoolcraft scoring system (Gardner & Schoolcraft, 1999). Briefly, blastocysts were assessed for the degree of expansion: early

blastocysts were assigned a score of 1 or 2; those with a clearly defined cavity were graded as 3 or 4; blastocysts initiating hatching were graded as 5; and fully hatched blastocysts were graded as 6. The quality of the inner cell mass (ICM) and trophectoderm (TE) was graded as A, B, or C, with A representing the highest quality and C the lowest.

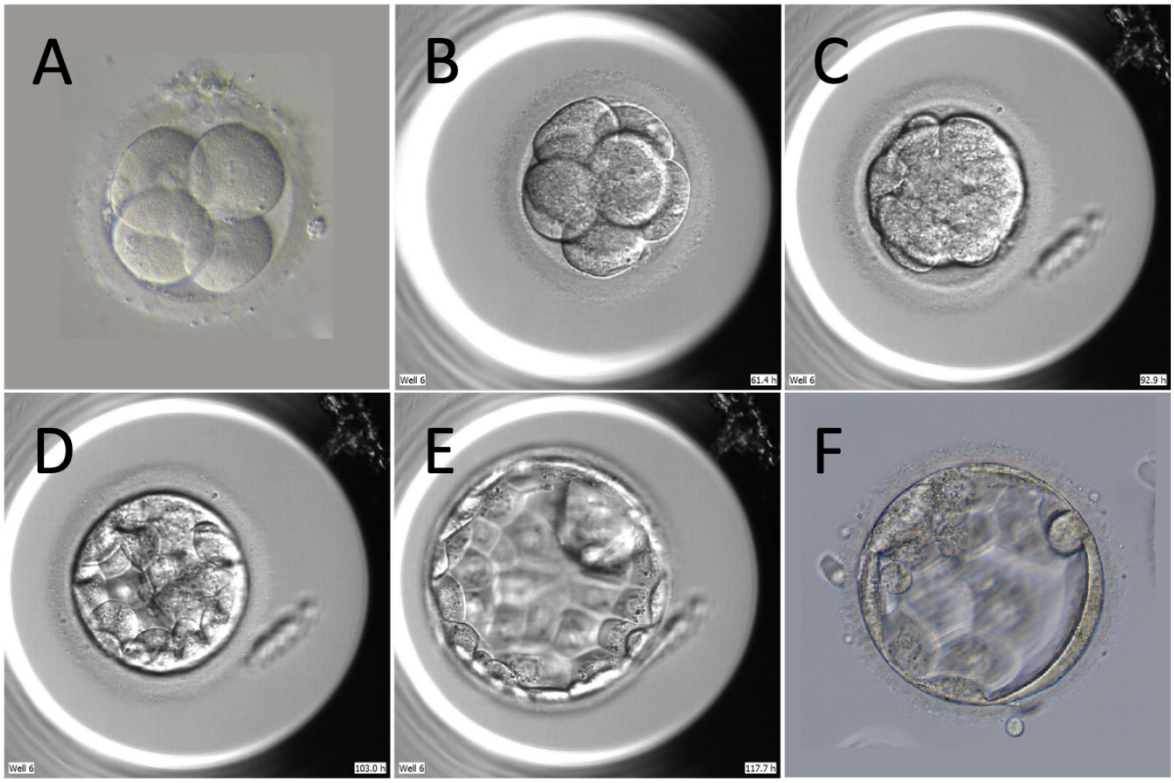

Figure 2.5. Representative images of embryo morphology at key developmental stages. Images showing (A) a 4-cell embryo with even sized blastomeres, visual nuclei and no fragmentation, (B) an 8-cell embryo with even sized blastomeres and no fragmentation, (C) a morula, (D) an early blastocyst with grade 2 cavity expansion, (E) a 4AA blastocyst with grade 4 expansion top quality ICM and TE, (F) a 4CC blastocyst with grade 4 expansion poorly defined ICM and TE.

4.2.14 Embryo Transfer

Embryos were most commonly transferred on Day 5 at the blastocyst stage, either as a fresh transfer or as a frozen embryo transfer (FET) in a subsequent cycle. A smaller group of patients with few fertilised embryos, or with a history of poor embryo development, had embryos

transferred on Day 2 at the 2–4-cell stage or on Day 3 at the 6–8-cell stage. In all cases, the highest-quality embryo, as assessed by morphology (Section 4.2.13), was selected for transfer.

Following grading, the embryo designated for transfer was placed into a centre-well dish containing 1 ml of pre-equilibrated EmbryoGlue™ (Vitrolife) up to 60 minutes before transfer for blastocysts, and 20 minutes before transfer for Day 2 and Day 3 embryos.

Transfer was performed once the catheter (Guardia™ Access, Cook Medical, O'Halloran Road, Nat Tech Park, Limerick, Ireland) had been correctly positioned by the clinician. After identity checks were completed, the embryo was loaded into the inner catheter using a syringe containing warmed G-2™ Plus and then transferred to the patient.

4.2.15 Embryo Freezing and Thawing

Embryos were frozen at two developmental stages. At the 2PN stage on Day 1, embryos were slow-frozen into straws (Cryo Bio System Groupe, IMV Technologies, Saint Ouen, France) using Freeze Kit Cleave™ (Vitrolife). On Day 5, blastocysts were vitrified using Rapid Vit Blast™ (Vitrolife) and loaded onto Rapid-i™ straws (Vitrolife). Freezing at both stages was performed in accordance with the manufacturer's instructions.

Embryos were thawed at the 2PN stage using Thaw Kit Cleave™ (Vitrolife) following the manufacturer's protocol and cultured to Day 2, Day 3, or Day 5 for transfer, depending on the number of embryos available and the patient's previous embryo-development history. Vitrified blastocysts were warmed using Rapid Warm Blast™ (Vitrolife) as per the manufacturer's instructions and allowed 2–3 hours for re-expansion prior to grading for transfer.

4.2.16 Pregnancy Determination and Clinical Definitions

The following criteria were applied to all outcome data in the study:

- Positive pregnancy: a serum β-hCG level >5 IU measured 14 days after embryo transfer.

- Implantation: confirmed by ultrasound detection of ≥1 gestational sac within the uterine cavity 6–8 weeks after embryo transfer.

- Clinical pregnancy: defined as a positive serum β-hCG result together with ultrasound confirmation of ≥1 gestational sac within the uterine cavity 6–8 weeks after embryo transfer.

- Ongoing pregnancy: confirmed by the presence of a viable fetal heartbeat detected by ultrasound from 6 weeks after embryo transfer.

- Live birth: recorded together with gestational age at delivery, birthweight, infant sex, and any reported congenital abnormalities or maternal complications.

- Biochemical pregnancy: defined as a positive serum β-hCG result with no gestational sac visible on ultrasound at 6–8 weeks.

- Miscarriage: recorded when a positive β-hCG result and ultrasound detection of ≥1 gestational sac and fetal pole at 6–8 weeks were followed by absence of a detectable fetal heartbeat.

- Blighted ovum: defined as a positive β-hCG result with ultrasound detection of ≥1 gestational sac but no fetal pole at 6–8 weeks.

4.2.17 Statistical Analysis

Statistical analysis was not performed due to the circumstances outlined in Section 4.2.1. In general, for the type of data intended for this study, a generalised linear mixed model (GLMM) would be used to analyse fertilisation rates across the ICSI cohorts subjected to different sperm-preparation protocols. GLMMs would also be applied to outcomes including embryo grade, utilisation rate, pregnancy, miscarriage, and live-birth rates. A p-value < 0.05 would be considered statistically significant. The modelling would account for relevant covariates such as female age at the time of oocyte retrieval and whether the embryo transferred was fresh or frozen–thawed.

4.3 Results

Due to the absence of site-specific approval (SSA), no patient data could be accessed, extracted, or analysed for this retrospective cohort study. As outlined in Section 4.2.1, the project met ethical requirements under the National Statement on Ethical Conduct in Human Research (2023) and received HREC approval; however, without SSA, the study could not progress to data collection. Consequently, no clinical, embryological, or laboratory outcomes relating to the different sperm preparation techniques, including clinical use of GM501 SpermMobil (THEO), were available for evaluation.

Although the intended analyses could not be performed, the study design would have enabled comparison of fertilisation, embryo development, utilisation, pregnancy, miscarriage, and live-birth outcomes across preparation methods used for ejaculated, epididymal, and testicular spermatozoa. The planned statistical approach, including generalised linear mixed models (GLMMs), is described in Section 4.2.17.

As no data were obtained, no statistical analyses were conducted, and no results are presented in this chapter.

4.4 Chapter Summary

Although this study was unable to proceed to data collection, the chapter outlines a robust methodological framework for evaluating the clinical impact of different sperm preparation techniques in MAR cycles. The rationale for this work remains highly relevant: epididymal and testicular samples vary widely in quality, and the effectiveness of laboratory preparation directly influences the likelihood of identifying viable sperm for ICSI. Clinical experience and published evidence consistently show that approaches such as density-gradient preparation, erythrocyte lysis, and targeted mechanical processing improve the recovery of usable spermatozoa from surgically retrieved samples. Likewise, the use of motility-enhancing agents such as GM501 SpermMobil can facilitate the identification of viable sperm in cases of immotility, particularly in testicular or severely compromised ejaculated samples.

The absence of retrospective data limits the ability to draw conclusions specific to the WFC patient population; however, the methodological structure developed for this chapter provides a strong foundation for future evaluation once appropriate approvals are secured. The broader implications of sperm preparation strategies—and their reported effects on fertilisation, embryo development, and clinical outcomes—are explored in Chapter 5 in the context of current literature.

Chapter 5

Discussion

5.0 Discussion

The overarching aim of this thesis was to evaluate the safety and developmental consequences of exposing mammalian embryos and spermatozoa to phosphodiesterase (PDE) inhibitors, specifically pentoxifylline (PTX) and theophylline (THEO), within the context of assisted reproductive technologies (ART). Across three complementary chapters, this work examined: (i) the developmental competence and cell-number outcomes of mouse embryos following microinjection of PTX or THEO (Chapter 2); (ii) the morphokinetic consequences of these exposures using time-lapse imaging (Chapter 3); and (iii) the clinical rationale and methodological framework for assessing sperm preparation techniques, including PDE inhibitor use, in human fertility treatment (Chapter 4). Together, these chapters provide a multi-layered evaluation of PDE inhibitors use in ART, spanning controlled laboratory experimentation, embryological kinetics, and clinical practice.

Although the clinical component could not proceed due to the absence of site-specific approval, the experimental findings offer important insights into the biological effects of PTX and THEO, while the methodological design of Chapter 4 highlights the ongoing need for rigorous evaluation of sperm preparation strategies in clinical settings. This discussion synthesises the findings across the thesis, situates them within the broader literature, and considers their implications for laboratory practice, clinical decision-making, and future research.

The increasing reliance on PDE inhibitors to activate viable but immotile sperm in severe male-factor infertility makes it essential to examine whether these compounds have any unintended downstream effects on the earliest stages of embryo development. Although their ability to stimulate motility can provide a pathway to fertilisation in otherwise intractable cases, the consequences of exposing gametes or resulting embryos to such agents remain incompletely understood. Much of the ART literature has focused on the benefits of

motility enhancement, whereas the possibility that even transient exposure may influence embryogenesis, cleavage dynamics, or later fetal development has received far less attention.

Since the introduction of pentoxifylline in 1988 (Yovich et al., 1988), its usefulness, optimal dosing, and potential adverse effects have remained subjects of debate. Evidence suggests a dualistic profile: PTX enhances sperm motility (Pereira et al., 2017), yet elevated concentrations have been associated with reduced embryo viability (Fisher & Gunaga, 1975), compromised membrane integrity (Tournaye et al., 1994a), and increased oxidative stress (Mirończuk-Chodakowska et al., 2018; Perk et al., 2008). Clinical findings are similarly mixed, with some studies reporting improved fertilisation outcomes (Mahaldashtian et al., 2021), while others caution against dose-dependent toxicity (Tournaye et al., 1995). Oral administration studies show potential benefits for both male and female reproductive parameters (Dadgar et al., 2023; Vitale et al., 2022), yet multicentre data highlight persistent inconsistencies (Navas et al., 2017). This variability underscores the need for controlled experimental models capable of isolating true compound-specific effects.

5.1 Effects of PDE Inhibitor Microinjection on Embryo Development

Although PDE inhibitors are widely used to enhance sperm motility in ART, their impact on early embryo development is poorly defined. Most mouse studies expose zygotes to these agents in culture, an approach that neither reflects clinical use nor provides a functional assessment of developmental competence. Whether clinically relevant concentrations of PTX or THEO pose any risk when introduced in a clinically realistic manner therefore remains unknown.

In the current work we addressed this gap using a functional mouse embryo assay which replicates ICSI-like exposure by microinjecting PTX or THEO directly into zygotes. PVP-injected, medium-injected, and non-injected controls provided a framework for separating injection-related effects from true compound-specific outcomes. Through detailed assessment of cleavage, blastocyst development, blastocysts cell composition and morphokinetic profile, we evaluated the developmental safety of PDE inhibitors at the point of gamete manipulation. The initial work established a technically robust microinjection

protocol and demonstrated that mouse zygotes tolerate microinjection well when performed under optimised conditions.

Early developmental outcomes, cleavage and blastocyst formation at 96 hours, were broadly comparable across groups, indicating that neither PTX nor THEO impaired early viability. Cleavage rates did not differ significantly between groups with proportions ranging from 71.4% in the iPVP group to 87.0% in both the CON and iCON groups, indicating that microinjection with the various solutions did not impair early embryo viability or the ability to cleave.

Blastocyst development, a key indicator of pre-implantation competence, also showed no significant differences between groups. The highest blastulation rate at 96 h was observed in the non-injected CON group (87.0%), while THEO-, PTX-, and PVP-injected embryos showed modestly lower rates (62.5–71.2%). Importantly, all embryos that cleaved progressed to the blastocyst stage by 114 h. These values remained above the ≥70% threshold commonly referenced in MEA validation guidelines (Scott et al., 1993). Current guidelines from the US food and drug administration, FDA for MEA in assisted reproduction technology devices suggests a more stringent limit of ≥80% embryos developed to expanded blastocyst at 96 hours in culture (120 h post hCG)(US Food Drug Administration, 2021). Most experimental groups met or approached this threshold, although THEO-injected embryos were marginally below and PVP-injected embryos lower still.

Conventional MEA exposes 1-cell embryos to the test agent in culture, whereas the present study used a functional microinjection approach. This distinction is critical because manual zygote microinjection itself can reduce developmental potential. Liu and colleagues reported <30% blastocyst development following manual microinjection of HTF medium, increasing to 45–50% with automated injection and to 89% when injected embryos were cultured in KSOM (Liu et al., 2011). These findings highlight both the technical complexity of manual zygote injection and the importance of using a functional assay to appropriately evaluate toxicity and safety. The consistently high blastocyst development rates observed across all injected groups in the present study therefore provide reassurance that the injection procedure was well-tolerated and that any differences observed are unlikely to reflect procedural artefact.

This finding further underscores the importance of appropriate injection controls in experimental embryology.

When more sensitive endpoints were examined, important differences emerged in the present study. The media-only injection control (iCON) consistently underperformed, particularly in hatching and in the proportion of top-quality 5AA blastocysts, indicating that the act of injecting medium alone can introduce a detrimental effect not seen with PVP, PTX, or THEO. This observation aligns with findings from gene-editing research where zygote microinjection is routinely used, particularly for introducing CRISPR (clustered regularly interspaced short palindromic repeats)–Cas (CRISPR-associated) components into the embryo. In a recent study evaluating the most efficient method for CRISPR-Cas9 delivery, the authors used piezo-driven microinjection and included a culture-medium injection group as a procedural control. Although 96.6% of medium-injected zygotes cleaved and 90.7% of cleaved embryos reached the blastocyst stage, only 55.8% of these blastocysts were classified as high-grade (Stamatiadis et al., 2021). This pattern mirrors the present findings and reinforces that microinjection itself, independent of any test compound, can subtly impair blastocyst quality even when overall developmental progression appears normal.

Total cell count provides a more sensitive measure of embryo quality than simple progression to the blastocyst stage, as it reflects the embryo's proliferative capacity rather than its ability to reach a structural milestone. In this study, total cell-number analysis revealed the most striking divergence between the two PDE inhibitors. PTX-injected embryos showed a clear and statistically significant reduction in total cell number (145 ± 25, $p<0.05$) compared with untreated controls (168 ± 37), indicating that PTX imposes a measurable constraint on proliferative capacity even when overall development to the blastocyst stage appears normal. In contrast, THEO-injected embryos displayed cell numbers indistinguishable from controls (171 ± 27, ns), suggesting that THEO does not adversely affect cell proliferation.

These findings are consistent with those of Satish et al., who reported that sperm exposed to PTX during preparation produced blastocysts with significantly reduced total cell numbers and a markedly higher apoptotic index (Satish et al., 2021). Importantly, these detrimental effects were alleviated when a modified PTX analogue was used. Together, these results reinforce the

view that PTX can negatively influence early embryonic development and cell survival, even when exposure occurs indirectly via treated sperm, and highlight a pattern of PTX-specific developmental toxicity that is not observed with THEO.

Further, the clinical analogue control, zygotes injected with PVP (167 ± 15), performed equivalently to the non-injected group. This finding is reassuring, as PVP is routinely introduced into oocytes during ICSI to facilitate sperm immobilisation and handling. The absence of any reduction in cell number in the iPVP group confirms the developmental safety of standard ICSI practice and underscores that the proliferative deficit observed in the PTX group reflects a compound-specific effect rather than an artefact of the injection environment.

The media-only control (iCON) also exhibited significantly lower cell numbers, suggesting that microinjection with medium alone can reduce proliferative capacity, possibly due to subtle variations in injection volume or flow rate in the absence of PVP.

5.2 Morphokinetic Consequences of PDE Inhibitor Exposure

Time-lapse imaging enabled detailed assessment of whether PTX or THEO disrupt the intrinsic timing and coordination of early cleavage events. Because early cleavage timings are exquisitely sensitive to biological stressors, morphokinetics provide a powerful means of detecting subtle disturbances that may not manifest in blastocyst rates (Coticchio et al., 2020).

In this study, several differences were initially observed when timings were referenced to hCG, but these largely disappeared when normalised to pronuclear fading (tPNf), indicating that variation in mating and fertilisation timing contributed more to the observed differences than the treatments themselves. Neither PTX nor THEO disrupted cleavage-cycle duration or synchrony. The only remaining difference was a modest delay in morula formation in iPTX, which did not persist into later stages.

Morphokinetic timings can be altered by minor deviations in temperature or gas composition during embryo culture (Nguyen et al., 2020; Walters et al., 2020). Mouse embryo morphokinetics have been proposed as highly sensitive markers of in-vitro stress and may

represent a stronger primary endpoint for MEA than blastocyst formation, which is used in standard quality-control assays (Morbeck, 2017; Wolff et al., 2013). Early cleavage timings were found to be particularly sensitive indicators of embryotoxicity, capable of detecting disturbances at concentrations that do not affect blastocyst formation. The study reported that the cell-cycle events most vulnerable to toxic insult occur within the first 72 h of culture (Wolff et al., 2013). In the present study, these key early morphokinetic indicators of embryo health, ECC2, ECC3, and the synchronisation parameters s2 and s3, were comparable across all groups. The consistency observed suggests that neither THEO nor PTX perturbs the intracellular regulatory mechanisms governing early cleavage timing.

Taken together, these findings show that PTX affects cell number but does not disrupt the fundamental kinetic architecture of early development, whereas THEO appears benign across both morphological and kinetic endpoints. Although embryos exposed to PTX or THEO appear to develop normally based on cleavage timing and blastocyst formation, the reduction in cell number associated with PTX indicates that more sensitive developmental features may be affected. Because blastocyst cell number correlates with implantation potential (Gardner et al., 2000; Richter et al., 2001), such subtler effects may still have clinical relevance.

5.3 Clinical Context and Methodological Framework

Although no clinical data could be analysed, Chapter 4 established a rigorous framework for evaluating sperm preparation techniques in human ART. Sperm retrieved from ejaculates, epididymal aspirates, or testicular biopsies vary widely in quality, and preparation methods, including density gradients, erythrocyte lysis, mechanical teasing, and motility-enhancing agents, directly influence the embryologist's ability to identify viable sperm for ICSI.

Clinical experience and published evidence indicate that PDE inhibitor-based motility enhancers, such as GM501 SpermMobil, can facilitate the identification of viable sperm in cases of immotility, particularly in testicular samples (Ebner et al., 2014; Ebner et al., 2011; Wöber et al., 2015). The absence of data from this study highlights the need for future evaluation but does not diminish the clinical relevance of the methodological design

5.4 Integrating Experimental and Clinical Perspectives

Clinically, the findings are broadly reassuring. Embryos in human ART are unlikely to experience direct cytoplasmic exposure to PTX or THEO; any exposure occurs during sperm preparation, and only trace residues would enter the oocyte during ICSI rather than being introduced directly into the zygote. The absence of major developmental disturbances in this study therefore supports the general safety of these compounds under typical laboratory conditions. Nevertheless, the observation that PTX reduces cellular proliferation indicates that some caution remains warranted. Several clinical studies report mixed outcomes when PTX is used for motility enhancement (Mahaldashtian et al., 2021; Pereira et al., 2017; Perk et al., 2008), and the present findings provide a biological rationale for conservative exposure protocols. THEO, by contrast, showed no detrimental effects on morphokinetics or total cell number, making it a potentially less disruptive option when motility enhancement is required (Ebner et al., 2015; Ebner et al., 2014; Ebner et al., 2011; Sandi-Monroy et al., 2019).

The clinical application of PDE inhibitors in ART is primarily dictated by the motility of retrieved spermatozoa, whether from ejaculated or testicular sources. In cases of necrozoospermia or severe asthenozoospermia, where motile sperm are absent or exceptionally rare, these agents serve as a vital tool for salvaging the cycle by stimulating the vital but immotile sperm to move. This stimulation facilitates the accurate identification and selection of viable sperm for ICSI, thereby maximizing fertilisation and pregnancy potential for this challenging patient cohort. Furthermore, the efficiency of the sperm collection step is critical due to the narrow oocyte's injection window. As the collected eggs have a definite time window for injection post triggering which shouldn't be exceeded otherwise any delay may affect the success rate for the whole treatment.

A key contribution of this thesis is the demonstration that different developmental endpoints capture different aspects of embryo health. Early cleavage and blastocyst formation were insensitive to PTX, whereas total cell number revealed a clear deficit. Morphokinetics showed no disruption of cell-cycle timing or synchrony. This underscores the importance of using multiple complementary endpoints when assessing embryo safety.

5.5 Limitations and Reasons for Caution

Several limitations must be acknowledged. First, the embryo experiments were conducted in a mouse model, which does not fully replicate human embryonic physiology. Second, the microinjection model introduces exposure directly into the cytoplasm of zygotes, which may not reflect the exposure route in clinical sperm preparation and ICSI. Third, the absence of clinical data in Chapter 4 limits the ability to evaluate the real-world impact of sperm preparation techniques within the WFC population.

Caution is also required when extrapolating findings across PDE inhibitors. PTX and THEO differ in potency, pharmacokinetics, and intracellular effects, and their safety profiles cannot be assumed to be equivalent. Finally, the suppressive effect of PTX on cell number, although consistent, was modest, and its clinical significance remains uncertain.

5.6 Concluding Remarks and Clinical Significance

This thesis provides a comprehensive evaluation of PDE inhibitor exposure in ART, integrating experimental embryology, morphokinetics, and clinical methodology. The findings demonstrate that:

- THEO appears safe across all measured endpoints.
- PTX reduces total cell number, indicating a subtle effect on proliferative capacity.
- Neither compound disrupts morphokinetics, suggesting that the fundamental architecture of early development remains intact.
- Clinical sperm preparation techniques warrant systematic evaluation, particularly in cases involving immotile or surgically retrieved sperm.

The clinical significance of this work lies in its contribution to the evidence base supporting safe and effective laboratory practice. As ART continues to evolve, the refinement of sperm preparation techniques and the careful evaluation of laboratory interventions will remain essential for optimising outcomes and ensuring the long-term health of children conceived through fertility treatment.

In conclusion, this investigation demonstrates that both THEO and PTX are compatible with normal preimplantation development when present at concentrations exceeding those encountered in clinical ART practice. The preservation of blastocyst formation rates and developmental timing across all treatment groups provides strong evidence that these compounds do not compromise fundamental developmental competence. However, the observation that PTX produces a mild but measurable reduction in blastocyst cell number, while THEO does not, indicates that these compounds exert differential effects on cellular proliferation that should be considered when selecting PDE inhibitors for clinical use.

Appendix 1.1

Abbreviations

ADP	Adenosine diphosphate
AEC	Animal ethics committee
AMP	Adenosine monophosphate
ANOVA	Analysis of Variance
ANZARD	Australia and New Zealand Assisted Reproduction Database
ART	Assisted reproductive techniques
ATP	Adenosine triphosphate
BTB	Blood-testis barrier
cAMP	Cyclic adenosine monophosphate
cc	Blastomere cell-cycle duration
CG	Chorionic gonadotrophin
COC	Cumulus–oocyte complex
CON	Control
COVID-19	Coronavirus disease 2019
CRC4	C-X-C chemokine receptor type 4
DNA	Deoxyribonucleic acid
ECC	Embryo cell cycle
ED	Erectile dysfunction
EGA	Embryonic genome activation
EPI	Epiblast
ET	Embryo transfer
FAE	Freeze all embryos
FDR	False discovery rate
FET	Frozen embryo transer
FSH	Follicle-stimulating hormone
GLMM	Generalised linear mixed model
GnRH	Gonadotropin-releasing hormone
hCG	Human chorionic gonadotrophin
HEPES	N-2-hydroxyethylpiperazine-N'-2-ethanesulfonic acid
HREC	Human research ethics committee
HSA	Human serum albumin
i.p.	Intraperitoneal
ICM	Inner cell mass
ICMART	Committee for monitoring assisted reproductive technologies
ICSI	Intra cytoplasmic sperm injection
IQR	Interquartile ranges
IU	International unit

IVF	*In vitro* fertilisation
LH	Luteinizing hormone
LOS	Large offspring syndrome
MAR	Medical assisted reproduction
MEA	Mouse embryo assay
MOPS	3-N-morpholino-propanesulphonic acid
MRT	Mitochondrial Replacement Therapy
OPU	Oocyte pick-up
PBS	Phosphate buffer saline
PDE	Phosphodiesterase
PDE	Phosphodiesterase
PESA	Percutaneous sperm aspiration
PFA	Paraformaldehyde
PGT-A	Preimplantation genetic testing for aneuploidy
PI	Propidium iodide
PKA	Protein kinase A
PLCζ	Sperm-specific phospholipase C zeta
PMSG	Pregnant-mare-serum-gonadotrophin
PMSG	Pregnant mare's serum gonadotrophin
PN	Pronuclei
PrE	Primitive endoderm
PTX	Pentoxifylline
PVP	Polyvinylpyrrolidone
QC	Quality control
RCF	Relative Centrifugal Force
RNA	Ribonucleic acid
ROS	Reactive Oxygen Species
RTAC	Reproductive technology accreditation committee
SD	Standard deviation
SSA	Site-specific approval
SSC	Spermatogonial stem cells
STF-1	Stromal-derived factor-1
TE	Trophectoderm
TESA	Testicular sperm aspirate
TESE	Testicular sperm extraction
TGA	Therapeutic Goods Administration
THEO	Theophylline
VOC	Volatile organic compound
WHO	World Health Organisation
WSLHD	Western Sydney Local Health District
ZGA	Zygote genome activation
ZP	Zona pellucida

Appendix 2.1

Culture Medium Composition

G-MOPS
Is a MOPS buffered culturing media used when handling the zygotes and embryos in ambient atmosphere.

Composition: Alanine, Alanyle-glutamine, Aspartame, Cacium chloride, Glucose, Glutamate, Glycine, Magnesium sulphate, MOPS, Penicillin G, Potassium chloride, Proline, Serine, Sodium bicarbonate, Sodium chloride, Sodium dihydrogen phosphate, Sodium lactate, Sodium pyruvate, Taurine, Water for injection.

G1 Plus
Medium used for supporting the embryos development from the pronucleate stage (Zygote) to day 3 stage (6-8 cells)

Composition: Alanine, Alanyl-glutamine, Asparagine, Aspartame, EDTA, Calcium chloride, Gentamicin, Glucose, Glutamate, Glycine, Human serum albumin, Hyaluronan, Magnesium sulphate, Penicillin G, Potassium chloride, Proline, Serine, Sodium bicarbonate, Sodium chloride, Sodium dihydrogen phosphate, Sodium lactate, Sodium pyruvate, Taurine, Water for injection.

G2 Plus
Medium used for culturing embryos from day 3 (6-8 cells) to the blastocyst stage (day5)

Composition: Alanine, Alanyl-glutamine, Arginine, Asparagine, Aspatame, Calcium chloride, Calcium pantothenate, Cystine, Gentamicin, Glucose, Glutamate, Glycine, Histidine, Human serum albumin, Hyaluronan, Isoeucine, Leucine, Lysine, Magnesium sulphate, Methionine, Penicillin G, Phenylalanine, Potassium chloride, Proline, Pyridoxine, Riboflavine, Serine, Sodium bicarbonate, Sodium chloride, Sodium dihydrogen phosphate, Sodium lactate, Sodium pyruvate, Thiamine, Tryptophan, Tyrosine, Valine, Water for injection.

Appendix 2.2

Harvesting of Mouse Zygotes

The collection of pre-implantation embryos from superovulated female mice is a well-established technique used to obtain embryos at defined developmental stages for experimental analysis. The procedures outlined in this appendix describe the steps involved in the humane sacrifice of the animal, dissection of the reproductive tract, and recovery of embryos ranging from the pronuclear 1-cell stage to the blastocyst stage. These methods follow standard laboratory practice for murine embryo collection and were performed under sterile conditions to ensure embryo viability and experimental consistency.

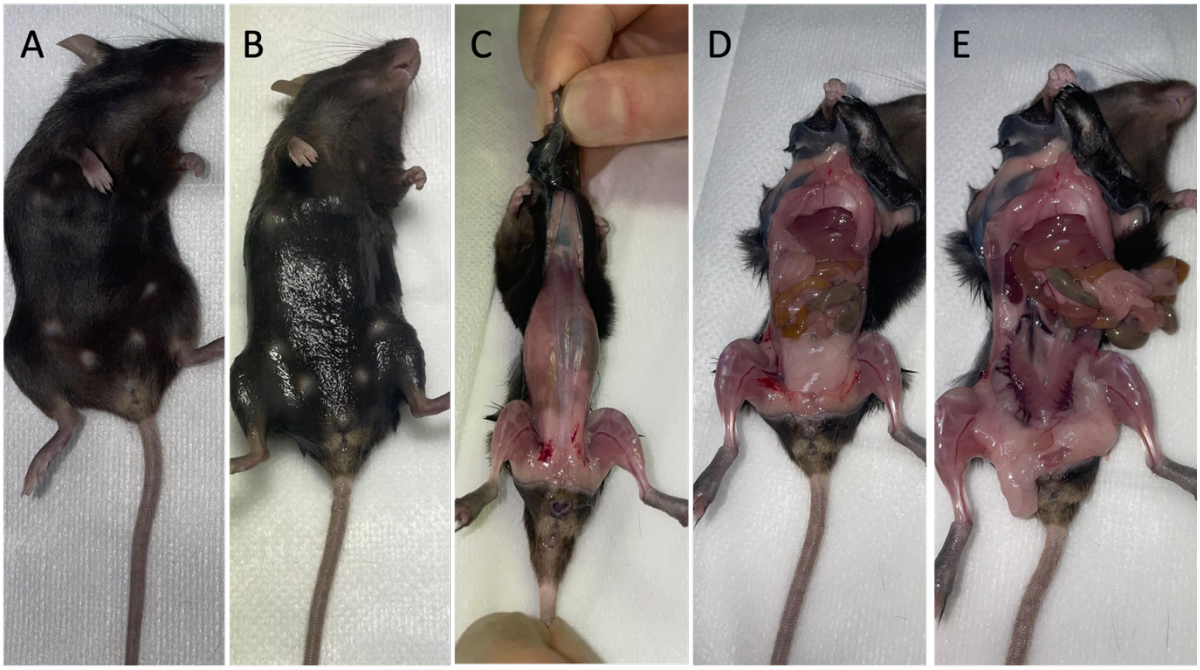

Figure A2.1: Dissection of a Female Mouse to Obtain the Reproductive Organs.

The dead mouse was placed on absorbent paper (A) and swabbed with 70% ethanol (B) to minimise the risk of contamination. A small lateral incision was made in the skin at the midline using surgical scissors, and the skin was then pulled towards the head and tail until the abdomen was fully exposed (C). The body wall (peritoneum) was incised (D), and the coils of gut were gently moved aside. The two uterine horns, oviducts, and ovaries were then located and removed from the body cavity (E).

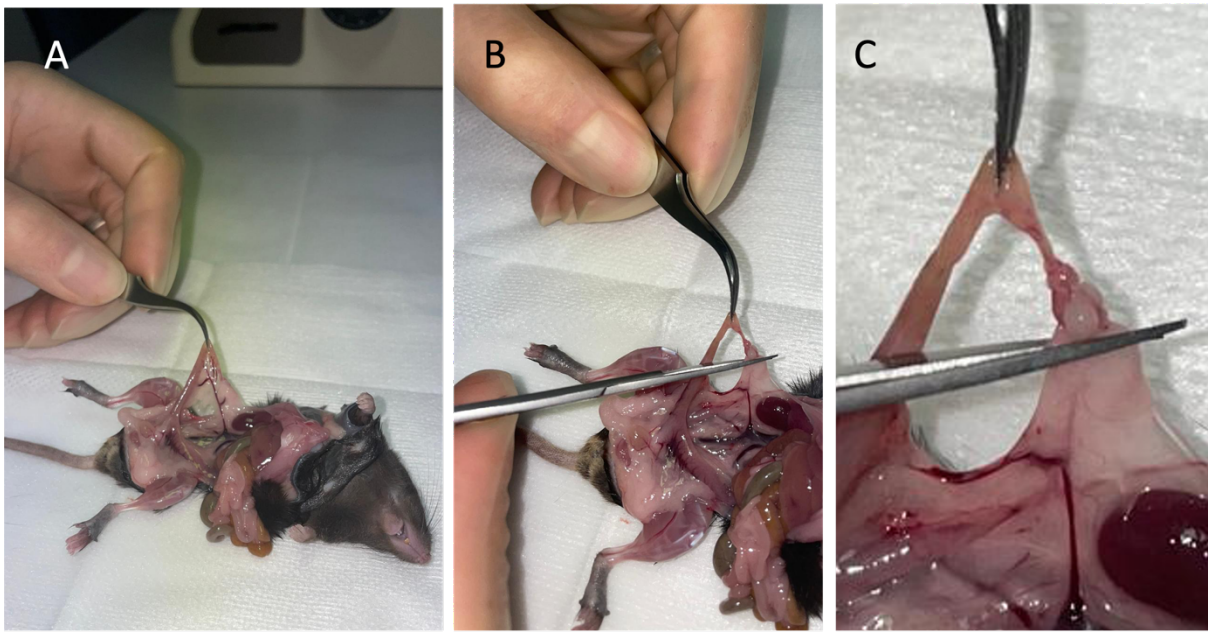

Figure A2.2: Locating and Dissecting the Reproductive Tract

The ovary, oviduct, and the upper portion of the uterus were separated from the mesometrium using fine forceps (A). A cut was made to detach the ovary from the mesometrium (B and C).

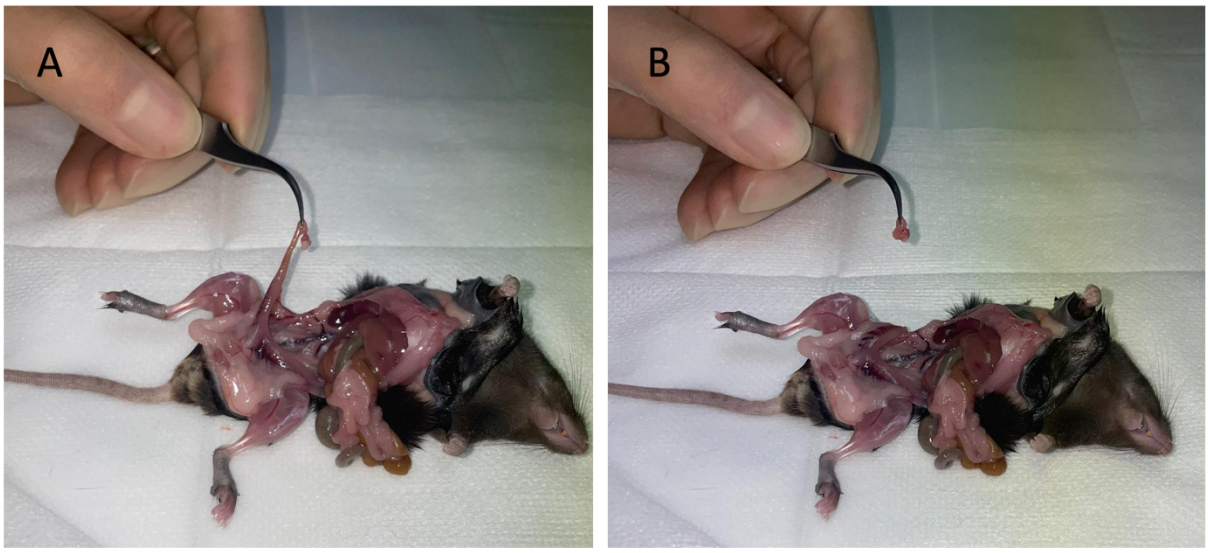

Figure A2.3. Dissection of the Oviduct

A second cut separates the oviduct from the uterus (A and B).

Appendix 2.3

Micromanipulation Set-Up

All micro manipulation was done using a Nikon Ti eclipse inverted microscope fitted with Narishige MTK-1 Takanome Micromanipulators (Narishige Group, Tokyo Japan) and a heated stage (Thermo Plate, Tokai Hit, Shizuoka-ken, Japan). Holding and injection pipettes (Vitrolife AB; Product Ref. 15305 and 15430) were attached and precisely aligned as detailed below.

To set up the Narishige Takanome micromanipulation system with the needles positioned correctly for zygote micromanipulation, the following steps were followed:

- Use the 4× objective and focus on a marked dish placed on the microscope stage.
- Ensure that all micromanipulation joysticks and pumps are centred and stable.
- Load the pipettes and raise them fully to the upper position.
- Lower each pipette slowly, one at a time, bring it into focus, and then tighten the holding screws to secure it.
- Rotate the pipettes so that they face each other directly and are parallel to the heated microscope stage.
- Press the air-pressure release buttons on both the injection and holding pumps.
- Switch to the 20× objective and perform fine-focus adjustments.
- Confirm that both pipettes are in sharp focus and correctly aligned for use.

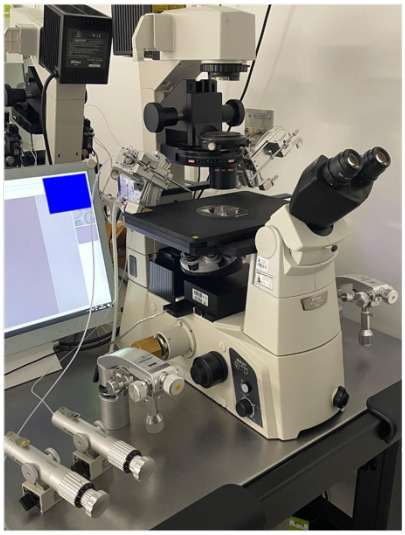
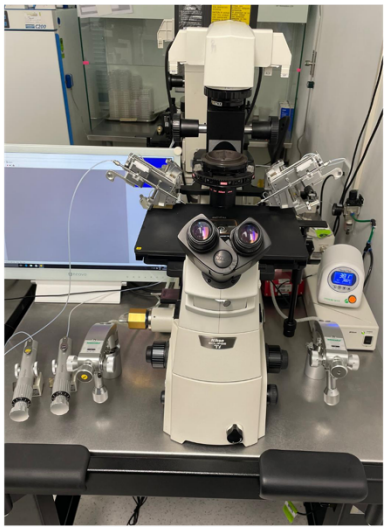


When ready to begin micromanipulating zygotes, raise the needles to the upper position and place the culture dish containing the zygotes onto the heated microscope stage. Focus on an empty culture drop and lower the pipettes into the field of view. Use the joystick controls to make fine adjustments so that the glass pipettes move freely without touching the bottom of the dish. Throughout the procedure, keep the zygotes in focus and use the micromanipulation controls to maintain the pipettes in focus as they are moved around the dish.

Appendix 2.4

Propidium Iodide Staining Solutions

Reagents

3.7% Paraformaldehyde (PFA), Phosphate buffered Saline (PBS), Polyvinylpyrrolidone (PVP), Triton X-100, Propidium Iodide (PI), RNase and Glycerol. All laboratory chemicals and reagents were purchased from Sigma-Aldrich / Merck (Bayswater, VIC, Australia).

Solution preparation

1mg/ml PVP in PBS

A total of 0.1 g of PVP was weighed on an electronic balance and added to a glass beaker containing 100 ml of PBS. The mixture was stirred with a glass rod until the PVP had fully dissolved. The PBS/PVP solution was then transferred into a sterile, lidded flask, labelled, and stored at 4 °C.

0.5% Triton X-100

A total of 0.5 ml of Triton X-100 was added slowly to a glass beaker containing 99.5 ml of PBS and stirred with a glass rod until fully mixed. The solution was then labelled and stored at 4 °C until use.

50pg/ml PI

Stock 1mg/ml of PI in PBS was prepared (0.001g PI in 1ml PBS). 50ul of the stock were then added to 950ml of PBS and solution was labelled and stored at 4°C in a dark flask wrapped with aluminium foil (light sensitive).

50pg/ml RNase

A 1 mg/ml stock solution of RNase was prepared (0.001 g RNase dissolved in 1 ml PBS). From this stock, 50 µl were added to 950 µl of PBS to obtain a final concentration of 50 µg/ml. The solution was labelled and stored at −20 °C until use.

Appendix 2.5

Supplementary Tables for Chapter 2.

This appendix presents the full statistical output supporting the analyses described in Chapter 2. For each dataset, both parametric (one-way ANOVA with Tukey's post-hoc test) and non-parametric (Kruskal–Wallis with Dunn's FDR-corrected post-hoc test) approaches were performed to ensure robustness across potential deviations from normality and unequal variances. The tables below provide the complete pairwise comparison results for all experimental groups in both 2D and 3D culture systems, including mean differences or mean rank differences, confidence intervals, adjusted p- or q-values, and significance classifications. These outputs correspond directly to the summary statistics and significance statements reported in the Results chapter.

Across both 2D and 3D culture systems, a consistent pattern emerged in which iTHEO and CON displayed significantly higher total cell counts than iPTX, with this relationship confirmed by both parametric (Tukey) and non-parametric (Dunn FDR-corrected) approaches. In contrast, iPVP did not differ significantly from iTHEO or CON in either system, indicating that its effects on total cell number were broadly comparable to untreated controls. The most reproducible differences were observed between iPTX and the higher-performing groups (iTHEO, CON), and between iCON and CON, where the direction and magnitude of effects were stable across statistical methods. Importantly, no contradictory outcomes were detected between ANOVA/Tukey and Kruskal–Wallis/Dunn analyses, supporting the robustness of the findings even in the presence of non-normal distributions or unequal variances. Overall, the combined statistical outputs demonstrate a clear and biologically coherent hierarchy of group effects that is maintained across both dimensional systems and analytical frameworks.

Tukey's multiple comparisons test for 2D and 3D total cell counts

Table S1. Tukey's Multiple Comparisons Test for 2D Total Cell Counts

Comparison	Mean difference	95% CI	Adjusted p value	Significant?
iTHEO vs iPTX	32.94	10.54 to 55.34	0.0009	***
iTHEO vs iPVP	–0.75	–27.56 to 26.06	>0.9999	ns
iTHEO vs iCON	33.11	7.94 to 58.28	0.0038	**
iTHEO vs CON	1.53	–25.97 to 29.03	0.9999	ns
iPTX vs iPVP	–33.70	–59.90 to –7.50	0.0050	**
iPTX vs iCON	0.17	–24.36 to 24.70	>0.9999	ns
iPTX vs CON	–31.41	–58.32 to –4.50	0.0138	*
iPVP vs iCON	33.87	5.25 to 62.49	0.0121	*
iPVP vs CON	2.28	–28.39 to 32.95	0.9996	ns
iCON vs CON	–31.58	–60.85 to –2.30	0.0278	*

Footnote: Tukey's multiple comparisons test following one way ANOVA

Table S2. Tukey's Multiple Comparisons Test for 3D Total Cell Counts

Comparison	Mean difference	95% CI	Adjusted p value	Significant?
iTHEO vs iPTX	26.35	5.77 to 46.93	0.0053	**
iTHEO vs iPVP	4.89	–19.74 to 29.52	0.9812	ns
iTHEO vs iCON	29.96	6.83 to 53.09	0.0046	**
iTHEO vs CON	–4.89	–30.16 to 20.38	0.9828	ns
iPTX vs iPVP	–21.46	–45.54 to 2.62	0.1037	ns
iPTX vs iCON	3.61	–18.93 to 26.15	0.9916	ns
iPTX vs CON	–31.25	–55.97 to –6.53	0.0061	**
iPVP vs iCON	25.07	–1.22 to 51.36	0.0690	ns (trend)
iPVP vs CON	–9.78	–37.97 to 18.41	0.8688	ns
iCON vs CON	–34.85	–61.74 to –7.96	0.0046	**

Footnote: Tukey's multiple comparisons test following one way ANOVA

Dunn's multiple comparisons test (FDR-corrected) for 2D and 3D total cell counts

Table S3. Dunn's Multiple Comparisons Test (FDR-Corrected) for 2D Total Cell Counts

Comparison	Mean rank difference	Adjusted q-value	Significant?
iTHEO vs iPTX	28.61	0.0013	**
iTHEO vs iPVP	–0.16	>0.9999	ns
iTHEO vs iCON	28.79	0.0060	**
iTHEO vs CON	–1.69	>0.9999	ns
iPTX vs iPVP	–28.77	0.0099	**
iPTX vs iCON	0.18	>0.9999	ns
iPTX vs CON	–26.92	0.0270	*
iPVP vs iCON	28.95	0.0240	*
iPVP vs CON	1.86	>0.9999	ns
iCON vs CON	–27.09	0.0548	ns (trend)

Footnote: Dunn's test with Benjamini–Hochberg FDR correction following Kruskal–Wallis.

Table S4. Dunn's Multiple Comparisons Test (FDR-Corrected) for 3D Total Cell Counts

Comparison	Mean rank difference	Adjusted q-value	Significant?
iTHEO vs iPTX	25.67	0.0059	**
iTHEO vs iPVP	3.68	>0.9999	ns
iTHEO vs iCON	28.35	0.0073	**
iTHEO vs CON	–3.10	>0.9999	ns
iPTX vs iPVP	–21.98	0.1183	ns
iPTX vs iCON	2.68	>0.9999	ns
iPTX vs CON	–28.77	0.0134	*
iPVP vs iCON	24.67	0.0970	ns (trend)
iPVP vs CON	–6.78	>0.9999	ns
iCON vs CON	–31.45	0.0126	*

Footnote: Dunn's test with Benjamini–Hochberg FDR correction following Kruskal–Walli

References

Agarwal, A., Mulgund, A., Hamada, A., & Chyatte, M. R. (2015). A unique view on male infertility around the globe. *Reprod Biol Endocrinol*, *13*, 37. https://doi.org/10.1186/s12958-015-0032-1

Ahmadi, H., Aghebati-Maleki, L., Rashidiani, S., Csabai, T., Nnaemeka, O. B., & Szekeres-Bartho, J. (2023). Long-Term Effects of ART on the Health of the Offspring. *Int J Mol Sci*, *24*(17). https://doi.org/10.3390/ijms241713564

Aitken, R. J. (2020). Impact of oxidative stress on male and female germ cells: implications for fertility. *Reproduction*, *159*(4), R189-r201. https://doi.org/10.1530/rep-19-0452

Aitken, R. J. (2024). Paternal age, de novo mutations, and offspring health? New directions for an ageing problem. *Hum Reprod*, *39*(12), 2645-2654. https://doi.org/10.1093/humrep/deae230

Animal Research Act 1985, New South Wales Consolidated Acts (1985). https://legislation.nsw.gov.au/view/html/inforce/current/act-1985-123

Asami, M., & Perry, A. C. F. (2025). Mouse and human embryonic genome activation initiate at the one-cell stage. *Front Cell Dev Biol*, *13*, 1594995. https://doi.org/10.3389/fcell.2025.1594995

Austin, C. R. (1952). The capacitation of the mammalian sperm. *Nature*, *170*(4321), 326. https://doi.org/10.1038/170326a0

Australian Code for the Care and Use of Animals for Scientific Purposes, (2013). https://www.nhmrc.gov.au/about-us/publications/australian-code-care-and-use-animals-scientific-purposes

Azevedo, M. F., Faucz, F. R., Bimpaki, E., Horvath, A., Levy, I., de Alexandre, R. B., Ahmad, F., Manganiello, V., & Stratakis, C. A. (2014). Clinical and molecular genetics of the phosphodiesterases (PDEs). *Endocr Rev*, *35*(2), 195-233. https://doi.org/10.1210/er.2013-1053

Barnes, F. L., Crombie, A., Gardner, D. K., Kausche, A., Lacham-Kaplan, O., Suikkari, A. M., Tiglias, J., Wood, C., & Trounson, A. O. (1995). Blastocyst development and birth after in-vitro maturation of human primary oocytes, intracytoplasmic sperm injection and assisted hatching. *Hum Reprod*, *10*(12), 3243-3247. https://doi.org/10.1093/oxfordjournals.humrep.a135896

Barratt, C. L. (2007). Semen analysis is the cornerstone of investigation for male infertility. *Practitioner*, *251*(1690), 8-10, 12, 15-17.

Behringer, R., Gertsenstein, M., Nagy, K. V., & Nagy, A. (2014). *Manipulating the Mouse Embryo: A Laboratory Manual*. Cold Spring Harbor Laboratory Press. https://books.google.com.au/books?id=LR2anQEACAAJ

Berntsen, S., Zedeler, A., Nøhr, B., Rønn Petersen, M., Grøndahl, M. L., Andersen, L. F., Løssl, K., Løkkegaard, E., Englund, A. L., Vestergaard Gabrielsen, A., Prætorius, L., Behrendt-Møller, I., Langhoff Thuesen, L., Vomstein, K., Petri Lauritsen, M., Ivanoska Trajcevski, A., Frøding Skipper, D., Westergaard, D., Pinborg, A., . . . la Cour Freiesleben, N. (2025). IVF versus ICSI in patients without severe male factor infertility: a randomized clinical trial. *Nat Med*, *31*(6), 1939-1948. https://doi.org/10.1038/s41591-025-03621-x

Bhabha, G., Johnson, G. T., Schroeder, C. M., & Vale, R. D. (2016). How Dynein Moves Along Microtubules. *Trends Biochem Sci*, *41*(1), 94-105. https://doi.org/10.1016/j.tibs.2015.11.004

Biggers, J. D., McGinnis, L. K., & Lawitts, J. A. (2004). Enhanced effect of glycyl-L-glutamine on mouse preimplantation embryos in vitro. *Reprod Biomed Online*, *9*(1), 59-69. https://doi.org/10.1016/s1472-6483(10)62111-6

Biggers, J. D., McGinnis, L. K., & Lawitts, J. A. (2005). One-step versus two-step culture of mouse preimplantation embryos: is there a difference? *Hum Reprod*, *20*(12), 3376-3384. https://doi.org/10.1093/humrep/dei228

Blakeley, P., Fogarty, N. M., del Valle, I., Wamaitha, S. E., Hu, T. X., Elder, K., Snell, P., Christie, L., Robson, P., & Niakan, K. K. (2015). Defining the three cell lineages of the human blastocyst by single-cell RNA-seq. *Development*, *142*(18), 3151-3165. https://doi.org/10.1242/dev.123547

Boitrelle, F., Shah, R., Saleh, R., Henkel, R., Kandil, H., Chung, E., Vogiatzi, P., Zini, A., Arafa, M., & Agarwal, A. (2021). The Sixth Edition of the WHO Manual for Human Semen Analysis: A Critical Review and SWOT Analysis. *Life (Basel)*, *11*(12). https://doi.org/10.3390/life11121368

Boswell-Smith, V., Spina, D., & Page, C. P. (2006). Phosphodiesterase inhibitors. *Br J Pharmacol*, *147 Suppl 1*(Suppl 1), S252-257. https://doi.org/10.1038/sj.bjp.0706495

Boussouar, F., & Benahmed, M. (2004). Lactate and energy metabolism in male germ cells. *Trends in Endocrinology & Metabolism*, *15*(7), 345-350. https://doi.org/https://doi.org/10.1016/j.tem.2004.07.003

Braude, P., Bolton, V., & Moore, S. (1988). Human gene expression first occurs between the four- and eight-cell stages of preimplantation development. *Nature*, *332*(6163), 459-461. https://doi.org/10.1038/332459a0

Breitbart, H., & Grinshtein, E. (2023). Mechanisms That Protect Mammalian Sperm from the Spontaneous Acrosome Reaction. *Int J Mol Sci*, *24*(23). https://doi.org/10.3390/ijms242317005

Brison, D. R., & Schultz, R. M. (1997). Apoptosis during Mouse Blastocyst Formation: Evidence for a Role for Survival Factors Including Transforming Growth Factor α1. *Biology of Reproduction*, *56*(5), 1088-1096. https://doi.org/10.1095/biolreprod56.5.1088

Campbell, A., & Fishel, S. (2015). *Atlas of Time Lapse Embryology* (A. Campbell & S. Fishel, Eds. 1st ed.). CRC Press. https://doi.org/10.1201/b18006

Cappelaere, L., Le Cour Grandmaison, J., Martin, N., & Lambert, W. (2021). Amino Acid Supplementation to Reduce Environmental Impacts of Broiler and Pig Production: A Review. *Front Vet Sci*, *8*, 689259. https://doi.org/10.3389/fvets.2021.689259

Carrasquel Martínez, G., Aldana, A., Carneiro, J., Treviño, C. L., & Darszon, A. (2022). Acrosomal alkalinization occurs during human sperm capacitation. *Mol Hum Reprod*, *28*(3). https://doi.org/10.1093/molehr/gaac005

Carson, S. A., & Kallen, A. N. (2021). Diagnosis and Management of Infertility: A Review. *Jama*, *326*(1), 65-76. https://doi.org/10.1001/jama.2021.4788

Castillo, C. M., Harper, J., Roberts, S. A., O'Neill, H. C., Johnstone, E. D., & Brison, D. R. (2020). The impact of selected embryo culture conditions on ART treatment cycle outcomes: a UK national study. *Hum Reprod Open*, *2020*(1), hoz031. https://doi.org/10.1093/hropen/hoz031

Cauffman, G., De Rycke, M., Sermon, K., Liebaers, I., & Van de Velde, H. (2009). Markers that define stemness in ESC are unable to identify the totipotent cells in human preimplantation embryos. *Hum Reprod*, *24*(1), 63-70. https://doi.org/10.1093/humrep/den351

Ceelen, M., & Vermeiden, J. P. (2001). Health of human and livestock conceived by assisted reproduction. *Twin Res*, *4*(5), 412-416. https://doi.org/10.1375/1369052012614

Cheng, C. Y., & Mruk, D. D. (2012). The blood-testis barrier and its implications for male contraception. *Pharmacol Rev*, *64*(1), 16-64. https://doi.org/10.1124/pr.110.002790

Chiang, C., Mahalingam, S., & Flaws, J. A. (2017). Environmental Contaminants Affecting Fertility and Somatic Health. *Semin Reprod Med*, *35*(3), 241-249. https://doi.org/10.1055/s-0037-1603569

Ciray, H. N., Campbell, A., Agerholm, I. E., Aguilar, J., Chamayou, S., Esbert, M., & Sayed, S. (2014). Proposed guidelines on the nomenclature and annotation of dynamic human embryo monitoring by a time-lapse user group. *Hum Reprod*, *29*(12), 2650-2660. https://doi.org/10.1093/humrep/deu278

Cockburn, K., & Rossant, J. (2010). Making the blastocyst: lessons from the mouse. *J Clin Invest*, *120*(4), 995-1003. https://doi.org/10.1172/jci41229

Coticchio, G., Apter, S., Ebner, T., Freour, T., Guns, Y., Kovacic, B., Le Clef, N., Marques, M., Meseguer, M., Montjean, D., Sfontouris, I., Sturmey, R., & technology, E. W. g. o. T.-l. (2020). Good practice recommendations for the use of time-lapse technology†. *Human reproduction open*, *2020*(2). https://doi.org/10.1093/hropen/hoaa008

Dadgar, Z., Shariatzadeh, S. M. A., Mehranjani, M. S., & Kheirolahi, A. (2023). The therapeutic effect of co-administration of pentoxifylline and zinc in men with idiopathic infertility. *Irish Journal of Medical Science (1971 -)*, *192*(1), 431-439. https://doi.org/10.1007/s11845-022-02931-0

Davidson, A., Vermesh, M., Lobo, R. A., & Paulson, R. J. (1988). Mouse embryo culture as quality control for human in vitro fertilization: the one-cell versus the two-cell model. *Fertil Steril*, *49*(3), 516-521. https://doi.org/10.1016/s0015-0282(16)59783-0

de Kretser, D. M. (1997). Male infertility. *The Lancet*, *349*(9054), 787-790. https://doi.org/10.1016/S0140-6736(96)08341-9

De Paepe, C., Krivega, M., Cauffman, G., Geens, M., & Van de Velde, H. (2014). Totipotency and lineage segregation in the human embryo. *Mol Hum Reprod*, *20*(7), 599-618. https://doi.org/10.1093/molehr/gau027

Del Carmen Nogales, M., Bronet, F., Basile, N., Martínez, E. M., Liñán, A., Rodrigo, L., & Meseguer, M. (2017). Type of chromosome abnormality affects embryo morphology dynamics. *Fertil Steril*, *107*(1), 229-235.e222. https://doi.org/10.1016/j.fertnstert.2016.09.019

Delaunay, C., Santos, M. J. D. S., & Gouveia, L. (2021). In-vitro metaphors: ART beneficiaries' meaning-making about human embryos in the context of IVF in Portugal. *Reproductive Biomedicine & Society Online*, *13*, 62-74. https://doi.org/https://doi.org/10.1016/j.rbms.2021.05.003

Dhikhirullahi, O., & Zhang, Z. (2025). Male infertility. *Syst Biol Reprod Med*, *71*(1), 416-438. https://doi.org/10.1080/19396368.2025.2548492

Dong, J., Yin, M., Wu, L., Wang, T., Li, M., Zhang, W., Ma, M., & Li, B. (2024). Pregnancy and neonatal outcomes of ICSI using pentoxifylline to identify viable spermatozoa in patients with frozen-thawed testicular spermatozoa. *Front Endocrinol (Lausanne)*, *15*, 1364285. https://doi.org/10.3389/fendo.2024.1364285

Drobnis, E. Z., & Nangia, A. K. (2017). Phosphodiesterase Inhibitors (PDE Inhibitors) and Male Reproduction. *Adv Exp Med Biol*, *1034*, 29-38. https://doi.org/10.1007/978-3-319-69535-8_5

Dumoulin, J. M., Coonen, E., Bras, M., Bergers-Janssen, J. M., Ignoul-Vanvuchelen, R. C., van Wissen, L. C., Geraedts, J. P., & Evers, J. L. (2001). Embryo development and chromosomal anomalies after ICSI: effect of the injection procedure. *Hum Reprod*, *16*(2), 306-312. https://doi.org/10.1093/humrep/16.2.306

Duranthon, V., Watson, A. J., & Lonergan, P. (2008). Preimplantation embryo programming: transcription, epigenetics, and culture environment. *Reproduction*, *135*(2), 141-150. https://doi.org/10.1530/rep-07-0324

Dyer, S., Chambers, G. M., Jwa, S. C., Baker, V. L., Banker, M., de Mouzon, J., Elgindy, E., Fu, B., Ishihara, O., Kupka, M. S., Zegers-Hochschild, F., & Adamson, G. D. (2025). International Committee for Monitoring Assisted Reproductive Technologies world report: assisted reproductive technology, 2019. *Fertil Steril*, *124*(4), 679-693. https://doi.org/10.1016/j.fertnstert.2025.06.003

Ebner, T., Maurer, M., Oppelt, P., Mayer, R. B., Duba, H. C., Costamoling, W., & Shebl, O. (2015). Healthy twin live-birth after ionophore treatment in a case of theophylline-resistant Kartagener syndrome. *J Assist Reprod Genet*, *32*(6), 873-877. https://doi.org/10.1007/s10815-015-0486-2

Ebner, T., Shebl, O., Mayer, R. B., Moser, M., Costamoling, W., & Oppelt, P. (2014). Healthy live birth using theophylline in a case of retrograde ejaculation and absolute asthenozoospermia. *Fertil Steril*, *101*(2), 340-343. https://doi.org/10.1016/j.fertnstert.2013.10.006

Ebner, T., Tews, G., Mayer, R. B., Ziehr, S., Arzt, W., Costamoling, W., & Shebl, O. (2011). Pharmacological stimulation of sperm motility in frozen and thawed testicular sperm using the dimethylxanthine theophylline. *Fertil Steril*, *96*(6), 1331-1336. https://doi.org/10.1016/j.fertnstert.2011.08.041

Fauque, P., Mondon, F., Letourneur, F., Ripoche, M. A., Journot, L., Barbaux, S., Dandolo, L., Patrat, C., Wolf, J. P., Jouannet, P., Jammes, H., & Vaiman, D. (2010). In vitro fertilization and embryo culture strongly impact the placental transcriptome in the mouse model. *PLoS One*, *5*(2), e9218. https://doi.org/10.1371/journal.pone.0009218

Female age-related fertility decline. Committee Opinion No. 589. (2014). *Fertil Steril*, *101*(3), 633-634. https://doi.org/10.1016/j.fertnstert.2013.12.032

Fisher, D. L., & Gunaga, K. P. (1975). Theophylline induced variations in cyclic AMP content of the superovulated preimplantation mouse embryo. *Biol Reprod*, *12*(4), 471-476. https://doi.org/10.1095/biolreprod12.4.471

Fortier, A. L., Lopes, F. L., Darricarrère, N., Martel, J., & Trasler, J. M. (2008). Superovulation alters the expression of imprinted genes in the midgestation mouse placenta. *Hum Mol Genet*, *17*(11), 1653-1665. https://doi.org/10.1093/hmg/ddn055

Fowler, R. E., & Edwards, R. G. (1957). Induction of superovulation and pregnancy in mature mice by gonadotrophins. *J Endocrinol*, *15*(4), 374-384. https://doi.org/10.1677/joe.0.0150374

Gardner, D. K. (1994). Mammalian embryo culture in the absence of serum or somatic cell support. *Cell Biol Int*, *18*(12), 1163-1179. https://doi.org/10.1006/cbir.1994.1043

Gardner, D. K., & Harvey, A. J. (2015). Blastocyst metabolism. *Reprod Fertil Dev*, *27*(4), 638-654. https://doi.org/10.1071/rd14421

Gardner, D. K., & Lane, M. (1993). Amino acids and ammonium regulate mouse embryo development in culture. *Biol Reprod*, *48*(2), 377-385. https://doi.org/10.1095/biolreprod48.2.377

Gardner, D. K., & Lane, M. (1998). Culture of viable human blastocysts in defined sequential serum-free media. *Hum Reprod*, *13 Suppl 3*, 148-159; discussion 160. https://doi.org/10.1093/humrep/13.suppl_3.148

Gardner, D. K., & Lane, M. (2005). Ex vivo early embryo development and effects on gene expression and imprinting. *Reprod Fertil Dev*, *17*(3), 361-370. https://doi.org/10.1071/rd04103

Gardner, D. K., Lane, M., Stevens, J., Schlenker, T., & Schoolcraft, W. B. (2000). Blastocyst score affects implantation and pregnancy outcome: towards a single blastocyst transfer. *Fertility and Sterility*, *73*(6), 1155-1158. https://doi.org/https://doi.org/10.1016/S0015-0282(00)00518-5

Gardner, D. K., & Leese, H. J. (1990). Concentrations of nutrients in mouse oviduct fluid and their effects on embryo development and metabolism in vitro. *J Reprod Fertil*, *88*(1), 361-368. https://doi.org/10.1530/jrf.0.0880361

Gardner, D. K., & Sakkas, D. (1993). Mouse embryo cleavage, metabolism and viability: role of medium composition. *Hum Reprod*, *8*(2), 288-295. https://doi.org/10.1093/oxfordjournals.humrep.a138039

Gardner, D. K., & Schoolcraft, W. B. (1999). In vitro culture of human blastocysts. *Towards reproductive certainty: fertility and genetics beyond*, *1999*, 378-388.

Gleicher, N., Gayete-Lafuente, S., Guijarro-Baude, L., Patrizio, P., Albertini, D. F., & Barad, D. H. (2026). The declining efficiency of IVF in the USA. *Hum Reprod Open*, *2026*(1), hoag004. https://doi.org/10.1093/hropen/hoag004

Gordon, U. D. (2002). Assisted conception in the azoospermic male. *Hum Fertil (Camb)*, *5*(1 Suppl), S9-s14. https://doi.org/10.1080/1464727022000199851

Gupta, S. K. (2021). Human Zona Pellucida Glycoproteins: Binding Characteristics With Human Spermatozoa and Induction of Acrosome Reaction. *Front Cell Dev Biol*, *9*, 619868. https://doi.org/10.3389/fcell.2021.619868

Hamatani, T., Carter, M. G., Sharov, A. A., & Ko, M. S. (2004). Dynamics of global gene expression changes during mouse preimplantation development. *Dev Cell*, *6*(1), 117-131. https://doi.org/10.1016/s1534-5807(03)00373-3

Handelsman, D. J., Hirschberg, A. L., & Bermon, S. (2018). Circulating Testosterone as the Hormonal Basis of Sex Differences in Athletic Performance. *Endocrine Reviews*, *39*(5), 803-829. https://doi.org/10.1210/er.2018-00020

Handyside, A. H. (1981). Immunofluorescence techniques for determining the numbers of inner and outer blastomeres in mouse morulae. *J Reprod Immunol*, *2*(6), 339-350. https://doi.org/10.1016/0165-0378(81)90004-8

Hardy, K., & Spanos, S. (2002). Growth factor expression and function in the human and mouse preimplantation embryo. *J Endocrinol*, *172*(2), 221-236. https://doi.org/10.1677/joe.0.1720221

Hertig, A. T., & Rock, J. (1973). Searching for early fertilized human ova. *Gynecol Invest*, *4*(3), 121-139. https://doi.org/10.1159/000301716

Hertig, A. T., Rock, J., Adams, E. C., & Menkin, M. C. (1959). Thirty-four fertilized human ova, good, bad and indifferent, recovered from 210 women of known fertility; a study of biologic wastage in early human pregnancy. *Pediatrics*, *23*(1 Part 2), 202-211.

Hillyear, L. M. (2022). *In Vitro Embryo Production in Agricultural Animals: Morphokinetic Profiling as a Tool to Investigate Embryo Viability* Canterbury Christ Church University (United Kingdom)].

Hoorsan, H., Mirmiran, P., Chaichian, S., Moradi, Y., Hoorsan, R., & Jesmi, F. (2017). Congenital Malformations in Infants of Mothers Undergoing Assisted Reproductive Technologies: A Systematic Review and Meta-analysis Study. *J Prev Med Public Health*, *50*(6), 347-360. https://doi.org/10.3961/jpmph.16.122

Houston, B. J., Riera-Escamilla, A., Wyrwoll, M. J., Salas-Huetos, A., Xavier, M. J., Nagirnaja, L., Friedrich, C., Conrad, D. F., Aston, K. I., Krausz, C., Tüttelmann, F., O'Bryan, M. K., Veltman, J. A., & Oud, M. S. (2021). A systematic review of the validated monogenic causes of human male infertility: 2020 update and a discussion of emerging gene-disease relationships. *Hum Reprod Update*, *28*(1), 15-29. https://doi.org/10.1093/humupd/dmab030

Howlett, S. K., & Bolton, V. N. (1985). Sequence and regulation of morphological and molecular events during the first cell cycle of mouse embryogenesis. *J Embryol Exp Morphol*, *87*, 175-206.

IRAC, Working Group, & on the Evaluation of Carcinogenic Risks to Humans. (1991). *Coffee, Tea, Mate, Methylxanthines and Methylglyoxal.* International Agency for Research on Cancer. https://www.ncbi.nlm.nih.gov/books/NBK507021/

Jacobs, L. A., & Vaughn, D. J. (2012). Hypogonadism and infertility in testicular cancer survivors. *J Natl Compr Canc Netw*, *10*(4), 558-563. https://doi.org/10.6004/jnccn.2012.0053

Johnson, M. T., & Gardner, D. K. (2011). Embryo culture in the twenty-first century. In D. K. Gardner, B. R. M. B. Rizk, & T. Falcone (Eds.), *Human Assisted Reproductive Technology: Future Trends in Laboratory and Clinical Practice* (pp. 232-247). Cambridge University Press. https://doi.org/DOI: 10.1017/CBO9780511734755.022

Joris, H., Nagy, Z., Van de Velde, H., De Vos, A., & Van Steirteghem, A. (1998). Intracytoplasmic sperm injection: laboratory set-up and injection procedure. *Hum Reprod*, *13 Suppl 1*, 76-86. https://doi.org/10.1093/humrep/13.suppl_1.76

Kaji, K., Oda, S., Shikano, T., Ohnuki, T., Uematsu, Y., Sakagami, J., Tada, N., Miyazaki, S., & Kudo, A. (2000). The gamete fusion process is defective in eggs of Cd9-deficient mice. *Nat Genet*, *24*(3), 279-282. https://doi.org/10.1038/73502

Kane, M., Morgan, P., & Coonan, C. (1997). Peptide growth factors and preimplantation development. *Human Reproduction Update*, *3*(2), 137-157. https://doi.org/10.1093/humupd/3.2.137

Katz, D. J., O'Donnell, L., McLachlan, R. I., Moss, T. J., Boothroyd, C. V., Jayadev, V., & Catford, S. R. (2025). The first Australian evidence-based guidelines on male infertility. *Med J Aust*, *223*(11), 653-663. https://doi.org/10.5694/mja2.70080

Kaur, G., Mital, P., & Dufour, J. M. (2013). Testisimmune privilege - Assumptions versus facts. *Anim Reprod*, *10*(1), 3-15.

Khan, Z., Wolff, H. S., Fredrickson, J. R., Walker, D. L., Daftary, G. S., & Morbeck, D. E. (2013). Mouse strain and quality control testing: improved sensitivity of the mouse embryo assay with embryos from outbred mice. *Fertility and Sterility*, *99*(3), 847-854.e842. https://doi.org/10.1016/j.fertnstert.2012.10.046

Khoudja, R. Y., Xu, Y., Li, T., & Zhou, C. (2013). Better IVF outcomes following improvements in laboratory air quality. *Journal of Assisted Reproduction and Genetics*, *30*(1), 69-76. https://doi.org/10.1007/s10815-012-9900-1

Kidder, G. M., & Watson, A. J. (2005). Roles of Na,K-ATPase in early development and trophectoderm differentiation. *Semin Nephrol*, *25*(5), 352-355. https://doi.org/10.1016/j.semnephrol.2005.03.011

Kim, E., Yamashita, M., Kimura, M., Honda, A., Kashiwabara, S., & Baba, T. (2008). Sperm penetration through cumulus mass and zona pellucida. *Int J Dev Biol*, *52*(5-6), 677-682. https://doi.org/10.1387/ijdb.072528ek

Kimber, S. J., Sneddon, S. F., Bloor, D. J., El-Bareg, A. M., Hawkhead, J. A., Metcalfe, A. D., Houghton, F. D., Leese, H. J., Rutherford, A., Lieberman, B. A., & Brison, D. R. (2008). Expression of genes involved in early cell fate decisions in human embryos and their regulation by growth factors. *Reproduction*, *135*(5), 635-647. https://doi.org/10.1530/rep-07-0359

Kleijkers, S. H. M., Mantikou, E., Slappendel, E., Consten, D., van Echten-Arends, J., Wetzels, A. M., van Wely, M., Smits, L. J. M., van Montfoort, A. P. A., Repping, S., Dumoulin, J. C. M., & Mastenbroek, S. (2016). Influence of embryo culture medium (G5 and HTF) on pregnancy and perinatal outcome after IVF: a multicenter RCT. *Human Reproduction*, *31*(10), 2219-2230. https://doi.org/10.1093/humrep/dew156

Kotevski, D., Newman, J., Chaitarvornkit, A., Paul, R., & Chambers, G. (2025). Assisted reproductive technology in Australia and New Zealand 2023. *National Perinatal Epidemiology and Statistics Unit, the University of New South Wales, Sydney.*

Kovacic, B., Vlaisavljevic, V., & Reljic, M. (2006). Clinical use of pentoxifylline for activation of immotile testicular sperm before ICSI in patients with azoospermia. *J Androl*, *27*(1), 45-52. https://doi.org/10.2164/jandrol.05079

LadyofHats. (2006). Complete diagram of a human spermatozoa. In *Wikimedia Commons*.

Lane, M., & Gardner, D. K. (1997). Differential regulation of mouse embryo development and viability by amino acids. *Journal of Reproduction and Fertility*, *109*(1), 153-164. https://doi.org/10.1530/jrf.0.1090153

Lane, M., & Gardner, D. K. (2000). Lactate regulates pyruvate uptake and metabolism in the preimplantation mouse embryo. *Biol Reprod*, *62*(1), 16-22. https://doi.org/10.1095/biolreprod62.1.16

Lane, M., & Gardner, D. K. (2003). Ammonium induces aberrant blastocyst differentiation, metabolism, pH regulation, gene expression and subsequently alters fetal development in the mouse. *Biol Reprod*, *69*(4), 1109-1117. https://doi.org/10.1095/biolreprod.103.018093

Lazzari, E., Potančoková, M., Sobotka, T., Gray, E., & Chambers, G. M. (2023). Projecting the Contribution of Assisted Reproductive Technology to Completed Cohort Fertility. *Population Research and Policy Review*, *42*(1), 6. https://doi.org/10.1007/s11113-023-09765-3

Leese, H. J., Conaghan, J., Martin, K. L., & Hardy, K. (1993). Early human embryo metabolism. *Bioessays*, *15*(4), 259-264. https://doi.org/10.1002/bies.950150406

Li, M., Drury, K. C., & Williams, R. S. (2001). Suitability of mouse embryos for human IVF QC: zygotes vs. 2-cell embryos. *Fertility and Sterility*, *76*(3), S230. https://doi.org/10.1016/S0015-0282(01)02685-1

Lin, J. B., & Troyer, D. (2014). Testicular Anatomy and Physiology. In L. M. McManus & R. N. Mitchell (Eds.), *Pathobiology of Human Disease* (pp. 2464-2475). Academic Press. https://doi.org/https://doi.org/10.1016/B978-0-12-386456-7.05102-9

Linck, R. W., Chemes, H., & Albertini, D. F. (2016). The axoneme: the propulsive engine of spermatozoa and cilia and associated ciliopathies leading to infertility. *Journal of*

Assisted Reproduction and Genetics, *33*(2), 141-156. https://doi.org/10.1007/s10815-016-0652-1

Linehan, L. A., Hennessy, M., & O'Donoghue, K. (2025). Recurrent Miscarriage and Infertility Services and Supports: A Qualitative Study of Views and Experiences in the Republic of Ireland. *Health Expect*, *28*(4), e70396. https://doi.org/10.1111/hex.70396

Liperis, G., & Sjöblom, C. (2017). Quality Control in the IVF Laboratory: Continuous Improvement. In D. E. Morbeck & M. H. M. Montag (Eds.), *Principles of IVF Laboratory Practice: Optimizing Performance and Outcomes* (pp. 79-87). Cambridge University Press. https://doi.org/DOI: 10.1017/9781316569238.014

Liu, W., Du, L., Li, J., He, Y., & Tang, M. (2024). Microenvironment of spermatogonial stem cells: a key factor in the regulation of spermatogenesis. *Stem Cell Res Ther*, *15*(1), 294. https://doi.org/10.1186/s13287-024-03893-z

Liu, X., Fernandes, R., Gertsenstein, M., Perumalsamy, A., Lai, I., Chi, M., Moley, K. H., Greenblatt, E., Jurisica, I., Casper, R. F., Sun, Y., & Jurisicova, A. (2011). Automated microinjection of recombinant BCL-X into mouse zygotes enhances embryo development. *PLoS One*, *6*(7), e21687. https://doi.org/10.1371/journal.pone.0021687

Loughlin, K. R., & Agarwal, A. (1992). Use of theophylline to enhance sperm function. *Arch Androl*, *28*(2), 99-103. https://doi.org/10.3109/01485019208987686

Lu, Y., Su, H., Zhang, J., Wang, Y., & Li, H. (2021). Treatment of Poor Sperm Quality and Erectile Dysfunction With Oral Pentoxifylline: A Systematic Review. *Front Pharmacol*, *12*, 789787. https://doi.org/10.3389/fphar.2021.789787

Lucifero, D., Mertineit, C., Clarke, H. J., Bestor, T. H., & Trasler, J. M. (2002). Methylation dynamics of imprinted genes in mouse germ cells. *Genomics*, *79*(4), 530-538. https://doi.org/10.1006/geno.2002.6732

Luck, D. J. (1984). Genetic and biochemical dissection of the eucaryotic flagellum. *J Cell Biol*, *98*(3), 789-794. https://doi.org/10.1083/jcb.98.3.789

Lundin, K., & Park, H. (2020). Time-lapse technology for embryo culture and selection. *Ups J Med Sci*, *125*(2), 77-84. https://doi.org/10.1080/03009734.2020.1728444

Ma, M., Zhang, L., Liu, Z., Teng, Y., Li, M., Peng, X., & An, L. (2024). Effect of blastocyst development on hatching and embryo implantation. *Theriogenology*, *214*, 66-72. https://doi.org/https://doi.org/10.1016/j.theriogenology.2023.10.011

Maezawa, T., Yamanaka, M., Hashimoto, S., Amo, A., Ohgaki, A., Nakaoka, Y., Fukuda, A., Ikeda, T., Inoue, M., & Morimoto, Y. (2014). Possible selection of viable human blastocysts after vitrification by monitoring morphological changes. *J Assist Reprod Genet*, *31*(8), 1099-1104. https://doi.org/10.1007/s10815-014-0260-x

Mahaldashtian, M., Khalili, M. A., Nottola, S. A., Woodward, B., Macchiarelli, G., & Miglietta, S. (2021). Does in vitro application of pentoxifylline have beneficial effects in assisted male reproduction? *Andrologia*, *53*(1), e13722. https://doi.org/10.1111/and.13722

Mahutte, N. G., & Arici, A. (2003). Failed fertilization: is it predictable? *Curr Opin Obstet Gynecol*, *15*(3), 211-218. https://doi.org/10.1097/00001703-200306000-00001

Mangoli, V., Mangoli, R., Dandekar, S., Suri, K., & Desai, S. (2011). Selection of viable spermatozoa from testicular biopsies: a comparative study between pentoxifylline and hypoosmotic swelling test. *Fertil Steril*, *95*(2), 631-634. https://doi.org/10.1016/j.fertnstert.2010.10.007

Mayeur, A., Magnan, F., Mathieu, S., Rubens, P., Sperelakis Beedham, B., Sonigo, C., Steffann, J., & Frydman, N. (2024). What importance do donors and recipients attribute to the

nuclear DNA-related genetic heritage of oocyte donation? *Hum Reprod*, *39*(4), 770-778. https://doi.org/10.1093/humrep/deae030

McLay, D. W., & Clarke, H. J. (2003). Remodelling the paternal chromatin at fertilization in mammals. *Reproduction*, *125*(5), 625-633. https://doi.org/10.1530/rep.0.1250625

Ménézo, Y. J. R., & Hérubel, F. (2002). Mouse and bovine models for human IVF*. *Reproductive BioMedicine Online*, *4*(2), 170-175. https://doi.org/https://doi.org/10.1016/S1472-6483(10)61936-0

Merritt, B. A., Behr, S. C., & Khati, N. J. (2020). Imaging of Infertility, Part 1: Hysterosalpingograms to Magnetic Resonance Imaging. *Radiol Clin North Am*, *58*(2), 215-225. https://doi.org/10.1016/j.rcl.2019.10.010

Meseguer, M., Rubio, I., Cruz, M., Basile, N., Marcos, J., & Requena, A. (2012). Embryo incubation and selection in a time-lapse monitoring system improves pregnancy outcome compared with a standard incubator: a retrospective cohort study. *Fertil Steril*, *98*(6), 1481-1489.e1410. https://doi.org/10.1016/j.fertnstert.2012.08.016

Miller, D., Brinkworth, M., & Iles, D. (2010). Paternal DNA packaging in spermatozoa: more than the sum of its parts? DNA, histones, protamines and epigenetics. *Reproduction*, *139*(2), 287-301. https://doi.org/10.1530/rep-09-0281

Mirończuk-Chodakowska, I., Witkowska, A. M., & Zujko, M. E. (2018). Endogenous non-enzymatic antioxidants in the human body. *Adv Med Sci*, *63*(1), 68-78. https://doi.org/10.1016/j.advms.2017.05.005

Morbeck, D. E. (2017). Mouse Embryo Assay for Quality Control in the IVF Laboratory. In M. H. M. Montag & D. E. Morbeck (Eds.), *Principles of IVF Laboratory Practice: Optimizing Performance and Outcomes* (pp. 69-72). Cambridge University Press. https://doi.org/DOI: 10.1017/9781316569238.012

Moriyama, Makri, D., Maalouf, M. N., Adamova, P., de Moraes, G. F. A., Pinheiro, M. O., Bernardineli, D. L., Massaia, I., Maalouf, W. E., & Lo Turco, E. G. (2022). The effects of temperature variation treatments on embryonic development: a mouse study. *Scientific Reports*, *12*(1), 2489. https://doi.org/10.1038/s41598-022-06158-y

Morris, S. A., & Zernicka-Goetz, M. (2012). Formation of distinct cell types in the mouse blastocyst. *Results Probl Cell Differ*, *55*, 203-217. https://doi.org/10.1007/978-3-642-30406-4_11

Nagy, A., Gertsenstein, M., Vintersten, K., & Behringer, R. (2003). *Manipulating the Mouse Embryo: A Laboratory Manual*. Cold Spring Harbor Laboratory Press.

Navas, P., Paffoni, A., Intra, G., González-Utor, A., Clavero, A., Gonzalvo, M. C., Díaz, R., Peña, R., Restelli, L., Somigliana, E., Papaleo, E., Castilla, J. A., & Viganò, P. (2017). Obstetric and neo-natal outcomes of ICSI cycles using pentoxifylline to identify viable spermatozoa in patients with immotile spermatozoa. *Reprod Biomed Online*, *34*(4), 414-421. https://doi.org/10.1016/j.rbmo.2017.01.009

Newman, J., Paul, R., & Chambers, G. (2022). Assisted reproductive technology in Australia and New Zealand 2020. *National Perinatal Epidemiology and Statistics Unit, the University of New South Wales, Sydney*.

Ng, K. Y. B., Mingels, R., Morgan, H., Macklon, N., & Cheong, Y. (2017). In vivo oxygen, temperature and pH dynamics in the female reproductive tract and their importance in human conception: a systematic review. *Human Reproduction Update*, *24*(1), 15-34. https://doi.org/10.1093/humupd/dmx028

Nguyen, A. Q., Bardua, I., Greene, B., Wrenzycki, C., Wagner, U., & Ziller, V. (2020). Mouse embryos exposed to oxygen concentrations that mimic changes in the oviduct and

uterus show improvement in blastocyst rate, blastocyst size, and accelerated cell division. *Reprod Biol*, *20*(2), 147-153. https://doi.org/10.1016/j.repbio.2020.03.011

Noda, T., Blaha, A., Fujihara, Y., Gert, K. R., Emori, C., Deneke, V. E., Oura, S., Panser, K., Lu, Y., Berent, S., Kodani, M., Cabrera-Quio, L. E., Pauli, A., & Ikawa, M. (2022). Sperm membrane proteins DCST1 and DCST2 are required for sperm-egg interaction in mice and fish. *Commun Biol*, *5*(1), 332. https://doi.org/10.1038/s42003-022-03289-w

Nomikos, M., Blayney, L. M., Larman, M. G., Campbell, K., Rossbach, A., Saunders, C. M., Swann, K., & Lai, F. A. (2005). Role of phospholipase C-zeta domains in Ca2+-dependent phosphatidylinositol 4,5-bisphosphate hydrolysis and cytoplasmic Ca2+ oscillations. *J Biol Chem*, *280*(35), 31011-31018. https://doi.org/10.1074/jbc.M500629200

O'Donnell, L., Nicholls, P. K., O'Bryan, M. K., McLachlan, R. I., & Stanton, P. G. (2011). Spermiation: The process of sperm release. *Spermatogenesis*, *1*(1), 14-35. https://doi.org/10.4161/spmg.1.1.14525

O'Donnell, L., & Smith, L. B. (2000). Endocrinology of the Testis and Spermatogenesis. In K. R. Feingold, R. A. Adler, S. F. Ahmed, B. Anawalt, M. R. Blackman, G. Chrousos, E. Corpas, W. W. de Herder, K. Dhatariya, K. Dungan, E. Hamilton, J. Hofland, S. Jan de Beur, S. Kalra, G. Kaltsas, N. Kapoor, M. Kim, C. Koch, P. Kopp, M. Korbonits, C. S. Kovacs, W. Kuohung, B. Laferrère, M. Levy, E. A. McGee, R. McLachlan, R. Muzumdar, J. Purnell, R. Rey, R. Sahay, A. S. Shah, M. A. Sperling, C. A. Stratakis, D. L. Trence, & D. P. Wilson (Eds.), *Endotext*. MDText.com, Inc. Copyright © 2000-2026, MDText.com, Inc. https://www.ncbi.nlm.nih.gov/books/NBK279031/

O'Donnell, L., Stanton, P., & de Kretser, D. M. (2015). Endocrinology of the male reproductive system and spermatogenesis.

O'Neill, C. L., Chow, S., Rosenwaks, Z., & Palermo, G. D. (2018). Development of ICSI. *Reproduction*, *156*(1), F51-f58. https://doi.org/10.1530/rep-18-0011

O'Shaughnessy, P. J. (2014). Hormonal control of germ cell development and spermatogenesis. *Semin Cell Dev Biol*, *29*, 55-65. https://doi.org/10.1016/j.semcdb.2014.02.010

Olson, G. E., & Winfrey, V. P. (1990). Mitochondria-cytoskeleton interactions in the sperm midpiece. *J Struct Biol*, *103*(1), 13-22. https://doi.org/10.1016/1047-8477(90)90081-m

Palermo, G., Joris, H., Devroey, P., & Van Steirteghem, A. C. (1992). Pregnancies after intracytoplasmic injection of single spermatozoon into an oocyte. *Lancet*, *340*(8810), 17-18. https://doi.org/10.1016/0140-6736(92)92425-f

Payne, D., Flaherty, S. P., Barry, M. F., & Matthews, C. D. (1997). Preliminary observations on polar body extrusion and pronuclear formation in human oocytes using time-lapse video cinematography. *Hum Reprod*, *12*(3), 532-541. https://doi.org/10.1093/humrep/12.3.532

Pereira, R., Sá, R., Barros, A., & Sousa, M. (2017). Major regulatory mechanisms involved in sperm motility. *Asian J Androl*, *19*(1), 5-14. https://doi.org/10.4103/1008-682x.167716

Perk, H., Armagan, A., Naziroğlu, M., Soyupek, S., Hoscan, M. B., Sütcü, R., Ozorak, A., & Delibas, N. (2008). Sildenafil citrate as a phosphodiesterase inhibitor has an antioxidant effect in the blood of men. *J Clin Pharm Ther*, *33*(6), 635-640. https://doi.org/10.1111/j.1365-2710.2008.00962.x

Piliszek, A., Grabarek, J. B., Frankenberg, S. R., & Plusa, B. (2016). Cell fate in animal and human blastocysts and the determination of viability. *Mol Hum Reprod*, *22*(10), 681-690. https://doi.org/10.1093/molehr/gaw002

Plant, T. M., & Marshall, G. R. (2001). The Functional Significance of FSH in Spermatogenesis and the Control of Its Secretion in Male Primates. *Endocrine Reviews*, *22*(6), 764-786. https://doi.org/10.1210/edrv.22.6.0446

Pribenszky, C., Nilselid, A. M., & Montag, M. (2017). Time-lapse culture with morphokinetic embryo selection improves pregnancy and live birth chances and reduces early pregnancy loss: a meta-analysis. *Reprod Biomed Online*, *35*(5), 511-520. https://doi.org/10.1016/j.rbmo.2017.06.022

Puga Molina, L. C., Luque, G. M., Balestrini, P. A., Marín-Briggiler, C. I., Romarowski, A., & Buffone, M. G. (2018). Molecular Basis of Human Sperm Capacitation. *Front Cell Dev Biol*, *6*, 72. https://doi.org/10.3389/fcell.2018.00072

Quinn, P., & Horstman, F. C. (1998). Is the mouse a good model for the human with respect to the development of the preimplantation embryo in vitro? *Hum Reprod*, *13 Suppl 4*, 173-183. https://doi.org/10.1093/humrep/13.suppl_4.173

Rawe, V. Y., Díaz, E. S., Abdelmassih, R., Wójcik, C., Morales, P., Sutovsky, P., & Chemes, H. E. (2008). The role of sperm proteasomes during sperm aster formation and early zygote development: implications for fertilization failure in humans. *Hum Reprod*, *23*(3), 573-580. https://doi.org/10.1093/humrep/dem385

Reproductive Technology Accreditation Committee. (2021). *Code of Practice for Assisted Reproductive Technology Units. Fertility Society of Australia Reproductive Technology Accreditation Committee (RTAC)*. Retrieved 1/3/2022 from https://www.fertilitysociety.com.au/wp-content/uploads/20211124-RTAC-ANZ-COP.pdf

Richter, K. S., Harris, D. C., Daneshmand, S. T., & Shapiro, B. S. (2001). Quantitative grading of a human blastocyst: optimal inner cell mass size and shape. *Fertility and Sterility*, *76*(6), 1157-1167. https://doi.org/https://doi.org/10.1016/S0015-0282(01)02870-9

Roque, M., Haahr, T., Geber, S., Esteves, S. C., & Humaidan, P. (2019). Fresh versus elective frozen embryo transfer in IVF/ICSI cycles: a systematic review and meta-analysis of reproductive outcomes. *Hum Reprod Update*, *25*(1), 2-14. https://doi.org/10.1093/humupd/dmy033

Russell, L. D., Ettlin, R. A., Hikim, A. P. S., & Clegg, E. D. (1993). Histological and Histopathological Evaluation of the Testis. *International Journal of Andrology*, *16*(1), 83-83. https://doi.org/https://doi.org/10.1111/j.1365-2605.1993.tb01156.x

Sacchi, L., Albani, E., Cesana, A., Smeraldi, A., Parini, V., Fabiani, M., Poli, M., Capalbo, A., & Levi-Setti, P. E. (2019). Preimplantation Genetic Testing for Aneuploidy Improves Clinical, Gestational, and Neonatal Outcomes in Advanced Maternal Age Patients Without Compromising Cumulative Live-Birth Rate. *J Assist Reprod Genet*, *36*(12), 2493-2504. https://doi.org/10.1007/s10815-019-01609-4

Sandi-Monroy, N. L., Musanovic, S., Zhu, D., Szabó, Z., Vogl, A., Reeka, N., Eibner, K., Bundschu, K., & Gagsteiger, F. (2019). Use of dimethylxanthine theophylline (SpermMobil(®)) does not affect clinical, obstetric or perinatal outcomes. *Arch Gynecol Obstet*, *300*(5), 1435-1443. https://doi.org/10.1007/s00404-019-05312-8

Sathananthan, A. H., Ratnam, S. S., Ng, S. C., Tarín, J. J., Gianaroli, L., & Trounson, A. (1996). The sperm centriole: its inheritance, replication and perpetuation in early human embryos. *Hum Reprod*, *11*(2), 345-356. https://doi.org/10.1093/humrep/11.2.345

Satish, M., Kumari, S., Deeksha, W., Abhishek, S., Nitin, K., Adiga, S. K., Hegde, P., Dasappa, J. P., Kalthur, G., & Rajakumara, E. (2021). Structure-based redesigning of pentoxifylline analogs against selective phosphodiesterases to modulate sperm functional competence for assisted reproductive technologies. *Sci Rep*, *11*(1), 12293. https://doi.org/10.1038/s41598-021-91636-y

Saunders, C. M., Larman, M. G., Parrington, J., Cox, L. J., Royse, J., Blayney, L. M., Swann, K., & Lai, F. A. (2002). PLC zeta: a sperm-specific trigger of Ca(2+) oscillations in eggs and embryo development. *Development*, *129*(15), 3533-3544. https://doi.org/10.1242/dev.129.15.3533

Scott, L., & Smith, S. (1995). Human sperm motility-enhancing agents have detrimental effects on mouse oocytes and embryos. *Fertil Steril*, *63*(1), 166-175.

Scott, L. F., Sundaram, S. G., & Smith, S. (1993). The relevance and use of mouse embryo bioassays for quality control in an assisted reproductive technology program**Presented in part at the 48th Annual Meeting of the American Fertility Society, New Orleans, Louisiana, November 2 to 5, 1992. *Fertility and Sterility*, *60*(3), 559-568. https://doi.org/https://doi.org/10.1016/S0015-0282(16)56176-7

Seshagiri, P. B., Sen Roy, S., Sireesha, G., & Rao, R. P. (2009). Cellular and molecular regulation of mammalian blastocyst hatching. *Journal of Reproductive Immunology*, *83*(1), 79-84. https://doi.org/https://doi.org/10.1016/j.jri.2009.06.264

Shahbazi, M. N., & Zernicka-Goetz, M. (2018). Deconstructing and reconstructing the mouse and human early embryo. *Nat Cell Biol*, *20*(8), 878-887. https://doi.org/10.1038/s41556-018-0144-x

Sharpe, A., Bhandari, H., & Miller, D. (2022). Is there a role for phosphodiesterase inhibitors in the treatment of male subfertility? *Hum Fertil (Camb)*, *25*(1), 13-23. https://doi.org/10.1080/14647273.2020.1793420

Siu, K. K., Serrão, V. H. B., Ziyyat, A., & Lee, J. E. (2021). The cell biology of fertilization: Gamete attachment and fusion. *J Cell Biol*, *220*(10). https://doi.org/10.1083/jcb.202102146

Sjoblom, C., & Swearman, H. (2019). Use of Medium Supplements for Oocyte and Embryo Culture. In G. Kovacs, A. Rutherford, & D. K. Gardner (Eds.), *How to Prepare the Egg and Embryo to Maximize IVF Success* (pp. 245-258). Cambridge University Press. https://doi.org/DOI: 10.1017/9781316756744.021

Skoracka, K., Eder, P., Łykowska-Szuber, L., Dobrowolska, A., & Krela-Kaźmierczak, I. (2020). Diet and Nutritional Factors in Male (In)fertility-Underestimated Factors. *J Clin Med*, *9*(5). https://doi.org/10.3390/jcm9051400

Smeenk, J., Wyns, C., De Geyter, C., Kupka, M., Bergh, C., Cuevas Saiz, I., De Neubourg, D., Rezabek, K., Tandler-Schneider, A., Rugescu, I., & Goossens, V. (2023). ART in Europe, 2019: results generated from European registries by ESHRE†. *Hum Reprod*, *38*(12), 2321-2338. https://doi.org/10.1093/humrep/dead197

Smeenk, J., Wyns, C., De Geyter, C., Kupka, M. S., Bergh, C., Cuevas Saiz, I., De Neubourg, D., Rezabek, K., Tandler-Schneider, A., Rugescu, I., Goossens, V., Reproduction, T. E. I. M. C. f. t. E. S. o. H., & Embryology. (2025). ART in Europe, 2020: results generated from European registries by ESHRE†. *Human Reproduction*, *40*(11), 2038-2055. https://doi.org/10.1093/humrep/deaf179

Sönmezer, M., & Oktay, K. (2008). Assisted reproduction and fertility preservation techniques in cancer patients. *Curr Opin Endocrinol Diabetes Obes*, *15*(6), 514-522. https://doi.org/10.1097/MED.0b013e32831a46fc

Sozen, B., Can, A., & Demir, N. (2014). Cell fate regulation during preimplantation development: a view of adhesion-linked molecular interactions. *Dev Biol*, *395*(1), 73-83. https://doi.org/10.1016/j.ydbio.2014.08.028

Squirrell, J. M., Lane, M., & Bavister, B. D. (2001). Altering intracellular pH disrupts development and cellular organization in preimplantation hamster embryos. *Biol Reprod*, *64*(6), 1845-1854. https://doi.org/10.1095/biolreprod64.6.1845

St. John, J., Sakkas, D., & Barratt, C. L. (2000). A Role for Mitochondrial DNA Review and Sperm Survival. *Journal of Andrology*, *21*(2), 189-199. https://doi.org/https://doi.org/10.1002/j.1939-4640.2000.tb02093.x

Stamatiadis, P., Boel, A., Cosemans, G., Popovic, M., Bekaert, B., Guggilla, R., Tang, M., De Sutter, P., Van Nieuwerburgh, F., Menten, B., Stoop, D., Chuva de Sousa Lopes, S. M., Coucke, P., & Heindryckx, B. (2021). Comparative analysis of mouse and human preimplantation development following POU5F1 CRISPR/Cas9 targeting reveals interspecies differences. *Human Reproduction*, *36*(5), 1242-1252. https://doi.org/10.1093/humrep/deab027

Strünker, T., Goodwin, N., Brenker, C., Kashikar, N. D., Weyand, I., Seifert, R., & Kaupp, U. B. (2011). The CatSper channel mediates progesterone-induced Ca2+ influx in human sperm. *Nature*, *471*(7338), 382-386. https://doi.org/10.1038/nature09769

Sun, F., Turek, P., Greene, C., Ko, E., Rademaker, A., & Martin, R. H. (2007). Abnormal progression through meiosis in men with nonobstructive azoospermia. *Fertility and Sterility*, *87*(3), 565-571. https://doi.org/https://doi.org/10.1016/j.fertnstert.2006.07.1531

Svingen, T., & Koopman, P. (2013). Building the mammalian testis: origins, differentiation, and assembly of the component cell populations. *Genes Dev*, *27*(22), 2409-2426. https://doi.org/10.1101/gad.228080.113

Swain, J. E. (2010). Optimizing the culture environment in the IVF laboratory: impact of pH and buffer capacity on gamete and embryo quality. *Reprod Biomed Online*, *21*(1), 6-16. https://doi.org/10.1016/j.rbmo.2010.03.012

Swearman, H., Liperis, G., Crittenden, J., & Sjoblom, C. (2018). Fertilization by ICSI results in significantly higher aneuploidy rates compared to IVF, in embryos analysed by next generation sequencing (NGS) or comparative genome hybridization (CGH) array. *Fertility and Sterility*, *110*(4), e346-e347.

Taft, R. A. (2008). Virtues and limitations of the preimplantation mouse embryo as a model system. *Theriogenology*, *69*(1), 10-16. https://doi.org/10.1016/j.theriogenology.2007.09.032

Tarkowski, A. K. (1959). Experiments on the development of isolated blastomers of mouse eggs. *Nature*, *184*, 1286-1287. https://doi.org/10.1038/1841286a0

Tash, J. S., & Means, A. R. (1983). Cyclic adenosine 3',5' monophosphate, calcium and protein phosphorylation in flagellar motility. *Biol Reprod*, *28*(1), 75-104. https://doi.org/10.1095/biolreprod28.1.75

Terriou, P., Hans, E., Giorgetti, C., Spach, J. L., Salzmann, J., Urrutia, V., & Roulier, R. (2000). Pentoxifylline initiates motility in spontaneously immotile epididymal and testicular spermatozoa and allows normal fertilization, pregnancy, and birth after intracytoplasmic sperm injection. *J Assist Reprod Genet*, *17*(4), 194-199. https://doi.org/10.1023/a:1009435732258

Tesarik, J. (1992). Control of the fertilization process by the egg coat: how does it work in humans. *J Assist Reprod Genet*, *9*(4), 313-317. https://doi.org/10.1007/bf01203952

The University of Sydney, T. U. o. (2024). Guidelines on attribution of generative AI use for research students. *The University of Sydney*. https://sydneyuni.service-now.com/sm?id=kb_article_view&sysparm_article=KB0035308

Thompson, J. G., Gardner, D. K., Pugh, P. A., McMillan, W. H., & Tervit, H. R. (1995). Lamb birth weight is affected by culture system utilized during in vitro pre-elongation development of ovine embryos. *Biol Reprod*, *53*(6), 1385-1391. https://doi.org/10.1095/biolreprod53.6.1385

Thompson, S. L., Konfortova, G., Gregory, R. I., Reik, W., Dean, W., & Feil, R. (2001). Environmental effects on genomic imprinting in mammals. *Toxicol Lett*, *120*(1-3), 143-150. https://doi.org/10.1016/s0378-4274(01)00292-2

Tomashov-Matar, R., Levi, M., & Shalgi, R. (2008). The involvement of Src family kinases (SFKs) in the events leading to resumption of meiosis. *Mol Cell Endocrinol*, *282*(1-2), 56-62. https://doi.org/10.1016/j.mce.2007.11.016

Toshimori, K., & Eddy, E. M. (2015). Chapter 3 - The Spermatozoon. In T. M. Plant & A. J. Zeleznik (Eds.), *Knobil and Neill's Physiology of Reproduction (Fourth Edition)* (pp. 99-148). Academic Press. https://doi.org/https://doi.org/10.1016/B978-0-12-397175-3.00003-X

Tournaye, H., Devroey, P., Camus, M., Van der Linden, M., Janssens, R., & Van Steirteghem, A. (1995). Use of pentoxifylline in assisted reproductive technology. *Hum Reprod*, *10 Suppl 1*, 72-79. https://doi.org/10.1093/humrep/10.suppl_1.72

Tournaye, H., Van der Linden, M., Van den Abbeel, E., Devroey, P., & Van Steirteghem, A. (1994a). The effect of pentoxifylline on mouse in-vitro fertilization and early embryonic development. *Hum Reprod*, *9*(10), 1903-1908. https://doi.org/10.1093/oxfordjournals.humrep.a138356

Tournaye, H., Van der Linden, M., Van den Abbeel, E., Devroey, P., & Van Steirteghem, A. (1994b). Fertilization and early embryology: The effect of pentoxifylline on mouse in-vitro fertilization and early embryonic development. *Human Reproduction*, *9*(10), 1903-1908. https://doi.org/10.1093/oxfordjournals.humrep.a138356

Turner, R. M. (2005). Moving to the beat: a review of mammalian sperm motility regulation. *Reproduction Fertility and Development*, *18*(2), 25-38. https://doi.org/10.1071/RD05120

US Food Drug Administration, C. f. D. R. H. (2021). *Mouse Embryo Assay for Assisted Reproduction Technology Devices* [Guidance Document]. https://www.fda.gov/regulatory-information/search-fda-guidance-documents/mouse-embryo-assay-assisted-reproduction-technology-devices

Veeck, L., & Zaninovic, N. (2003). *An Atlas of Human Blastocysts*. https://doi.org/10.3109/9780203008935

Venetis, C., Choi, S. K. Y., Jorm, L., Zhang, X., Ledger, W., Lui, K., Havard, A., Chapman, M., Norman, R. J., & Chambers, G. M. (2023). Risk for Congenital Anomalies in Children Conceived With Medically Assisted Fertility Treatment : A Population-Based Cohort Study. *Ann Intern Med*, *176*(10), 1308-1320. https://doi.org/10.7326/m23-0872

Vestweber, D., Gossler, A., Boller, K., & Kemler, R. (1987). Expression and distribution of cell adhesion molecule uvomorulin in mouse preimplantation embryos. *Dev Biol*, *124*(2), 451-456. https://doi.org/10.1016/0012-1606(87)90498-2

Vitale, S. G., Palumbo, M., Rapisarda, A. M. C., Carugno, J., Conde-López, C., Mendoza, N., Mendoza-Tesarik, R., & Tesarik, J. (2022). Use of pentoxifylline during ovarian

stimulation to improve oocyte and embryo quality: A retrospective study. *J Gynecol Obstet Hum Reprod*, *51*(6), 102398. https://doi.org/10.1016/j.jogoh.2022.102398
Walters, E. A., Brown, J. L., Krisher, R., Voelkel, S., & Swain, J. E. (2020). Impact of a controlled culture temperature gradient on mouse embryo development and morphokinetics. *Reprod Biomed Online*, *40*(4), 494-499. https://doi.org/10.1016/j.rbmo.2019.12.015
Wang, Y., Li, R., Yang, R., Zheng, D., Zeng, L., Lian, Y., Zhu, Y., Zhao, J., Liang, X., Li, W., Liu, J., Tang, L., Cao, Y., Hao, G., Wang, H., Zhang, H., Wang, R., Mol, B. W., Huang, H., & Qiao, J. (2024). Intracytoplasmic sperm injection versus conventional in-vitro fertilisation for couples with infertility with non-severe male factor: a multicentre, open-label, randomised controlled trial. *Lancet*, *403*(10430), 924-934. https://doi.org/10.1016/s0140-6736(23)02416-9
Watson, A. J. (1992). The cell biology of blastocyst development. *Mol Reprod Dev*, *33*(4), 492-504. https://doi.org/10.1002/mrd.1080330417
Winters, B. R., & Walsh, T. J. (2014). The epidemiology of male infertility. *Urol Clin North Am*, *41*(1), 195-204. https://doi.org/10.1016/j.ucl.2013.08.006
Wöber, M., Ebner, T., Steiner, S. L., Strohmer, H., Oppelt, P., Plas, E., & Obruca, A. (2015). A new method to process testicular sperm: combining enzymatic digestion, accumulation of spermatozoa, and stimulation of motility. *Arch Gynecol Obstet*, *291*(3), 689-694. https://doi.org/10.1007/s00404-014-3458-3
Wolff, H. S., Fredrickson, J. R., Walker, D. L., & Morbeck, D. E. (2013). Advances in quality control: mouse embryo morphokinetics are sensitive markers of in vitro stress. *Hum Reprod*, *28*(7), 1776-1782. https://doi.org/10.1093/humrep/det102
World Health Organisation. (2021). *WHO laboratory manual for the examination and processing of human semen* (L. Bjorndahl, Ed. sixth ed.). World Health Organisation. https://apps.who.int/iris/rest/bitstreams/1358672/retrieve
World Health Organization, W. H. (2025). *Guideline for the prevention, diagnosis and treatment of infertility*. World Health Organization. https://www.who.int/publications/i/item/9789240115774
Wu, B., Wong, D., Lu, S., Dickstein, S., Silva, M., & Gelety, T. J. (2005). Optimal use of fresh and frozen-thawed testicular sperm for intracytoplasmic sperm injection in azoospermic patients. *J Assist Reprod Genet*, *22*(11-12), 389-394. https://doi.org/10.1007/s10815-005-7481-y
Wu, T. F., & Chu, D. S. (2008). Epigenetic processes implemented during spermatogenesis distinguish the paternal pronucleus in the embryo. *Reprod Biomed Online*, *16*(1), 13-22. https://doi.org/10.1016/s1472-6483(10)60552-4
Xue, Z., Huang, K., Cai, C., Cai, L., Jiang, C. Y., Feng, Y., Liu, Z., Zeng, Q., Cheng, L., Sun, Y. E., Liu, J. Y., Horvath, S., & Fan, G. (2013). Genetic programs in human and mouse early embryos revealed by single-cell RNA sequencing. *Nature*, *500*(7464), 593-597. https://doi.org/10.1038/nature12364
Yamanaka, Y., Ralston, A., Stephenson, R. O., & Rossant, J. (2006). Cell and molecular regulation of the mouse blastocyst. *Dev Dyn*, *235*(9), 2301-2314. https://doi.org/10.1002/dvdy.20844
Yanagimachi, R. (1994). Fertility of mammalian spermatozoa: its development and relativity. *Zygote*, *2*(4), 371-372. https://doi.org/10.1017/S0967199400002240
Yang, L., Peavey, M., Kaskar, K., Chappell, N., Zhu, L., Devlin, D., Valdes, C., Schutt, A., Woodard, T., Zarutskie, P., Cochran, R., & Gibbons, W. E. (2022). Development of a dynamic machine learning algorithm to predict clinical pregnancy and live birth rate

with embryo morphokinetics. *F&S reports*, *3*(2), 116-123. https://doi.org/10.1016/j.xfre.2022.04.004

Yeung, Q. S., Briton-Jones, C. M., Tjer, G. C., Chiu, T. T., & Haines, C. (2004). The efficacy of test tube warming devices used during oocyte retrieval for IVF. *J Assist Reprod Genet*, *21*(10), 355-360. https://doi.org/10.1023/b:jarg.0000046203.44045.0e

Yoshioka, K., Suzuki, C., Itoh, S., Kikuchi, K., Iwamura, S., & Rodriguez-Martinez, H. (2003). Production of piglets derived from in vitro-produced blastocysts fertilized and cultured in chemically defined media: effects of theophylline, adenosine, and cysteine during in vitro fertilization. *Biol Reprod*, *69*(6), 2092-2099. https://doi.org/10.1095/biolreprod.103.020081

Young, L. E., & Fairburn, H. R. (2000). Improving the safety of embryo technologies: possible role of genomic imprinting. *Theriogenology*, *53*(2), 627-648. https://doi.org/10.1016/s0093-691x(99)00263-0

Yovich, J. M., Edirisinghe, W. R., Cummins, J. M., & Yovich, J. L. (1988). Preliminary results using pentoxifylline in a pronuclear stage tubal transfer (PROST) program for severe male factor infertility. *Fertil Steril*, *50*(1), 179-181. https://doi.org/10.1016/s0015-0282(16)60030-4

Zegers-Hochschild, F., Adamson, G. D., Dyer, S., Racowsky, C., de Mouzon, J., Sokol, R., Rienzi, L., Sunde, A., Schmidt, L., Cooke, I. D., Simpson, J. L., & van der Poel, S. (2017). The International Glossary on Infertility and Fertility Care, 2017. *Hum Reprod*, *32*(9), 1786-1801. https://doi.org/10.1093/humrep/dex234

Zimmerman, S., & Sutovsky, P. (2009). The sperm proteasome during sperm capacitation and fertilization. *J Reprod Immunol*, *83*(1-2), 19-25. https://doi.org/10.1016/j.jri.2009.07.006

Ziomek, C. A., & Johnson, M. H. (1980). Cell surface interaction induces polarization of mouse 8-cell blastomeres at compaction. *Cell*, *21*(3), 935-942. https://doi.org/10.1016/0092-8674(80)90457-2

Zmuidinaite, R., Sharara, F. I., & Iles, R. K. (2021). Current Advancements in Noninvasive Profiling of the Embryo Culture Media Secretome. *Int J Mol Sci*, *22*(5). https://doi.org/10.3390/ijms22052513

Zuccarello, D., Ferlin, A., Garolla, A., Menegazzo, M., Perilli, L., Ambrosini, G., & Foresta, C. (2011). How the human spermatozoa sense the oocyte: a new role of SDF1-CXCR4 signalling. *Int J Androl*, *34*(6 Pt 2), e554-565. https://doi.org/10.1111/j.1365-2605.2011.01158.x